1970

A study of the anodic oxidation of 1, 3-butadiene on platinum and gold electrodes

Arun Kumar Agrawal

A STUDY OF THE ANODIC OXIDATION OF 1,3-BUTADIENE

ON PLATINUM AND GOLD ELECTRODES

by

ARUN KUMAR AGRAWAL, 1940-

A DISSERTATION

Presented to the Faculty of the Graduate School of the

UNIVERSITY OF MISSOURI-ROLLA

In Partial Fulfillment of the Requirements for the Degree

DOCTOR OF PHILOSOPHY

in

CHEMICAL ENGINEERING

1970

Advisor

ABSTRACT

The anodic oxidation of 1,3-butadiene on Pt and Au electrodes was studied at 70°C in solutions of H_2SO_4, K_2SO_4, K_2CO_3, and KOH with pH's ranging from 0.35 to 12.5. Reaction rates (current) were measured as a function of potential, pH, temperature, and butadiene partial pressure. A transition region (apparently a shift in the rate determining step) in case of Pt was observed in the Tafel plots. The coulombic efficiencies of oxidation to CO_2 were 85 percent in 1 N H_2SO_4 on Pt, 93 percent in 1 N KOH on Pt, and 72 percent in 1 N KOH on Au.

The parameters found on Pt were:

(1) Below the transition region.

$\partial V/\partial \log i$	$\simeq$	140 mv
$\partial V/\partial pH$	$\simeq$	0 (in acid)
	$\simeq$	-70 mv (in base)
$\partial \log i/\partial pH$	$\simeq$	0 (in acid)
	$\simeq$	0.5 (in base)
$\partial i/\partial P_R$	$<$	0

(2) Above the transition region.

$\partial V/\partial \log i$	$\simeq$	70 mv
$\partial V/\partial pH$	$\simeq$	0 (in acid)
	$\simeq$	-70 mv (in base)
$\partial \log i/\partial pH$	$\simeq$	0 (in acid)
	$\simeq$	1 (in base)

$\partial i/\partial P_R$ < 0

$\partial E'_a/\partial V$ ≈ -23 Kcal/volt

The parameters found on Au were:

$\partial V/\partial \log i$ ≈ 70 mv

$\partial V/\partial pH$ ≈ -70 mv (in base)

$\partial \log i/\partial pH$ ≈ 1 (in base)

$\partial i/\partial P_R$ < 0 (above 0.1 atm)

> 0 (below 0.1 atm)

$\partial E'_a/\partial V$ ≈ -23 Kcal/volt

The reaction mechanism is interpreted in terms of the following sequence:

$$H_2O \approx H_2O(ads)$$

$$R \approx R(ads)$$

$$R(ads) + H_2O(ads) \rightarrow RHOH^+(ads) + e$$

$$RHOH^+(ads) + H_2O \rightarrow \overset{H_2O}{\cdots} \rightarrow CO_2, H^+, e, \text{ etc.}$$

The first electron transfer is the rate determining step on Pt below the transition region and the corresponding rate equation is

$$i = zFk'\theta_R(1-\theta_T)\exp(\alpha\nu F/RT)$$

The rate determining step on Pt above the transition region and on Au is the chemical step following the first electron discharge step. The corresponding rate equation is

$$i = zFk''\theta_R(1-\theta_T)\exp(\nu F/RT)$$

In the rate equations ν is the rational potential.

ACKNOWLEDGEMENTS

The author wishes to thank Dr. J. W. Johnson, Professor of Chemical Engineering, who served as research advisor, and Dr. W. J. James, Professor of Chemistry and Director of the Graduate Center for Materials Research, Space Sciences Research Center, University of Missouri-Rolla. Their help, guidance, and encouragement are sincerely appreciated.

The author gratefully acknowledges a Research Scholarship from the Graduate Center for Materials Research.

TABLE OF CONTENTS

	Page
ABSTRACT	ii
ACKNOWLEDGEMENTS	v
LIST OF FIGURES	x
LIST OF TABLES	xiii
I. INTRODUCTION	1
II. LITERATURE REVIEW	3
A. Potential of Zero Charge	3
1. Variation of the potential of zero charge	5
a. Platinum	6
b. Gold	9
B. Electrosorption	12
1. Theory	12
2. Potential dependence of electrosorption	16
C. Anodic Oxidation of Hydrocarbons	24
1. Oxidation on Pt	24
a. Alkenes	24
b. Acetylene	29
2. Oxidation on Au	33
a. Acetylene	33
b. Ethylene	36

III. EXPERIMENTAL..... 39
A. Materials..... 39
B. Electrodes..... 40
1. Platinum Anode..... 40
2. Gold Anode..... 40
3. Cathode..... 41
C. Current-Potential Studies..... 41
1. Apparatus..... 41
2. Procedure..... 45
a. Anode activation..... 45
b. Rest potential..... 46
c. Current-potential measurements..... 47
3. Data and Results..... 47
a. Grade-A butadiene..... 48
b. Grade-B butadiene..... 51
(1) Platinum..... 51
(2) Gold..... 63
D. Current-Partial Pressure Studies..... 66
1. Apparatus..... 66
2. Procedure..... 66
3. Data and Results..... 66
E. Current-Temperature Studies..... 70
1. Apparatus..... 70
2. Procedure..... 70
3. Data and Results..... 70

F. Coulombic Efficiency Studies..... 74
1. Apparatus..... 74
2. Procedure..... 74
3. Data and results..... 77
IV. DISCUSSION..... 79
A. Summary of Experimental Results..... 79
1. Platinum..... 79
2. Gold..... 81
B. Comparison of Present Work with that Reported in Literature..... 82
C. Postulation of a Reaction Mechanism.. 83
1. Potential of zero charge..... 84
2. Applicability of oxidation mechanisms from the literature to butadiene..... 85
a. Acetylene-Pt mechanism..... 85
b. Alkene-Pt mechanism..... 87
c. Acetylene, Ethylene-Au mechanisms..... 89
3. A mechanism for the anodic oxidation of butadiene..... 91
a. Case I (Tafel slope = $2.3RT/\alpha F$)..... 94
b. Case II (Tafel slope = $2.3RT/F$)..... 95

D. Correlation of Experimental Results with the Theoretical Rate Equations..... 96
1. Polarization and pH relation... 96
a. Case I (Tafel slope 2.3RT/αF)..... 96
b. Case II (Tafel slope 2.3RT/F)..... 97
2. Current-partial pressure relation..... 97
3. Current-temperature relation... 98
E. Applicability of the Postulated Reaction Mechanism to Other Hydrocarbons..... 99
1. Acetylene on Pt..... 99
2. Alkenes on Pt..... 99
3. Ethylene on Au..... 100
4. Acetylene on Au..... 101
V. RECOMMENDATIONS..... 103
VI. APPENDICES..... 104
A. NOTATION..... 105
B. MATERIALS..... 109
C. APPARATUS..... 112
D. SAMPLE CALCULATIONS..... 114
E. DATA..... 116
VII. BIBLIOGRAPHY..... 145
VIII. VITA..... 148

LIST OF FIGURES

Figure		Page
1.	Potential of zero charge of gold in 0.1 N solutions.....	10
2.	Coverage-potential relationship in the adsorption of ethylene on platinum from 1 N H_2SO_4.....	17
3.	Diagram of the apparatus used for potentiostatic studies in the anodic oxidation of butadiene.....	42
4.	Electrolytic cell.....	43
5.	Polarization curves for the anodic oxidation of Grade-A butadiene on Pt (P_R = 1 atm).....	50
6.	log i-pH relation at 0.5 volts(SHE) for the anodic oxidation of Grade-A butadiene on Pt at 70°C (P_R = 1 atm).....	52
7.	V-pH relation at 1.37 x 10^{-4} amp/cm^2 current density for the anodic oxidation of Grade-A butadiene on Pt at 70°C (P_R = 1 atm).....	53
8.	Polarization curves for the anodic oxidation of Grade-B butadiene on Pt at 70°C (P_R = 1 atm).....	55
9.	Polarization curves for the anodic oxidation of Grade-B butadiene on Pt at 70°C in 1 N H_2SO_4.....	56

10. Polarization curves for the anodic oxidation of Grade-B butadiene on Pt at 70°C in 1 N KOH..... 57
11. Polarization curves for the anodic oxidation of Grade-B butadiene on Au at 70°C (P_R = 1 atm)..... 58
12. Polarization curves for the anodic oxidation of Grade-B butadiene on Au at 70°C in 1 N KOH..... 59
13. log i-pH relation at 0.5 volts(SHE) for the anodic oxidation of Grade-B butadiene on Pt at 70°C (P_R = 1 atm)..... 61
14. V-pH relation at 1.37 x 10^{-4} amp/cm^2 current density for the anodic oxidation of Grade-B butadiene on Pt at 70°C (P_R = 1 atm)..... 62
15. log i-pH relation at 0.1 volts(SHE) for the anodic oxidation of Grade-B butadiene on Au at 70°C (P_R = 1 atm)..... 64
16. V-pH relation at 6.67 x 10^{-6} amp/cm^2 current density for the anodic oxidation of Grade-B butadiene on Au at 70°C (P_R = 1 atm)..... 65
17. Current-partial pressure relation for the anodic oxidation of Grade-B butadiene on Pt at 70°C in 1 N H_2SO_4..... 67

18. Current-partial pressure relation for the anodic oxidation of Grade-B butadiene on Pt at 70°C in 1 N KOH..... 68

19. Current-partial pressure relation for the anodic oxidation of Grade-B butadiene on Au at 70°C in 1 N KOH..... 69

20. Current-temperature relation for the anodic oxidation of Grade-B butadiene on Pt in 1 N H_2SO_4 (P_R = 1 atm)..... 71

21. Current-temperature relation for the anodic oxidation of Grade-B butadiene on Pt in 1 N KOH (P_R = 1 atm)..... 72

22. Current-temperature relation for the anodic oxidation of Grade-B butadiene on Au in 1 N KOH (P_R = 1 atm)..... 73

23. Electrical circuit used for galvanostatic studies in the anodic oxidation of butadiene..... 75

LIST OF TABLES

Table		Page
I.	Kinetic Paramenters for the Anodic Oxidation of Hydrocarbons on Pt at 80°C.....	25
II.	Kinetic Parameters for the Anodic Oxidation of Acetylene on Pt at 80°C.....	30
III.	Kinetic Parameters for the Anodic Oxidation of Acetylene and Ethylene on Au at 80°C.....	34
IV.	Rest Potentials for Grade-A Butadiene on Pt in Aqueous Solutions (P_R = 1 atm).....	49
V.	Rest Potentials for Grade-B Butadiene on Pt and Au in Aqueous Solutions at 70°C (P_R = 1 atm).....	54
VI.	Apparent Activation Energies for the Anodic Oxidation of Grade-B Butadiene on Pt and Au (P_R = 1 atm).....	76
VII.	Kinetic Parameters for the Anodic Oxidation of Grade-B Butadiene at 70°C.....	80
VIII.	Modified Parameters for the Anodic Oxidation of Grade-B Butadiene at 70°C..	93

IX. Current-Potential Values for the Anodic Oxidation of Grade-A Butadiene on Pt at 80°C (P_R = 1 atm) in 1 N H_2SO_4 (pH = 0.35)..... 117

X. Current-Potential Values for the Anodic Oxidation of Grade-A Butadiene on Pt at 70°C (P_R = 1 atm) in 1 N H_2SO_4 (pH = 0.35)..... 118

XI. Current-Potential Values for the Anodic Oxidation of Grade-A Butadiene on Pt at 70°C (P_R = 1 atm) in 1 N K_2SO_4 (pH = 4.4)..... 119

XII. Current-Potential Values for the Anodic Oxidation of Grade-A Butadiene on Pt at 70°C (P_R = 1 atm) in 1 N K_2CO_3 (pH = 10.8)..... 120

XIII. Current-Potential Values for the Anodic Oxidation of Grade-A Butadiene on Pt at 70°C (P_R = 1 atm) in 1 N KOH (pH = 12.5)..... 121

XIV. Current-Potential Values for the Anodic Oxidation of Grade-B Butadiene on Pt at 70°C (P_R = 1 atm) in 1 N H_2SO_4 (pH = 0.35)..... 122

XV. Current-Potential Values for the Anodic Oxidation of Grade-B Butadiene on Pt at 70°C (P_R = 1 atm) in H_2SO_4 + K_2SO_4 (pH = 1.3)..... 123

XVI. Current-Potential Values for the Anodic Oxidation of Grade-B Butadiene on Pt at 70°C (P_R = 1 atm) in H_2SO_4 + K_2SO_4 (pH = 2.6)..... 124

XVII. Current-Potential Values for the Anodic Oxidation of Grade-B Butadiene on Pt at 70°C (P_R = 1 atm) in K_2SO_4 + K_2CO_3 (pH = 9.9)..... 125

XVIII. Current-Potential Values for the Anodic Oxidation of Grade-B Butadiene on Pt at 70°C (P_R = 1 atm) in 1 N K_2CO_3 (pH = 10.8)..... 126

XIX. Current-Potential Values for the Anodic Oxidation of Grade-B Butadiene on Pt at 70°C (P_R = 1 atm) in 1 N KOH (pH = 12.5)..... 127

XX. Current-Potential Values for the Anodic Oxidation of Grade-B Butadiene on Pt at 70°C (P_R = 0.1 atm) in 1 N H_2SO_4 (pH = 0.35)..... 128

XXI. Current-Potential Values for the Anodic Oxidation of Grade-B Butadiene on Pt at 70°C (P_R = 0.01 atm) in 1 N H_2SO_4 (pH = 0.35)..... 129

XXII. Current-Potential Values for the Anodic Oxidation of Grade-B Butadiene on Pt at 70°C (P_R = 0.1 atm) in 1 N KOH (pH = 12.5)..... 130

XXIII. Current-Potential Values for the Anodic Oxidation of Grade-B Butadiene on Pt at 70°C (P_R = 0.01 atm) in 1 N KOH (pH = 12.5)..... 131

XXIV. Current-Potential Values for the Anodic Oxidation of Grade-B Butadiene on Au at 70°C (P_R = 1 atm) in 1 N H_2SO_4 (pH = 0.35)..... 132

XXV. Current-Potential Values for the Anodic Oxidation of Grade-B Butadiene on Au at 70°C (P_R = 1 atm) in K_2SO_4 + K_2CO_3 (pH = 9.9)..... 133

XXVI. Current-Potential Values for the Anodic Oxidation of Grade-B Butadiene on Au at 70°C (P_R = 1 atm) in 1 N K_2CO_3 (pH = 10.8)..... 134

XXVII. Current-Potential Values for the Anodic Oxidation of Grade-B Butadiene on Au at 70°C (P_R = 1 atm) in K_2SO_4 + KOH (pH = 11.6)..... 135

XXVIII. Current-Potential Values for the Anodic Oxidation of Grade-B Butadiene on Au at 70°C (P_R = 1 atm) in 1 N KOH (pH = 12.5)..... 136

XXIX. Current-Potential Values for the Anodic Oxidation of Grade-B Butadiene on Au at 70°C (P_R = 0.1 atm) in 1 N KOH (pH = 12.5)..... 137

XXX. Current-Potential Values for the Anodic Oxidation of Grade-B Butadiene on Au at 70°C (P_R = 0.01 atm) in 1 N KOH (pH = 12.5)..... 138

XXXI. Current-Pressure Values for the Anodic Oxidation of Grade-B Butadiene on Pt at 70°C in 1 N H_2SO_4 (pH = 0.35)..... 139

XXXII. Current-Pressure Values for the Anodic Oxidation of Grade-B Butadiene on Pt at 70°C in 1 N KOH (pH = 12.5)..... 140

XXXIII. Current-Pressure Values for the Anodic Oxidation of Grade-B Butadiene on Au at 70°C in 1 N KOH (pH = 12.5)..... 141

XXXIV. Current-Temperature Values for the Anodic Oxidation of Grade-B Butadiene on Pt in 1 N H_2SO_4 (P_R = 1 atm)..... 142

XXXV. Current-Temperature Values for the Anodic Oxidation of Grade-B Butadiene on Pt in 1 N KOH (P_R = 1 atm)..... 143

XXXVI. Current-Temperature Values for the Anodic Oxidation of Grade-B Butadiene on Au in 1 N KOH (P_R = 1 atm)..... 144

I. INTRODUCTION

The concept of direct conversion of the chemical energy of a fuel into electrical energy by an electrochemical process dates as far back as the year 1801 to Davy.[1] (Such electrochemical energy converters are popularly known as 'fuel cells'.) However, the systematic studies and development efforts of fuel cells were delayed until the past decade. Fuel cells hold promise of greater conversion efficiencies, by avoiding the intermediary heat cycle, than the conventional methods which have Carnot limitations. It was recently emphasized by Dr. G.E. Evans[2] that fuel cells will ultimately be used as reactors to produce various chemicals and the electricity generated during the process will be a by-product.

The establishment of reaction mechanisms for fuels and electrocatalytic activities of electrode substrates is important in the development and prediction of cell performance. Hydrocarbons, available as commercial fuels, have drawn considerable attention for use in such cells. The electroxidation of a number of these has been studied on noble metal electrodes.[3] In the present investigation, 1,3-butadiene was chosen for the anodic oxidation on Pt and Au electrodes in aqueous solutions. The steady state potentiostatic and galvanostatic methods

were employed to obtain the necessary kinetic parameters for elucidating the reaction mechanism.

II. LITERATURE REVIEW

Anodic oxidation of a number of hydrocarbons has been studied in the last decade largely because of the interest in fuel cells.[3] Such reactions are heterogeneous processes, and at least a portion of the reaction occurs on the electrode substrate. The rate of the reaction may depend upon the nature of the substrate, the concentrations of the reactants, solvent, reaction products, other species present at the electrode-electrolyte interface, and the potential difference across the interface. Literature pertinent to the present work and covering the above aspects is reviewed here in three sections: (1) potential of zero charge, (2) electrosorption, and (3) anodic oxidation of hydrocarbons.

A. Potential of Zero Charge

The potential of zero charge (p.z.c.) is an electrochemical parameter which plays a significant role in electrosorption and hence in electrode kinetics. The nature of the p.z.c. and its variation with electrolyte pH for Pt and Au are reviewed here.

When an electrode is placed in an electrolyte, a "double-layer" is formed at the metal-solution interface which acts as a capacitor. The excess charge*

*Excess or deficiency in electrons as compared to the neutral atoms.

developed on the metal side q_m is equivalent to the opposite charge on the solution side $-q_s$ that is necessary to maintain electrical neutrality of the system. The Gibbs adsorption isotherm for the system, at constant temperature and pressure, can be written as,*

$$\begin{aligned} d\gamma &= -\sum \Gamma_i d\bar{\mu}_i \\ &= -\sum \Gamma_i d\mu_i - \sum ze\Gamma_i d\phi_i \\ &= -\sum \Gamma_i d\mu_i - q_m dE \end{aligned} \tag{2.1}$$

This gives the Lippman equation[4] for the excess charge density,

$$\left(\frac{\partial \gamma}{\partial E}\right)_{P,T,\mu_i} = -q_m \tag{2.2}$$

The potential at which this derivative, i.e., q_m, is zero is defined as p.z.c. This corresponds to a situation where the metallic side of the double layer has no excess charge, i.e., $q_m = 0$.

At the p.z.c., the potential difference across the double layer is not necessarily zero.[5] From the definition of the electrochemical potential of a particle i with charge ze inside a phase α ,

$$\bar{\mu}_i^{\alpha} = \mu_i^{\alpha} + ze\phi^{\alpha} \tag{2.3}$$

---

*Terms are defined in nomenclature in Appendix A.

The chemical potential μ_i^α is the interaction of the particle with the phase devoid of the surface charge and dipoles within the phase α, and the inner or Galvani potential ϕ^α is the interaction of the particle with the surface layer containing the excess charge and the dipoles. The inner potential can be divided into a part ψ^α due to the free charge on the surface and a part χ^α due to the oriented dipoles in the surface. Thus,

$$\phi^\alpha = \psi^\alpha + \chi^\alpha \tag{2.4}$$

The absolute potential difference across the metal-solution interphase can be written as,

$$m_\Delta s = m_\Delta s_\psi + m_\Delta s_\chi \tag{2.5}$$

At zero charge, $m_\Delta s_\psi = 0$, and therefore,

$$m_\Delta s_{\phi_{q=0}} = m_\Delta s_{\chi_{q=0}} \tag{2.6}$$

Hence, at the p.z.c., a potential difference across the metal-solution interphase exists because of the electron overlap at the metal surface and oriented solvent dipoles in the double layer from the solution phase.

1. Variation of the potential of zero charge.

At the p.z.c., we have

$$m_\Delta s_{\phi_{q=0}} = m_\Delta s_{\chi_{q=0}} \tag{2.6}$$

and we can consider that,

$$ {}^{m}\Delta^{s}\chi_{q=0} = \chi^{m}_{q=0} - \chi^{s}_{q=0} \qquad (2.7) $$

The potentials χ^m and χ^s depend on the nature of the metal substrate and the solvent, respectively. Thus, the p.z.c. will be different for different metal-solution systems. Bockris and Argade[6] have shown by theoretical considerations that the p.z.c. measured with respect to a reference electrode is dependent upon the work-function of the metal. Petrii, et. al.,[7] have found experimentally that the variation in p.z.c. for platinum is dependent upon solution composition. Similar effects for Au and Ag were reported by Bode, Andersen, and Eyring,[8] where the p.z.c. depended upon the nature of anions in the aqueous electrolytes. Argade[5] (reporting a Russian work in his thesis) pointed out that the p.z.c. on some transition metals, e.g., Pt, Pd, Ni, Fe, and Co varies with pH, whereas no variation was observed for Hg, Au, Ag, Cu, Zn, and Pb.

a. Platinum. Gileadi, Argade, and Bockris[9] determined the p.z.c. on Pt in solutions of $HClO_4$+$NaClO_4$ and $NaClO_4$+NaOH over a pH range of 2.5 to 11.2 and found a linear relationship between the p.z.c. and pH. A completely hydrogen-free electrode (heat-treated, degassed, and non-pulsed) was used for the measurements. The relationship was expressed as,

$$ V_{pzc} = 0.56 - 2.3 \left(\frac{RT}{F}\right) pH \qquad (2.8) $$

where V_{pzc} is in volts (NHE). The presence of adsorbed/absorbed hydrogen on the Pt caused the p.z.c. to become more cathodic, but no specific relationship was reported.

Two recent Russian investigations[7,10] on Pt (presumably not hydrogen-free) show relationships different than reported above. Burshtein, et. al.,[10] measured the p.z.c. in $HClO_4$ + $NaClO_4$ solutions of pH's 2, 2.3, and 3. No pH dependence was found and a value of +0.1 volts was reported. Petrii, et. al.,[7] employed solutions of H_2SO_4 + Na_2SO_4 (pH 1.6-3.74), HCl + KCl (pH 1.2-3.34), HBr + KBr (pH 1.15-3.15), and KOH + KBr (pH 10.3-12.3). With increasing pH, the p.z.c. shifted in the negative direction. The magnitude of the shift depended on the composition of the solution. It was 18 mv per pH unit for sulfate, 30 mv for chloride , and 35 mv for bromide solutions. It increased in alkaline solutions.

An anomaly between the Russian work and that reported by Gileadi, et. al., seems to exist. Argade[5] has explained this is due to the presence of adsorbed hydrogen. Using the electrocapillary equations and data for mercury, he showed that the pH-dependence of the p.z.c. on Pt is likely due to ionic adsorption of H_3O^+ and OH^-. For the activated electrodes (hydrogen is known to penetrate into Pt during cathodic pulsing) used in the Russian work, the pH dependence of the p.z.c. in acidic solutions disappeared when the Pt-solution interphase

could be considered a non-polarizable system with respect to protons. The theoretical treatment by Argade of a non-polarizable electrode is presented here.

For a non-polarizable system when H^+ and $H^\cdot$ leak across the electrode-solution interface, one has,

$$-d\gamma = \Gamma_- d\mu_- + \Gamma_+ d\mu_+ + \Gamma_{H^+} d\mu_{H^+} + A_H d\mu_H + q_m dE \quad (2.9)$$

The subscripts + and - refer to the cations and anions of the salt. For the hydrogen adsorption-ionization equilibrium ($H^+ + e = Pt\text{-}H$) on the electrode,

$$\mu_{H^+} - F\psi = \mu_H \quad (2.10)$$

From equations 2.9 and 2.10,

$$-d\gamma = \Gamma_- d\mu_- + \Gamma_+ d\mu_+ + (\Gamma_{H^+} + A_H) d\mu_{H^+} + (q_m - A_H) dE \quad (2.11)$$

At constant μ_- and μ_+, $(\Gamma_{H^+} + A_H)$ and $(q_m - A_H)$ are independent variables. Hence,

$$\left(\frac{\partial E}{\partial \mu_{H^+}}\right)_{(q_m - A_H)} = -\left\{\frac{\partial (\Gamma_{H^+} + A_H)}{\partial (q_m - A_H)}\right\}_{\mu_{H^+}}$$

$$= -\left\{\frac{\partial \Gamma_{H^+} + \partial A_H}{\partial q_m - \partial A_H}\right\}_{\mu_{H^+}}$$

$$= -\left\{\frac{\left(\frac{\partial A_H}{\partial \Gamma_{H^+}}\right)^{-1} + 1}{\frac{\partial q_m}{\partial A_H} - 1}\right\}_{\mu_{H^+}} \quad (2.12)$$

But,

$$\left(\frac{\partial q_m}{\partial A_H}\right)_{\mu_{H^+}} = \frac{\left(\frac{\partial q_m}{\partial E}\right)}{\left(\frac{\partial A_H}{\partial E}\right)}$$

$$= - \frac{C_{dl}}{C_\phi} \qquad (2.13)$$

C_{dl} is approximately 70 $\mu F/cm^2$ for the equilibrium situation and C_ϕ is about 3 $\mu F/cm^2$ near the p.z.c. of the H-equilibrated electrode. Thus,

$$\left| \frac{\partial q_m}{\partial A_H} - 1 \right| >> 1 \qquad (2.14)$$

According to Frumkin, et. al.,[11]

$$\left| \frac{\partial A_H}{\partial \Gamma_{H^+}} \right| >> 1 \qquad (2.15)$$

Thus, the right hand side of equation 2.12 approaches zero and it can be seen that the p.z.c. of the non-polarizable electrode is pH independent provided A_H is relatively small compared to q_m.

b. Gold. The potential of zero charge on Au as reported by Bode, et. al.,[8] is shown in Figure 1. It is seen to be practically independent of pH in most cases over a wide range. At low pH's where some variation is seen, the accuracy of the results was

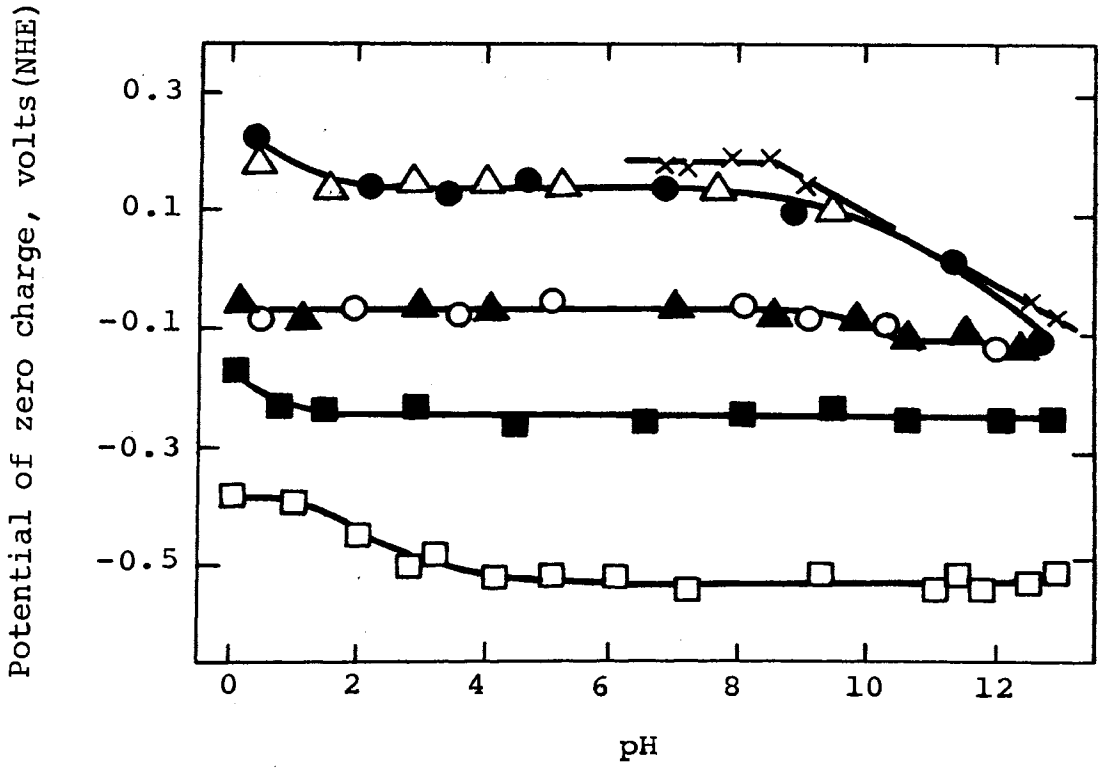

Figure 1. Potential of zero charge of Au in 0.1 N solutions.[8] (×, NaF; △, Na_2SO_4; ●, $NaClO_4$; ▲, NaCl; ○, LiCl; ■, NaBr; □, NaI)

uncertain because of the commencement of hydrogen evolution. In alkaline solutions (pH's ∿8 to 13), the p.z.c. decreased roughly 2.3RT/F volts per unit pH when either F^-, $SO_4^=$, or ClO_4^- anions were present with OH^- ions in the solution. No such shift was seen in the presence of either Cl^-, Br^-, or I^- ions. Bode concluded that OH^- ions coadsorb in the alkaline region and manifest themselves in the case of solutions containing less adsorbable ions such as F^-, etc. The anions shift the p.z.c. of Au to more positive values in the following order, $F^- > SO_4^= \simeq ClO_4^- > Cl^- > Br^- > I^-$.

Argade[5] measured the p.z.c. of Au by several methods in $HClO_4$ + $NaClO_4$ solutions. He compared his values with those reported in the literature by several investigators and found them to depend upon the way the electrodes were treated (activated) prior to measurements. The activated electrodes gave values more positive by about 0.1 to 0.2 volts than the non-activated ones. He concluded that the preferred value for Au (non-activated) is about 0.15 $\pm$ 0.10 volts. Argade also concluded that the positive shift of the p.z.c. for activated Au was probably due to a partial oxide coverage on the surface. Upon activation, an oxide film is formed during the anodic pulse and is reduced when the pulse is changed to cathodic. The resultant surface is probably not completely reduced because of the low hydrogen coverage

(θ_H = 0.03) and a slow rate of oxide reduction. The oxide would give rise to a higher work function and hence shift the p.z.c. in the positive direction.

2. Summary. The p.z.c. of Pt with adsorbed/absorbed hydrogen (i.e., pulsed or activated Pt) can be considered invarient with pH in strong acid solutions. In basic solutions or the hydrogen-free metal in acids, the relationship is approximately linear, with the variation depending upon the type of ions in the electrolyte. The probable cause of this pH effect is the adsorption of H_3O^+, OH^-, and/or other anions from the electrolyte.

The p.z.c. of Au is practically independent of pH up to values of $\sim$8, but its value may be affected by electrode activation. It decreases linearly in alkaline solutions when either F^-, $SO_4^=$, or ClO_4^- ions are present, but remains constant with Cl^-, Br^-, and I^- ions.

B. Electrosorption

In electrosorption, a potential difference exists between the solvated electrode and the solution. A theory of this phenomenon propounded by Bockris and coworkers[12,13] is presented here. The effect of potential and the electrosorption of hydrocarbons are discussed.

1. Theory. According to Bockris, et. al.,[12] the substrate is initially covered with water molecules (in aqueous solutions). When the organic species adsorb onto the surface, a number of water molecules is

replaced and finally equilibrium is attained. The electrosorption can thus be represented as a replacement reaction,

$$R(sol) + n\ H_2O(ads) = R(ads) + n\ H_2O(sol) \qquad (2.16)$$

At equilibrium,

$$\mu_{R,sol} + n\mu_{W,\ ads} = \mu_{R,ads} + n\mu_{W,sol} \qquad (2.17)$$

The standard free energy of adsorption

$$\Delta G^{o}_{ads} = (\mu^{o}_{R,ads} - \mu^{o}_{R,sol}) - n(\mu^{o}_{W,ads} - \mu^{o}_{W,sol}) \qquad (2.18)$$

is thus the difference between the standard free energies of adsorption of the organic and n water molecules.

Writing the chemical potentials in terms of mole fractions ($\simeq$ activities),

$$\mu_{R,sol} = \mu^{o}_{R,sol} + RT\ \ln(X_{R,sol}) \qquad (2.19)$$

$$\mu_{R,ads} = \mu^{o}_{R,ads} + RT\ \ln(X_{R,ads}) \qquad (2.20)$$

$$\mu_{W,sol} = \mu^{o}_{W,sol} + RT\ \ln(X_{W,sol}) \qquad (2.21)$$

$$\mu_{W,ads} = \mu^{o}_{W,ads} + RT\ \ln(X_{W,ads}) \qquad (2.22)$$

and substituting in the expression for the standard free energy of adsorption,

$$\Delta G^{o}_{ads} = -RT\ \ln \frac{(X_{R,ads})(X_{W,sol})^{n}}{(X_{W,ads})^{n}(X_{R,sol})} \qquad (2.23)$$

For dilute solutions $X_{W,sol} = 1$ and $X_{R,sol} = C_R/55.4$. On the surface,

$$X_{R,ads} = \frac{\Gamma_R}{\Gamma_R + \Gamma_W} \tag{2.24}$$

$$X_{W,ads} = \frac{\Gamma_W}{\Gamma_R + \Gamma_W} \tag{2.25}$$

Assuming that $\Gamma_{max,W} = n\Gamma_{max,R}$ and defining the fractional surface coverage by R as $\Gamma_R = \theta\Gamma_{max,R}$ gives

$$X_{R,ads} = \frac{\theta}{\theta + n(1-\theta)} \tag{2.26}$$

$$X_{W,ads} = \frac{n(1-\theta)}{\theta + n(1-\theta)} \tag{2.27}$$

This leads to,

$$\Delta G^o_{ads} = -RT \ln\{\frac{\theta}{\theta + n(1-\theta)} \cdot \frac{[\theta + n(1-\theta)]^n}{n^n(1-\theta)^n} \cdot \frac{55.4}{C_R}\} \tag{2.28}$$

or the isotherm,

$$\frac{\theta}{(1-\theta)^n} \cdot \frac{[\theta + n(1-\theta)]^{n-1}}{n^n} = \frac{C_R}{55.4} \cdot \exp(-\frac{\Delta G^o_{ads}}{RT}) \tag{2.29}$$

This reduces to the Langmuir isotherm if n = 1.

It was shown that ΔG^o_{ads} could be evaluated from certain estimated components of ΔG^o_{ads}, i.e.,

$$\Delta G^{o}_{ads} = \Delta G^{o}_{s,R} - n\,\Delta G^{o}_{s,W} \qquad (2.30)$$

$\Delta G^{o}_{s,W}$ and $\Delta G^{o}_{s,R}$ can be calculated from thermodynamic cycles, one for water and another for the organic compound.

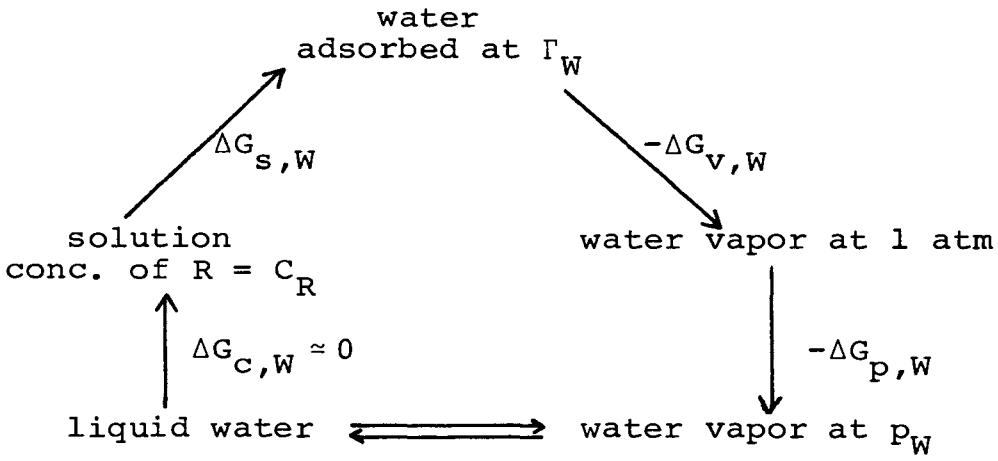

For water,

$$\Delta G_{s,W} = \Delta G_{p,W} + \Delta G_{v,W} \qquad (2.31)$$

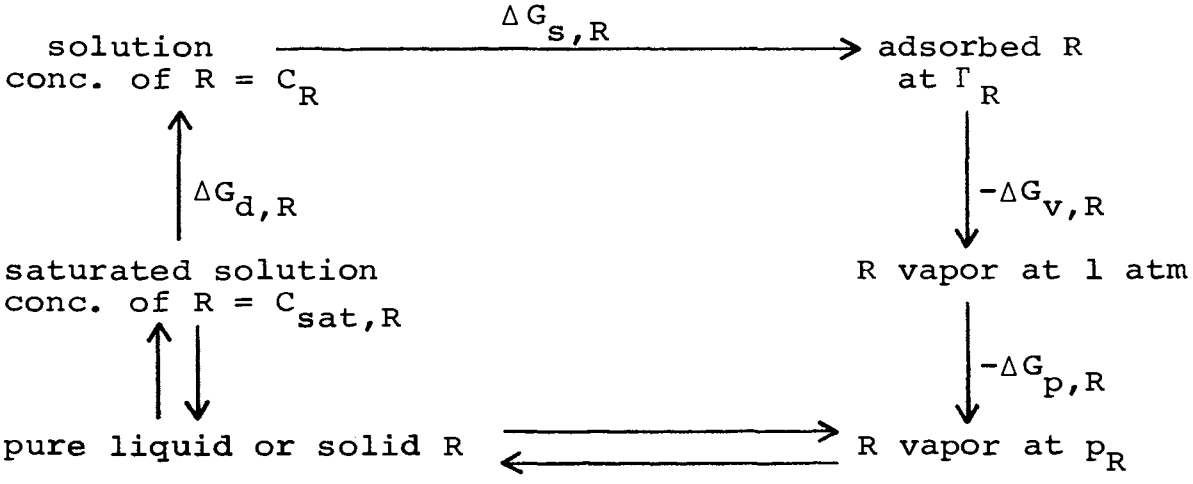

For the organic component,

$$\Delta G_{s,R} = -\Delta G_{d,R} + \Delta G_{p,R} + \Delta G_{v,R} \qquad (2.32)$$

Therefore,

$$\Delta G^{o}_{ads} = -\Delta G^{o}_{d,R} + \Delta G^{o}_{p,R} + \Delta G^{o}_{v,R} - n\Delta G^{o}_{p,W} - n\Delta G^{o}_{v,W}$$

$$= RT \ln \frac{C_R}{C_{sat,R}} - RT \ln \frac{p_R}{(p_W)^n} + \Delta G^{o}_{v,R} - n\,\Delta G^{o}_{v,W} \qquad (2.33)$$

The first two terms on the right hand side of equation 2.33 do not change with the metal and hence make the same contribution to ΔG^{o}_{ads} for all metals. The relative vapor pressures of the solvent and solute are other factors affecting the extent of adsorption. $\Delta G^{o}_{v,R}$ and $\Delta G^{o}_{v,W}$ can be estimated from gas phase adsorption.

2. Potential dependence of electrosorption. Investigations by Bockris and co-workers[12-15] of the electrosorption of n-decylamine, ethylene, benzene, and naphthalene on various metal electrodes, showed "bell-shaped" θ-V relationships. Such a plot for ethylene adsorption on platinum is shown in Figure 2. The results were interpreted on the basis of a competition between the organic and water molecules for surface sites and a field dependence of the standard free energy of adsorption of water, as discussed below.

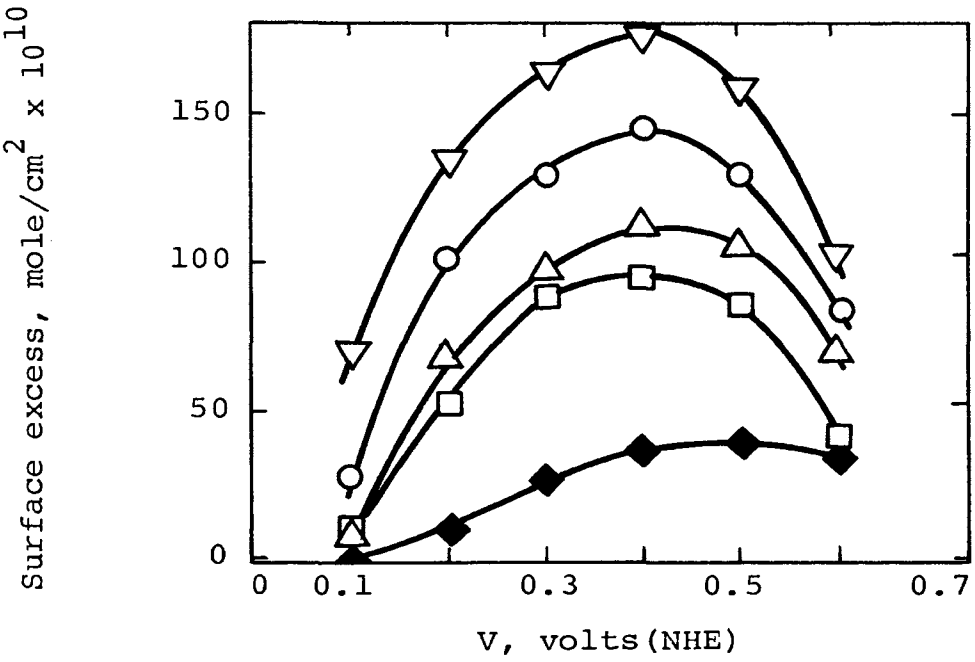

Figure 2. Coverage-potential relationship in the adsorption of ethylene on Pt from 1 N H_2SO_4.[14] (▽, 1.7×10^{-5} M; ○, 9.1×10^{-6} M; △, 4.6×10^{-6} M; □, 4.0×10^{-6} M; ◆, 2.1×10^{-6} M ethylene)

Consider first the water moelcules as symmetrical dipoles of moment ρ in field X of the double layer. (The free energy of adsorption of the neutral molecules is assumed to be independent of the field). The energy of interaction of solvent dipoles with the field is $\pm\rho X$* assuming that the dipoles completely align themselves with the field. At the p.z.c. and in the absence of any dipole potential, X will be zero and the solvent dipoles will be oriented in each direction in equal numbers. Since the effective free energy of adsorption depends on the difference between the values of the organic matter and water, maximum adsorption of the solute will occur at the p.z.c. In practice, the potential of maximum adsorption does not coincide with the p.z.c. and a somewhat more complex model is proposed.

Let N_1 and N_2 be the number of water molecules in the two possible orientations, and let the corresponding energies be E_1 and E_2. Then,

$$E_1 = E_1^c + \rho X - \left(\frac{N_1 - N_2}{N_t}\right) cE \qquad (2.34)$$

$$E_2 = E_2^c - \rho X + \left(\frac{N_1 - N_2}{N_t}\right) cE \qquad (2.35)$$

The average energy of a water molecule on the surface is

$$\bar{E} = \frac{N_1 E_1 + N_2 E_2}{N_t} \qquad (2.36)$$

---

*The sign depends upon orientation of the dipole.

The potential E_{max} at which the average energy is a maximum can be calculated from the condition,

$$\left(\frac{\partial \bar{E}}{\partial X}\right)_{N_t} = 0 \qquad (2.37)$$

Thus,

$$\left(\frac{\partial \bar{E}}{\partial X}\right)_{N_t} = \frac{1}{N_t}\left[N_1 \frac{\partial E_1}{\partial X} + E_1 \frac{\partial N_1}{\partial X} + N_2 \frac{\partial E_2}{\partial X} + E_2 \frac{\partial N_2}{\partial X}\right] \qquad (2.38)$$

Now,

$$\frac{\partial E_1}{\partial X} = -\frac{\partial E_2}{\partial X} \quad \text{and} \quad \frac{\partial N_1}{\partial X} = -\frac{\partial N_2}{\partial X} \qquad (2.39)$$

hence,

$$(N_1 - N_2)\frac{\partial E_1}{\partial X} + (E_1 - E_2)\frac{\partial N_1}{\partial X} = 0 \qquad (2.40)$$

Equation 2.40 can be satisfied only when,

$$N_1 = N_2 \text{ and } E_1 = E_2 \qquad (2.41)$$

Thus, if position 1 is stabilized by increasing the field, then $\partial E_1/\partial X < 0$ and $\partial N_1/\partial X > 0$, and vice versa. In the region where position 1 is more stable, $(E_1 - E_2) < 0$, and there will be more species oriented in this direction, i.e., $(N_1 - N_2) > 0$. Thus, the two products in equation 2.40 always have the same sign and they must therefore both be zero to fulfill equation 2.40. Since the two differential coefficients are not zero, the condition 2.41 must hold.

Substituting for E_1 and E_2, with $N_1 = N_2$, one has at the adsorption maximum,

$$E_1^c + \rho X = E_2^c - \rho X \tag{2.42}$$

$$\text{or} \quad -\Delta E^c = E_1^c - E_2^c = -2\rho X_{ads,max} \tag{2.43}$$

The field can be related to the charge per unit area q_m on the metal,

$$X_{ads,max} = \frac{4\pi\, q^m_{ads,max}}{\varepsilon} \tag{2.44}$$

hence,

$$\Delta E^c = -\frac{8\pi\rho q^m_{ads,max}}{\varepsilon} \tag{2.45}$$

where ε is the permittivity in the inner Helmholtz layer.

For most organic molecules, the functional group giving rise to the permanent dipole moment resides at a distance from the metal surface where the field (due to charge distribution in the diffuse layer) is small, and the permittivity is relatively high. Hence, the effect of potential and charge on the free energy of adsorption is small and the θ-V curve results. The existence of the π-bond interaction with the surface does not alter the situation substantially unless the energy of interaction is appreciably field dependent.

In the case of aqueous solutions, water is preferentially oriented with the oxygen towards the metal causing the charge density at the adsorption maximum to

be negative. Therefore, the potential of maximum adsorption E_m does not coincide with the p.z.c. It occurs at a negative potential on the rational scale,* where the total energy of interaction of water molecules with the surface is the same in both orientations. The field, and hence the charge, corresponding to E_m is characteristic of the metal and is related to the difference, ΔE^c in the field-independent parts of the interaction of water molecules with the surface in the two possible orientations. At the potential of maximum adsorption, equal numbers of water molecules are oriented in both directions and the dipole potential tends to zero.[16]

3. Electrosorption of hydrocarbons. Unsaturated hydrocarbons adsorb to a greater extent than saturated hydrocarbons on Pt. The nature of the electrolyte from which the adsorption is carried out affects the adsorption of saturated, but not unsaturated hydrocarbons.[3]

In the case of naphthalene and n-decylamine studied on four different metals (Pt, Cu, Fe, and Ni) the apparent standard free energy of adsorption was found to be essentially the same.[16] Naphthalene and n-decylamine are two very different compounds; the former replaces six H_2O molecules upon adsorption while the latter replaces only one. Gileadi[16] concluded that these two compounds

---

*Scale for which the zero point is equal to the p.z.c.

are physically adsorbed and that the observed values of ΔG^{o}_{ads} (-6 to -8 Kcal/mole) are characteristic of the replacement of a volume of water by an equal volume of organic ($-CH_2$) groups on the surface, independent of the nature of the remainder of the adsorbed molecule. However, ΔG^{o}_{ads} for ethylene[14] and benzene[15] on Pt is reported to be -2 to -4 and -6 to -8 Kcal/mole, respectively. Both are also considered to be chemisorbed; ethylene by replacing 4 and benzene by 9 water molecules. It therefore appears to this author that naphthalene and n-decylamine are also chemisorbed. The potential of maximum adsorption E_m on platinum for the four above mentioned hydrocarbons was found to be cathodic to the p.z.c.

The coverage-potential relationship for various concentrations of ethylene is shown in Figure 2. The symmetrical shapes of the curves indicate essentially no interaction of the organic molecule with the electric field in the double layer. This is consistent with the theory of the potential dependence of adsorption. A substantial dependence of E_m on θ would have indicated a contribution by the dipole potential of the organic molecule to the field in the compact double-layer.

In the absence of specific electrosorption data, ethylene adsorption can be considered to be typical of other double-bond hydrocarbons. Electrosorption

studies on Pt[13,16] with ethylene showed it to follow a simple Langmuir-type adsorption isotherm

$$\frac{\theta}{(1-\theta)^n} = K_c C \qquad (2.46)$$

with $K_c = (7.5 \pm 2.5) \times 10^8$ cm^3/gmole and n = 1. The value n = 1 indicates a one-point attachment of ethylene on the Pt surface. However, in an earlier isotherm developed from electroxidation studies, n was found to be four indicating four-point attachment. This difference was ascribed to a high mobility of the adsorbed ethylene on the Pt surface. The surface was assumed to be highly covered in the case of electroxidation so that lateral motion is hindered and behavior characteristic of localized adsorption is observed. The energetics of adsorption was shown to favor four-point attachment.

The value of the heat of adsorption ΔH^o_{ads} calculated from equilibrium constants at different temperatures was found to be 0.0 ± 4 Kcal/gmole. The value calculated from the following thermodynamic cycle is -2.0 Kcal/gmole and is considered to be in fair agreement with the above.

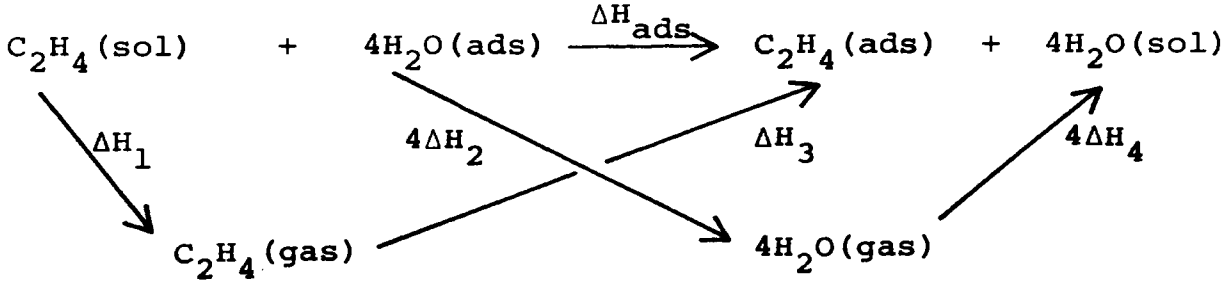

The values used in the above cycle were $\Delta H_1 = 4$, $\Delta H_2 = 22.6$, $\Delta H_3 = -58$, and $\Delta H_4 = -9.6$ Kcal/gmole.

C. Anodic Oxidation of Hydrocarbons

In this section, oxidation studies of hydrocarbons are reviewed under two headings: (1) oxidation on Pt, and (2) oxidation on Au.

1. Oxidation on Pt. Ethylene is one of the most frequently investigated hydrocarbons. Bockris, et. al.,[17] found that a number of unsaturated hydrocarbons with double-bonds follow a reaction sequence similar to that for ethylene. The sequence for acetylene was reported to be different.[18] The oxidation of saturated hydrocarbons proceeds by still other sequences.[19]

a. Alkenes. Bockris, et. al.,[3,17] studied the anodic oxidation of a number of double-bond hydrocarbons, including butadiene, on Pt. The observed kinetic parameters are listed in Table I. The proposed reaction mechanism which was the same for all is given below.

The primary product of oxidation in 1 N H_2SO_4 was found to be CO_2 for all the hydrocarbons. The reaction was represented as:

$$C_xH_y + 2x\ H_2O \rightarrow xCO_2 + (4x + y)\ H^+ + (4x + y)\ e \qquad (2.47)$$

Products other than CO_2 were reported to have been formed

TABLE I

KINETIC PARAMETERS FOR THE ANODIC OXIDATION OF HYDROCARBONS ON Pt AT 80°C*

Hydro-carbon	Tafel slope	$\partial \log i/\partial pH$	$\partial V/\partial pH$	$\partial \log i/\partial \log P_R$	E'_a	Q_{CO_2}
					Kcal/mole	Percent
C_2H_4	2(2.3RT/F)	0.45	-0.065	-0.20	21.0	100
C_3H_4	2(2.3RT/F)	0.46	-0.068	-0.17	19.7	93
C_3H_6	2(2.3RT/F)	0.46	-0.070	-0.14	23.7	97
C_4H_6	2(2.3RT/F)	0.39	-0.065	-0.13	20.1	60-90
C_4H_8-1	2(2.3RT/F)	0.47	-0.067	-0.16	22.3	70
C_4H_8-2	2(2.3RT/F)	0.47	-0.066	-0.20	23.0	85
C_6H_6	2(2.3RT/F)	0.40	-0.051	-0.11	22.9	60-90

*Ref. 3

for molecules larger than C_3H_6. The coulombic efficiencies Q_{CO_2} for butadiene and benzene were found to depend upon the current density.

The open circuit potentials were found to decrease by approximately 2.3RT/F per unit pH and were independent of temperature and partial pressure. Polarization curves were obtained at 80°C in 1 N H_2SO_4 by a steady-state potentiostatic method, and in other solutions of varying H_2SO_4 and NaOH concentrations by a galvanostatic method. The Tafel curves were linear over 2 to 3 decades of current with slopes of 2(2.3RT/F). Passivation of the anode in 1 N H_2SO_4 occurred at a potential of 0.85-0.9 volt for most of the hydrocarbon, but at a slightly higher value, 1.0 V, for allene and butadiene.

The pH dependence of current was $\partial \log i/\partial pH \simeq 0.5$. In the case of butadiene, polymerization occurred on the electrode surface in the pH range 4 to 10. Therefore, galvanostatic polarization was done very rapidly at pH's 3.3 and 6.5. Butadiene was also studied in solutions with pH's 0.55 and 12.5. The pH dependence for these four electrolytes was 0.39, which is slightly lower than that obtained for the other hydrocarbons. The pH dependence of potential in all cases was reported to be $\sim$-2.3RT/F.

In the linear Tafel region in 1 N H_2SO_4, the

hydrocarbon partial-pressure has an inverse effect on current. This effect is reported in Table I as a reaction order. The apparent energy of activation E'_a in 1 N H_2SO_4 was found to be approximately the same, 22 $\pm$ 2 Kcal/mole for all the hydrocarbons.

From these observations it was concluded that all seven of the hydrocarbons follow the same oxidation mechanism, (shown here for ethylene),

$$C_2H_2 \quad = \quad C_2H_2(ads) \tag{2.48}$$

$$H_2O \quad \overset{rds}{\rightarrow} \quad OH(ads) + H^+ + e \tag{2.49}$$

$$C_2H_2(ads) + OH(ads) \rightarrow C_2H_3^{\cdot}(ads) + H_2O \tag{2.50}$$

or

$$C_2H_4OH(ads)$$

$$C_2H_3^{\cdot}(ads),\ C_2H_4OH(ads) \overset{H_2O}{\rightarrow\cdots} \rightarrow 2\ CO_2 + 11\ H^+ + 11\ e \tag{2.51}$$

Thus, the rate equation for Langmuir-type adsorption can be written as:

$$i = k'(1-\theta_T)\exp(\alpha\nu F/RT) \tag{2.52}$$

where ν is the potential on the rational scale, $\nu = V - V_{pzc}$. The rate can also be expressed by the empirical equation:

$$i = kP_R^r C^{-0.5} \exp(\alpha VF/RT) \qquad (2.53)$$

The value of r depends upon the hydrocarbon species, $0.1 < r < 0.25$.

The V_{pzc} can be expressed as:

$$V_{pzc} = V_{pzc}^o + \frac{RT}{F} \ln(a_H+) \qquad (2.54)$$

Therefore, with the transfer coefficient α as 0.5, the theoretical rate equation becomes

$$i = k'(1-\theta_T)\exp[(V-V_{pzc}^o - \frac{RT}{F} \ln a_H+)F/2RT] \qquad (2.55)$$

$$= k''(1-\theta_T)(a_H+)^{-0.5}\exp(VF/2RT) \qquad (2.56)$$

Since, Langmuir's condition of adsorption is assumed

$$\frac{\theta_R}{(1-\theta_T)^n} = K_p P_R \qquad (2.57)$$

or

$$(1-\theta_T) = K_p^{-1/n} \theta_R^{1/n} P_R^{-1/n} \qquad (2.58)$$

If $\theta_R > 0.9$, over a limited pressure range we have,

$$(1-\theta_T) \simeq K'_p P_R^{-1/n} = K'_p P_R^r \quad (r = -1/n) \qquad (2.59)$$

Substituting $(1-\theta_T)$ in equation 2.56 gives the empirical rate equation. This equation yields parameters which are consistent with the observed values, $\partial \log i/\partial V = 2(2.3RT/F)$,

$\partial \log i/\partial P_E = -1/n$, $\partial \log i/\partial pH = 0.5$, and $\partial V/\partial pH = -2.3RT/F$.

From the observed order of reaction for butadiene, $r = -0.13$ (or $n = 8$), Bockris, et. al.,[3] concluded that C_4H_6 adsorbs with an 8-point attachment, also consistent with the molecular structure since it is twice as large as an ethylene molecule. The value of n for ethylene was approximately 4.

b. Acetylene. Johnson, Wroblowa, and Bockris[18] studied the oxidation of acetylene in aqueous solutions by steady-state galvanostatic and potentiostatic methods. The kinetic parameters obtained are listed here in Table II. The overall anodic oxidation reaction was found to be

$$C_2H_2 + 4\ H_2O \rightarrow 2\ CO_2 + 10\ H^+ + 10\ e \qquad (2.60)$$

throughout the pH range 0.3 to 12.6. The coulombic efficiency for conversion to CO_2 in the Tafel region was found to be virtually 100 percent.

The open circuit potential with acetylene was observed to vary linearly with pH of the electrolyte, $\partial V_{rest}/\partial pH = -2.3RT/F$. Linear Tafel curves over about one and one-half decades of current and with a slope of $\sim 2.3RT/F$ were obtained both in acidic and basic solutions. Below the linear sections (at low potentials), the current was independent of potential. Above the linear region, the slope increased rapidly and then passivation

TABLE II

KINETIC PARAMETERS FOR THE ANODIC OXIDATION OF ACETYLENE ON Pt AT 80°C *

Tafel slope	$\partial \log i/\partial pH$	$\partial V/\partial pH$	$\partial i/\partial P_A$	E'_a	Q_{CO_2}
				Kcal/mole	Percent
2.3RT/F	0.8	-0.050	< 0	21.5 (1 N H_2SO_4)	100
				26 (1 N KOH)	

*Ref. 18

occurred. The effects of pH on current and potential, determined from the Tafel curves, were $\partial \log i/\partial pH = 0.8$ and $\partial V/\partial pH = -50$ mv.

In both acidic and basic solutions, the steady state currents were observed to decrease with increase in C_2H_2 partial pressure, i.e., $\partial i/\partial P_A < 0$. Apparent activation energies calculated from Arrhenius plots were 21.5 $\pm$ 1 Kcal/mole in 1 N H_2SO_4 and 26 $\pm$ 1 Kcal/mole in 1 N NaOH. The shift in activation energy with potential was -25 Kcal/volt, roughly equal to the theoretical calculated value, $dE'_a/dV = -F = -23$ Kcal/volt.

The high coulombic efficiency was considered an indication of no branching in the reaction sequence leading to products other than CO_2 and H_2O (or protons). The negative pressure effect was interpreted as the involvement of a species other than or in addition to acetylene in the rate-determining reaction step. Under Langmuir conditions, the Tafel slope of 2.3RT/F indicates a rate determining chemical reaction following the first charge transfer step. For full coverage no pressure dependence would be expected. Thus, the following mechanism was suggested as consistent with the experimental observations:

$$C_2H_2 = C_2H_2(ads) \qquad (2.61)$$

$$H_2O = OH(ads) + H^+ + e \qquad (2.62)$$

$$C_2H_2(ads) + OH(ads) \xrightarrow{rds} \quad (2.63)$$

$$\xrightarrow{H_2O} \ldots \rightarrow 2\ CO_2 + 9\ H^+ + e \quad (2.64)$$

The discharge of water was proposed over the whole pH range since the experimental results indicated no change of parameters from acid to alkaline media and OH^- species would not be present in acidic solutions in sufficient quantity to support the observed currents. The rate of reaction for the proposed mechanism was written as,

$$i = k\ \theta_R \theta_{OH} \quad (2.65)$$

From quasi-equilibrium in steps prior to the rds (assuming Langmuir conditions),

$$\theta_{OH} = K(1-\theta_T)(a_{H^+})^{-1}\exp(VF/RT) \quad (2.66)$$

which gave

$$i = k'\ \theta_R(1-\theta_T)(a_{H^+})^{-1}\exp(VF/RT) \quad (2.67)$$

The coverage by OH radicals was assumed low in the Tafel region, and since the steps after the rate determining step are not in equilibrium as a result of the rapid removal of the product CO_2, the total coverage may be approximated as $\theta_T \approx \theta_R$. Thus, if $\theta_R > 0.5$, a negative pressure dependence is predicted. Langmuir isotherms from the theoretical rate equation $i = k''\theta_R(1-\theta_R)$ vs.

P_R were constructed to fit the observed i vs. P_R values. Fair agreement was obtained for four-point attachment (n = 4) and adsorption equilibrium constants $K_p = 10^4$ to 10^6 atm^{-1}. The other parameters compare favorably with $\partial \log i/\partial pH = 1$ and $\partial V/\partial pH = -2.3RT/F$.

2. Oxidation on Au. The oxidation reaction of a few hydrocarbons has been studied on Au. These kinetic parameters are presented in Table III and the proposed reaction mechanisms reviewed below.

a. Acetylene. Johnson, Reed, and James[20] studied the oxidation of acetylene at 80°C in aqueous solutions with pH ranging from 0.35 to 12.5. The most significant difference from that reported for Pt was the presence of a transition region (discontinuity) in the current-potential plots. The two linear regions, one below the transition region and the other above, had slopes of $\sim 2.3RT/\alpha F$. This behavior was observed in weakly acidic and basic solutions but not in strong acids. Another contrast was the absence of any pH effect in strong acid solutions, i.e., $\partial \log i/\partial pH = 0$. The partial pressure effect of acetylene on current was negative below and positive above the transition region. This was taken as an indication of different reaction mechanisms, one below (b.t.r.) and the other above the transition region (a.t.r.). The following reaction mechanisms satisfying the parameters were proposed.

TABLE III

KINETIC PARAMETERS FOR THE ANODIC OXIDATION OF C_2H_2 AND C_2H_4 ON Au AT 80°C *

Hydro-carbon	Electrolyte	Tafel slope	$\partial \log i/\partial pH$	$\partial i/\partial P_R$	E'_a	Q_{CO_2}
					Kcal/mole	Percent
C_2H_2	strong acid	2(2.3RT/F)	0	<0	19.5	60±5
	base & weak acid					
	b.t.r.**	2(2.3RT/F)	1	<0	19.5	
	a.t.r.***	2(2.3RT/F)	1	<0	13	80±10
C_2H_4	strong acid	2.3RT/F	0	>0	18.5	∿0
	base & weak acid					
	b.t.r.**	2(2.3RT/F)	1	>0		
	a.t.r.***	2.3RT/F	1	>0	26	

*Ref. 20 and 21.
**Below the transition region.
***Above the transition region.

Below the transition region:

$$C_2H_2 = C_2H_2(ads) \quad (2.68)$$

$$H_2O \rightarrow OH(ads) + H^+ + e \quad (2.69)$$

$$OH^- \rightarrow OH(ads) + e \quad (2.70)$$

(2.69) and (2.70): r.d.s.

$$C_2H_2(ads) + OH(ads) \rightarrow \overset{H_2O}{\cdots} \rightarrow CO_2 + H^+ + e, \text{ etc.} \quad (2.71)$$

Above the transition region:

$$C_2H_2 = C_2H_2(ads) \quad (2.72)$$

$$C_2H_2(ads) + H_2O \rightarrow C_2H_2OH(ads) + H^+ + e \quad (2.73)$$

$$C_2H_2(ads) + OH^- \rightarrow C_2H_2OH(ads) + e \quad (2.74)$$

(2.73) and (2.74): r.d.s.

$$C_2H_2OH(ads) \rightarrow \overset{H_2O}{\cdots} \rightarrow CO_2 + H^+ + e, \text{ etc.} \quad (2.75)$$

The discharge of H_2O and/or OH^- was necessary to explain the observed pH effect.

The oxidation rate equations were given as,

$$i_{b.t.r.} = zF(k_b a_{H_2O} + k_b' a_{OH^-})(1-\theta_T)\exp(\alpha VF/RT) \quad (2.76)$$

$$i_{a.t.r.} = zF(k_a a_{H_2O} + k_a' a_{OH^-})\theta_R \exp(\alpha VF/RT) \quad (2.77)$$

In equation 2.76, θ_T could be approximated by θ_R neglecting the adsorption of products. Adsorption isotherms obtained from i vs. P_R relations gave different n and K_p values in acid and base. In acid, n = 4 and

$K_p = 10^4$ atm^{-1} were obtained, while in base, n = 8 and $K_p = 2.5$ gave the best fit, but n = 4 and $K_p = 3.5$ were found to fit within a reasonable degree of accuracy.

b. Ethylene. Ethylene oxidation on Au and other noble metals has been studied by several investigators.[21-23] In a recent paper, Johnson, Lai and James[21] presented an oxidation mechanism which is discussed here.

The oxidation was studied at 80°C in aqueous electrolytes, pH 0.35 to 12.7. A transition in current-potential relationships (as with acetylene) was observed in weak acidic and basic solutions, but none in strong acids. Unlike acetylene, the Tafel slope changed from $\sim 2.3RT/\alpha F$ below to $\sim 2.3RT/F$ above the transition. The slope in strong acid was $\sim 2.3RT/F$. The effect of pH on current was approximately zero in strong acid and unity in basic solutions. A positive partial pressure effect was observed, i.e., a reduction in the partial pressure of C_2H_4 lowered the current.

Acetaldehyde was the only compound detected in product analyses. No CO_2 was produced in acidic solutions and determinations could not be made in basic solutions because of the very low currents obtainable.

In strong acidic solutions and above the transition region in other solutions the reaction mechanism

proposed was as follows:

$$C_2H_4 \quad = \quad C_2H_4(ads) \tag{2.78}$$

$$C_2H_4(ads) \quad = \quad C_2H_4^+(ads) + e \tag{2.79}$$

$$C_2H_4^+(ads) + H_2O \xrightarrow{rds} C_2H_4OH(ads) + H^+ \tag{2.80}$$

$$C_2H_4OH(ads) \rightarrow CH_3CHO + H^+ + e \tag{2.81}$$

or $$C_2H_4OH(ads) \rightarrow \overset{H_2O}{\cdots} \rightarrow CH_3CHO,\ CO_2,\ H^+,\ e \tag{2.82}$$

The corresponding rate equation is,

$$i \quad = \quad zFk\ a_{H_2O}\theta_R exp(VF/RT) \tag{2.83}$$

In weak acidic and basic solutions and below the transition region the mechanism was:

$$C_2H_4 \quad = \quad C_2H_4(ads) \tag{2.78}$$

$$\left.\begin{aligned} C_2H_4(ads) + H_2O &\rightarrow C_2H_4OH(ads) + H^+ + e \qquad (2.84)\\ C_2H_4(ads) + OH^- &\rightarrow C_2H_4OH(ads) + e \qquad (2.85)\end{aligned}\right\} \text{r.d.s.}$$

$$C_2H_4OH(ads) \rightarrow \overset{H_2O}{\cdots} \rightarrow CH_3CHO,\ CO_2,\ H^+,\ e \tag{2.82}$$

The rate equation for this sequence is

$$i \quad = \quad zF(k'a_{H_2O} + k''a_{OH^-})\theta_R exp(\alpha VF/RT) \tag{2.86}$$

Langmuir-type isotherms were obtained by correlating the i vs. P_R data. The best correlations in acid were obtained with n = 4 and K_p = 1, and in base with n = 8 and K_p = 1. The increased value of n for basic

electrolytes was similar to that found with C_2H_2. The increased value probably reflects an influence of the adsorbed organic species on water (or OH^-) discharge).

III. EXPERIMENTAL

The object of this investigation was to study the oxidation (anodic) reaction of 1,3-butadiene on platinum and gold electrodes. The following experiments were performed with each metal in acidic and basic electrolytes to elucidate a reaction mechanism,

1. current-potential studies
2. current-partial pressure studies
3. current-temperature studies
4. coulombic efficiency studies

Details of these experiments, including apparatus, procedure, and the results are presented in this chapter.

A. Materials

There were two sources for the butadiene used in this investigation. The initial experiments were done with an instrument grade gas obtained from the Matheson Co. Later, this grade was no longer available, and the remainder of the work was done with special purity gas supplied by the Phillips Petroleum Co. A description of the gas from both sources is given in Appendix B. Hereafter, that obtained from Matheson will be designated as Grade-A and that from Phillips as Grade B.

Acidic and basic electrolytes ranging in pH from 0.35 to 12.5 were prepared by mixing the requisite amounts of H_2SO_4, K_2SO_4, K_2CO_3, and KOH in conductivity

water. The normalities of the solutions were kept constant at unity to insure good conductance.

Complete lists of the materials and reagents are contained in Appendix B.

B. Electrodes

The working electrodes (anodes) were either platinized-Pt or Au. The auxiliary electrode (cathode) was platinized-Pt. Two reference electrodes were used, Hg,Hg_2Cl_2;1 N KCl for alkaline solutions, and Hg,Hg_2SO_4;1 N H_2SO_4 for acidic solutions.

1. Platinum anode. The platinized-Pt anode was made from a 2.7 cm x 2.7 cm piece of 52-mesh Pt gauze. The gauze was folded onto a 2 cm x 2 cm square Pt-wire frame. A Pt wire attached to the frame and sealed in a 5 mm pyrex glass tube was used as a lead to the outside of the cell. The electrode was cleaned in aqua regia and platinized in a platinic chloride solution containing a trace of lead acetate. The electrode was not re-platinized during the remainder of the study.

2. Gold anode. The Au anode was a 5 cm x 3 cm rectangular piece of Au foil (0.005 inch thick). A 26-gauge Au wire looped through a small hole at the top of the foil and sealed in a 5 mm pyrex glass tube served as a lead wire. The electrode was etched in aqua regia at the beginning of the study and subsequently only cleaned and activated.

3. Cathode. The cathode was a platinized-Pt electrode similar to the anode described above. Its geometric area was 3 cm x 3 cm.

C. Current-Potential Studies

1. Apparatus. A diagram of the assembled system is shown in Figure 3. The major electronic components are listed in Appendix C.

A front view of the H-type pyrex glass electrolytic cell used is shown in Figure 4. The anodic and cathodic compartments each had a 500 ml capacity and were connected through a ground-glass water-sealed stopcock. Each had a gas inlet near the bottom. The anodic compartment was provided with a Luggin capillary which was connected to the reference electrode through another ground-glass water-sealed stopcock outside the cell. A salt bridge was used with the calomel reference electrode to prevent contamination of the cell by chloride ions. The reference electrode was always at room temperature. The removable tops of the anodic and cathodic compartments had three and two ports, respectively. In each case, one port provided a water sealed outlet for the gas via an air condenser tube. The second port served as the electrode holder and the lead wire outlet. The third port of the anodic compartment held a thermometer which served as the measuring element for the temperature controller. The anodic compartment was heated with a

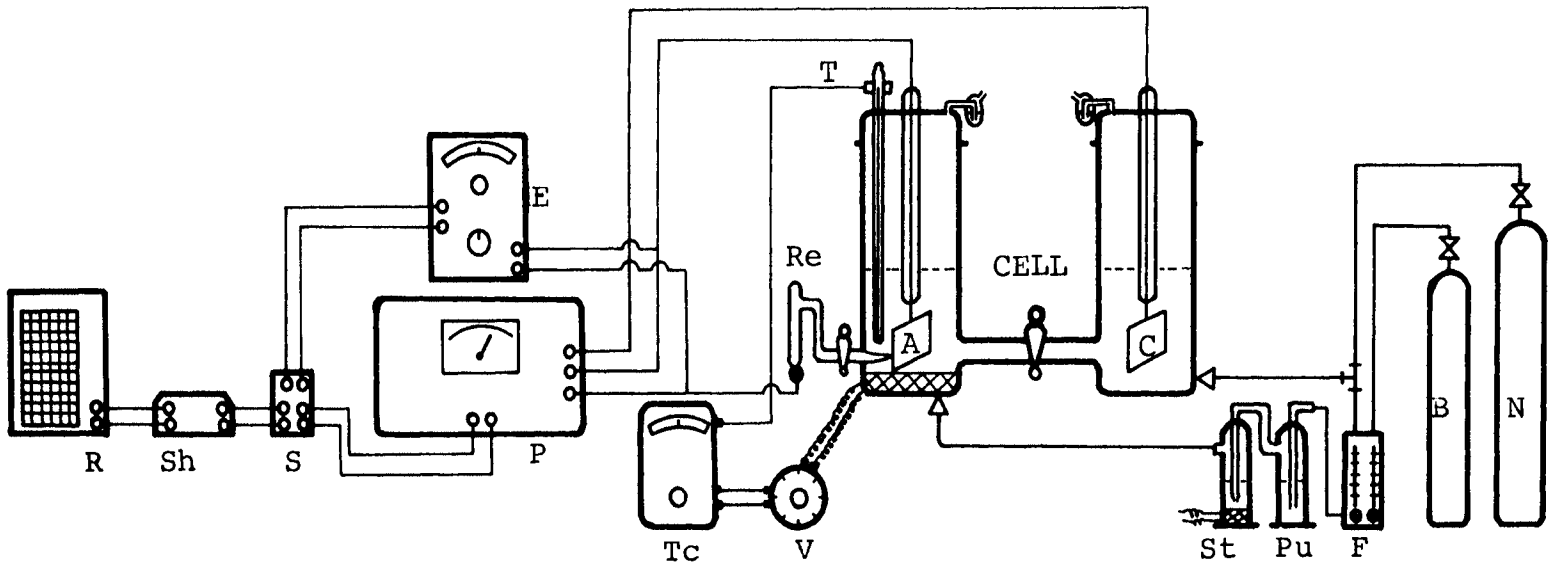

N.	Nitrogen	A.	Anode	P.	Potentiostat
B.	Butadiene	C.	Cathode	S.	DPDT Switch
F.	Flow Proportioner	Re.	Reference Electrode	Sh.	Shunt
Pu.	Purifier	T.	Thermometer	R.	Recorder
St.	Saturator	Tc.	Temperature Controller		
V.	Variac	E.	Electrometer		

Figure 3. Diagram of the apparatus used for potentiostatic studies in the anodic oxidation of butadiene.

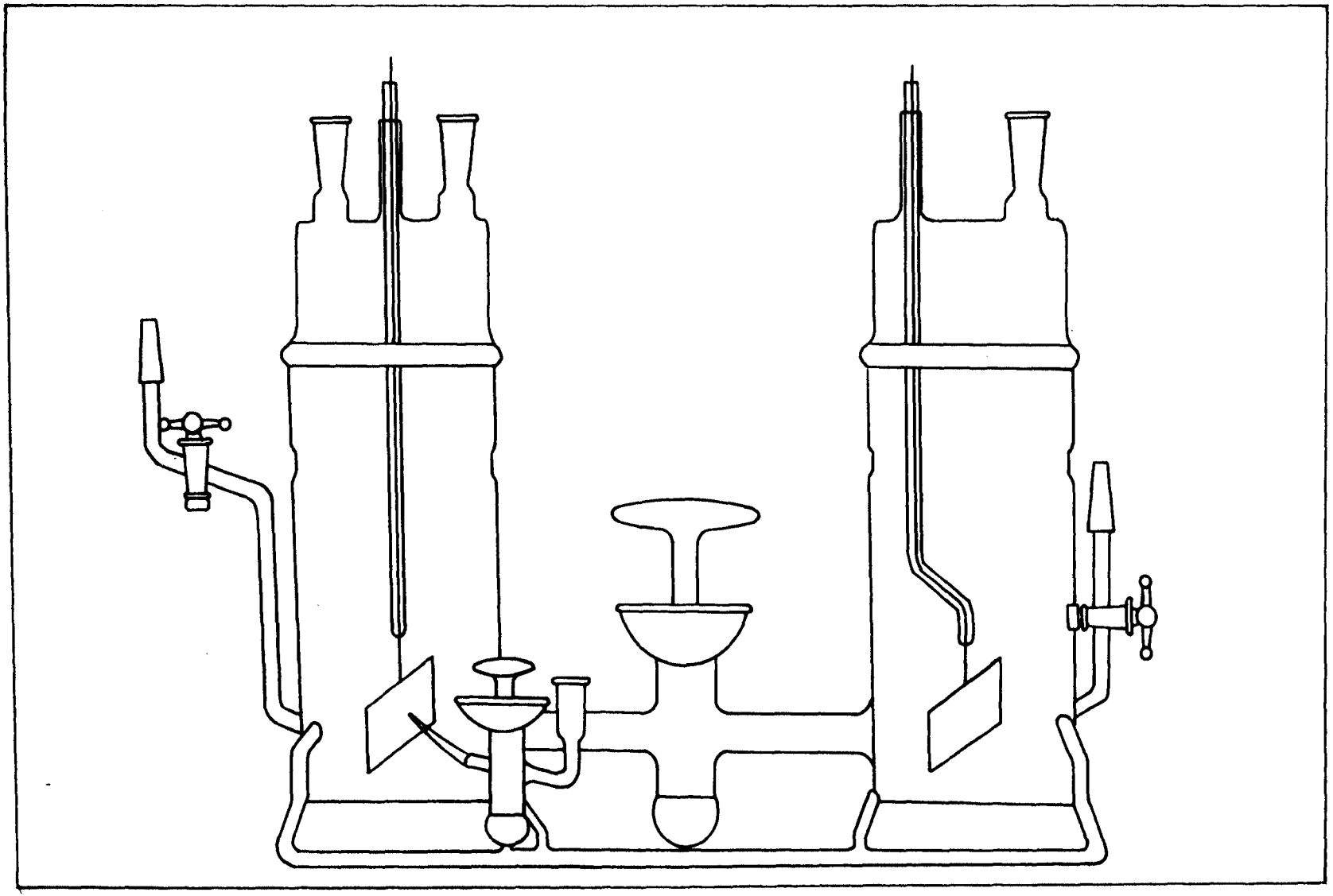

Figure 4. Electrolytic cell.

heating tape which was wrapped around it. The temperature was maintained within $\pm$ 0.5°C of the set point. The heating and cooling cycles were made approximately the same by adjusting the voltage applied to the tape with a variac.

The gas flow (N_2 and/or C_4H_6) through the anodic compartment was controlled with a dual-flow gas proportioner. The flow rate was kept constant at 30 cm^3/min. The gas passed through a scrubber and a washer-saturator before entering into the cell. The scrubber contained 1 N KOH which served to remove an additive, tertiary butyl catechol, from the butadiene. The washer-saturator contained the same solution as the cell, and was maintained at approximately the cell temperature. It removed any KOH solution droplets that were entrained in the gas, and simultaneously saturated it with water vapor. The saturation helped in preventing polymerization of butadiene in the cell inlet and in replenishing the water lost from the cell in the exit gases. Nitrogen to the cathode compartment was supplied directly from a separate cylinder.

Tygon tubing was initially used to connect the electrolysis cell and the gas cylinders. Later it was replaced with Teflon tubing in the butadiene line to check the possiblity of contamination of the butadiene from the tygon tubing. Several of the principle

experiments were repeated and showed no difference from the previous results.

A constant potential difference between the working and reference electrodes was maintained with a potentiostat and monitored with an electrometer. The current output from the potentiostat was recorded.

2. Procedure. Prior to beginning the experimental work, all the glass apparatus was thoroughly cleaned with sodium hydroxide and chromic acid solutions and rinsed with distilled water followed by conductivity water. In subsequent work, only conductivity water was used for washing and rinsing. A standard procedure was developed and adhered to throughout the investigation to assist in obtaining reproducible data. It is described here in three sections: (a) anode activation, (b) rest potentials, and (c) current-potential measurements.

a. Anode activation. The manner of anode activation can have an effect on the rest potentials and subsequent data. Because of this, the anode was activated before each experiment in a consistent manner throughout the study as follows: The anode (working electrode) was placed in a beaker containing 1 N H_2SO_4 along with a counter electrode of the same metal. (In the case of Au, before putting the electrodes into the activation solution, both were boiled in 1 N KOH for ten minutes to remove any polymer that may have been

formed on their surface during prior use.) The electrodes were connected to a d.c. power supply through a double-pole, double-throw switch which served to reverse their polarity. Four amperes of current were used to activate the Pt and two amperes to activate the Au electrodes. Initially, the working electrode was the cathode (H_2 evolution) and the counter electrode was the anode (O_2 evolution). Upon passage of the current, their polarity was reversed every 10 seconds for 2 minutes. At the end of this time, the working electrode was left cathodic (H_2 evolution) for another 2 minutes, then the current was switched off. The working electrode was immediately removed, rinsed with conductivity water, and quickly transferred to the anodic compartment of the cell which had been charged with approximately 500 ml of electrolyte. The auxiliary Pt electrode (cathode) was placed in the cathodic compartment of the cell. The positions of the electrodes were adjusted so that the anode and the cathode faced each other, and the lower edge of the anode touched a protruding tip of the Luggin capillary.

b. Rest potentials. When the electrodes were in position, nitrogen flow to the anodic and cathodic compartments was begun and heating and potential measurements commenced. The potential was recorded from the electrometer output. The N_2 purge of the anolyte was

stopped after one and one-half hours and butadiene flow started. In cases where a Tafel study was desired at a butadiene pressure of less than one atmosphere, N_2 and C_4H_6 were proportioned with the dual-flow proportioner to give the required partial pressure of C_4H_6. After a few minutes of butadiene flow, the anode potential normally shifted to a more active (cathodic) value and the steady-state (rest or open-circuit) potential was obtained in another 60 to 90 minutes.

c. Current-potential measurements. After the rest potential had been obtained, the anode potential was increased approximately 0.1 to 0.2 volts above the rest potential and held constant with the potentiostat. The current was recorded and after it had become steady, the potential was again increased by 0.02 to 0.05 volts. The steady state was arbitrarily defined as the value which remained constant for at least 10 minutes and was normally reached within 30 to 45 minutes after polarization was begun at a given potential. This procedure was continued until the current reached a limiting value.

3. Data and results. A considerable amount of the previous work on the anodic oxidation of hydrocarbons in aqueous solutions has been done at 80°C.[3] For the reasons of consistency in reporting data and for comparison purposes, it was attempted to study the

butadiene oxidation at 80°C. However, the butadiene was found to polymerize in the inlet nozzle and ultimately stop the flow. It was also feared that some of the polymer might reach the electrode and interfere with the oxidation reaction. Lowering the cell temperature to 70°C eliminated the problem, hence the study was made at this temperature.

As mentioned earlier, two qualities of butadiene were used. The experimental procedure with each was the same except that the Grade-A gas was not scrubbed in KOH solution.* The rest potentials and current-potential data for the two types were different and are reported separately in Appendix D.

a. Grade-A butadiene. The oxidation of Grade-A butadiene was studied only on Pt. The average value of the rest potentials is shown in Table IV. Polarization studies at 1 atm C_4H_6 pressure were made at 80°C in electrolyte with 0.35 pH, and at 70°C in electrolytes with pH's 0.35, 6.0, 10.8, and 12.5. The resulting curves shown in Figure 5 have linear sections with slopes of 135-140 mv.

From Figure 5, it is observed that at a fixed potential, current values are lower at lower pH values. The effect of pH on current density at a fixed potential

*At this time it was not known that the catechol could be removed by scrubbing the gas in KOH solution.

TABLE IV

REST POTENTIALS FOR GRADE-A BUTADIENE ON Pt IN AQUEOUS SOLUTIONS (P_R = 1 atm)

Temperature	Rest Potential			
°C	volts (SHE)			
	1 N H_2SO_4 (pH=0.35)	1 N K_2SO_4 (pH=6.0)	1 N K_2CO_3 (pH=10.8)	1 N KOH (pH=12.5)
80	+0.21	-	-	-
70	+0.21	-0.12	-0.44	-0.52

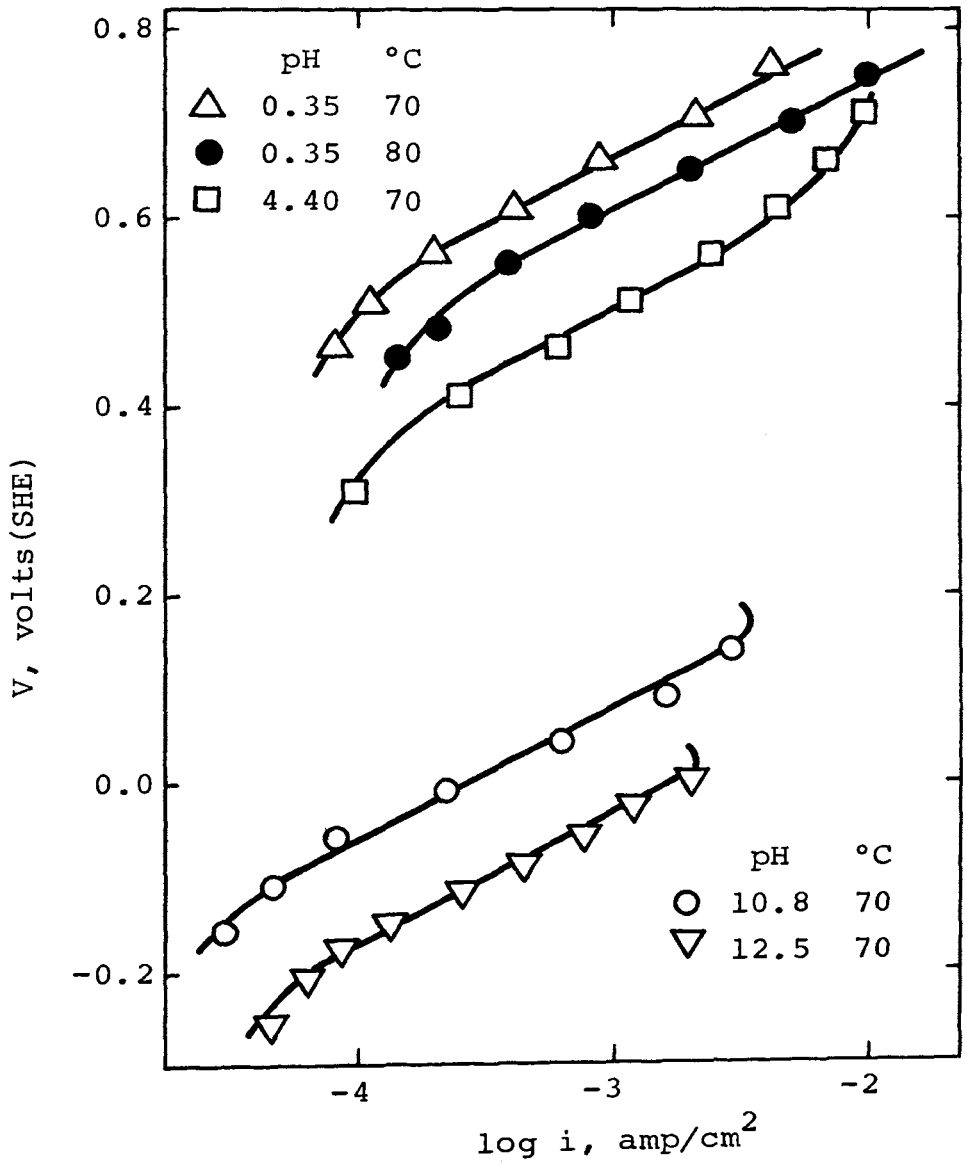

Figure 5. Polarization curves for the anodic oxidation of Grade-A butadiene on Pt (P_R = 1 atm).

is shown in Figure 6, and that on potential at fixed current density is shown in Figure 7. Values of the parameters $\partial \log i/\partial pH$ and $\partial V/\partial pH$ obtained from the above mentioned plots were $\sim$0.5 and -70 mv, respectively.

b. Grade-B butadiene. The average values of the rest potentials of Grade-B butadiene, P_R = 1 atm, on Pt and Au electrodes are shown in Table V. Rest potentials at reduced C_4H_6 partial pressures were practically the same as those at 1 atm. The polarization relationships are shown in Figures 8 to 12. Throughout the remainder of this chapter, all the results and discussion pertain to Grade-B butadiene unless mentioned otherwise.

(1) Platinum. The reaction on Pt was studied at 1 atm C_4H_6 pressure in electrolytes with pH's 0.35, 1.3, 2.6, 9.9, 10.8, and 12.5. As seen from Figure 8, the polarization curves appear to have two linear sections, $\sim$140 and $\sim$70 mv slopes, before the limitng current values are reached and passivation starts. The change in slope or transition occurs at approximately 2.0×10^{-4} amp/cm^2 current density. The lower (low i-V) portions of the curves, i.e., below the transition region (b.t.r.) have 140 mv slopes, and the upper (high i-V) portions, i.e., above the transition region (a.t.r.) have 70 mv slopes.

Experiments with reduced C_4H_6 pressure (P_B = 0.10 and 0.01 atm) were also made in electrolytes with pH's

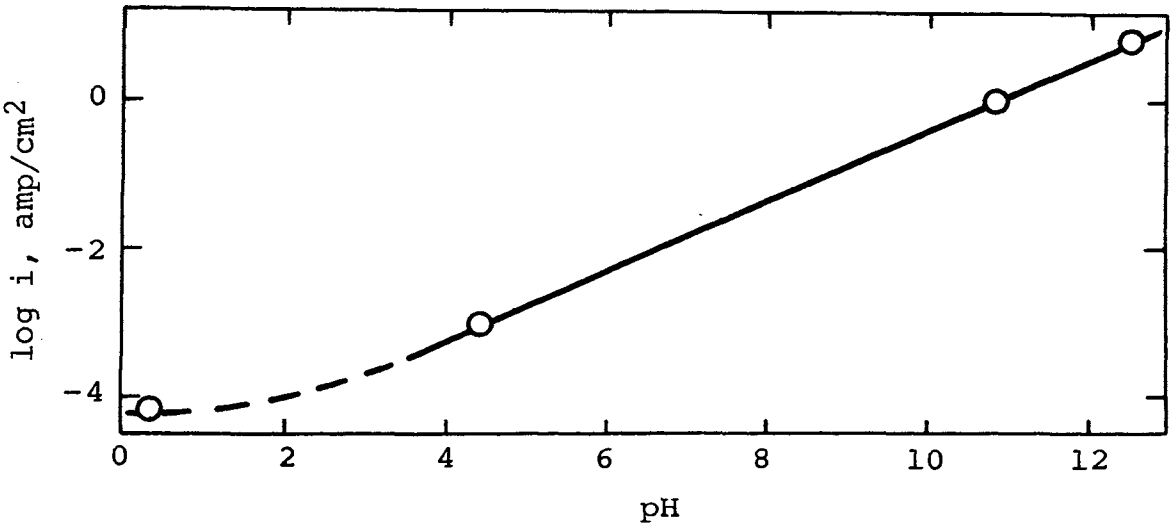

Figure 6. log i-pH relation at 0.5 volts(SHE) for the anodic oxidation of Grade-A butadiene on Pt at 70°C (P_R = 1 atm).

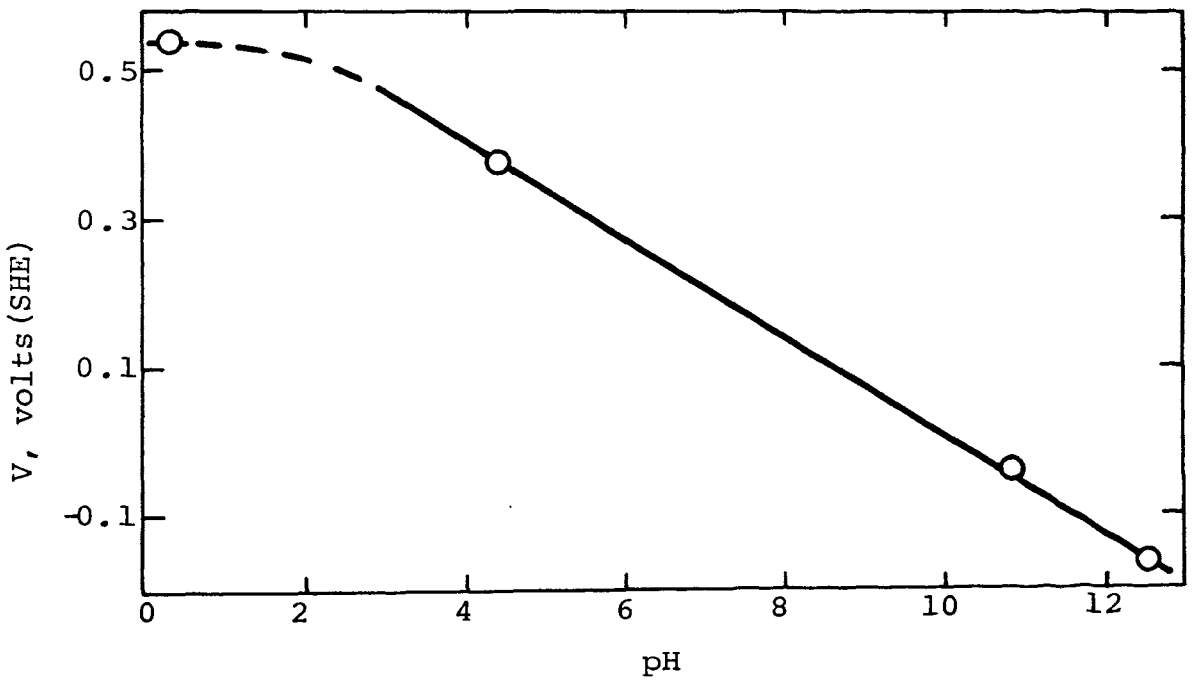

Figure 7. V-pH relation at 1.37×10^{-4} amp/cm^2 current density for the anodic oxidation of Grade-A butadiene on Pt at 70°C (P_R = 1 atm).

TABLE V

REST POTENTIALS FOR GRADE-B BUTADIENE ON Pt and Au

IN AQUEOUS SOLUTIONS AT 70°C

(P_R = 1 atm)

Electrode	Rest Potentials, volts (SHE)						
	pH						
	0.35	1.3	2.6	9.9	10.8	11.6	12.5
Pt	+0.27	+0.21	+0.16	-0.21	-0.30		-0.32
Au	+0.35			+0.03	-0.01	-0.045	-0.075

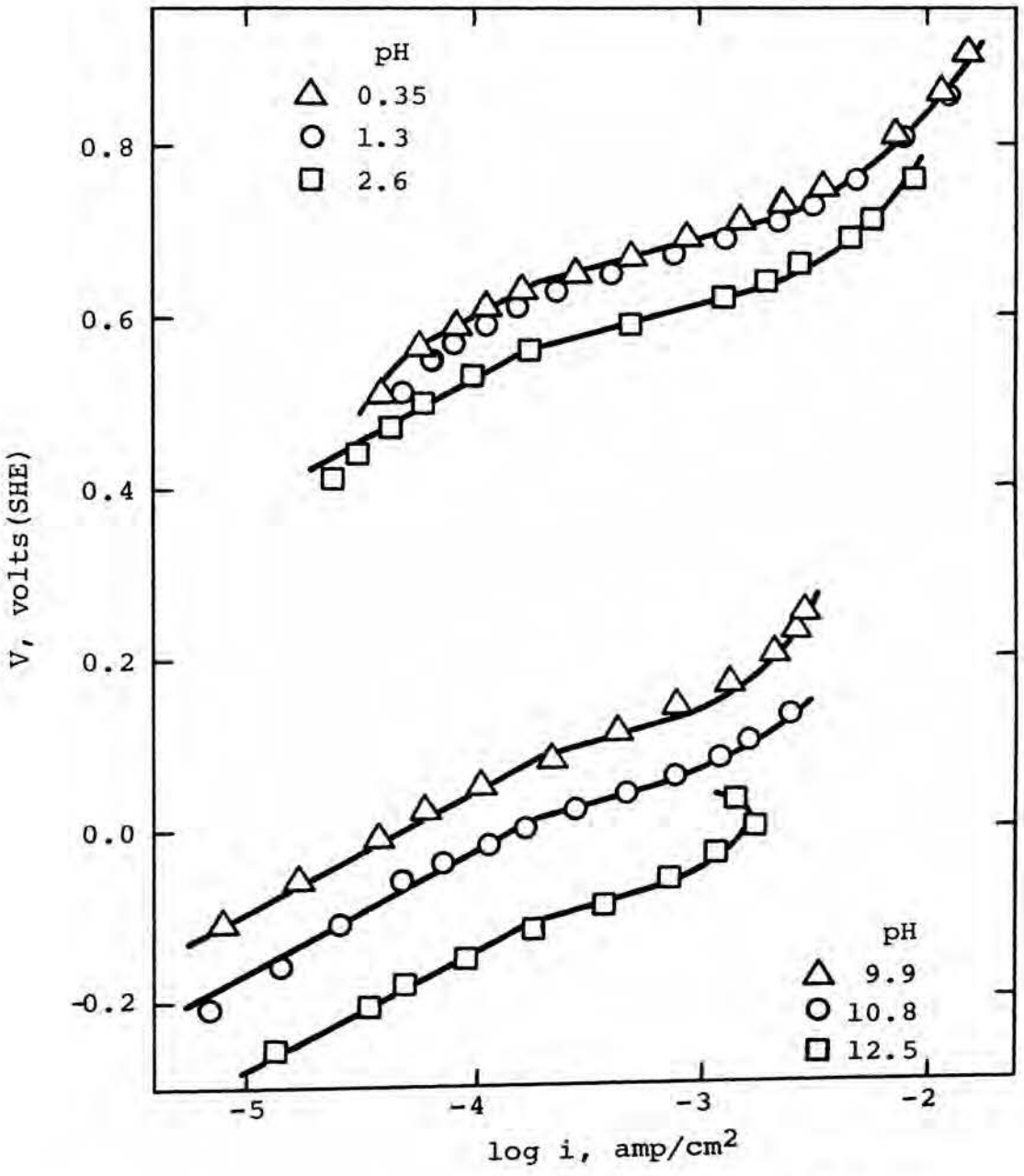

Figure 8. Polarization curves for the anodic oxidation of Grade-B butadiene on Pt at 70°C (P_R = 1 atm).

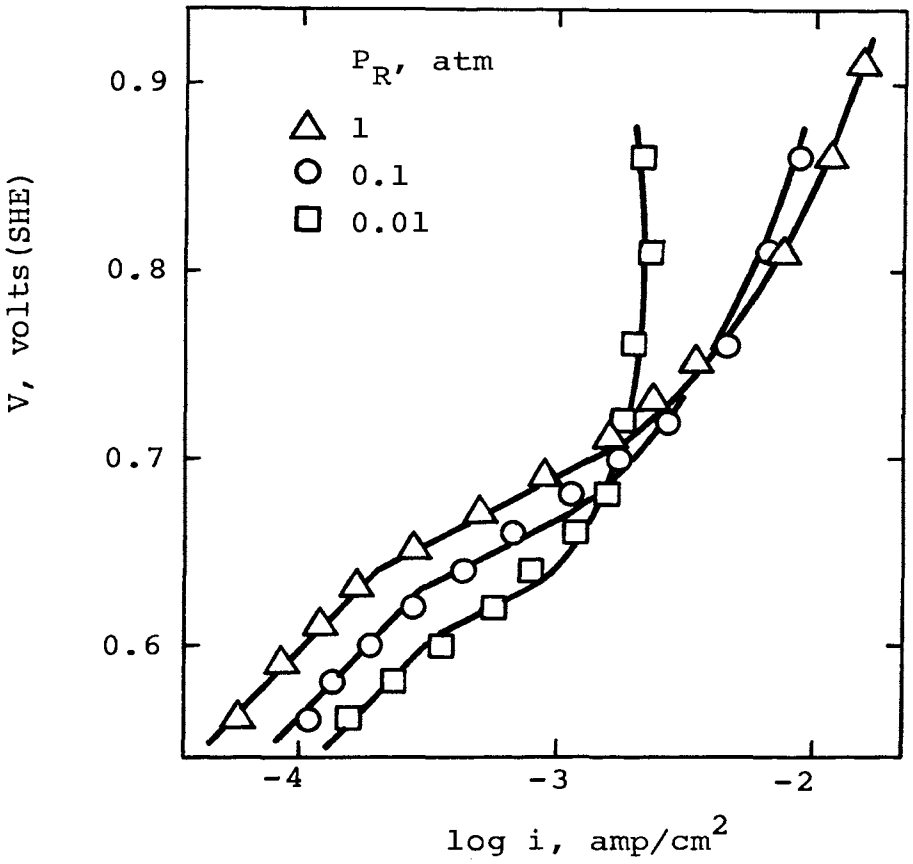

Figure 9. Polarization curves for the anodic oxidation of Grade-B butadiene on Pt at 70°C in 1 N H_2SO_4.

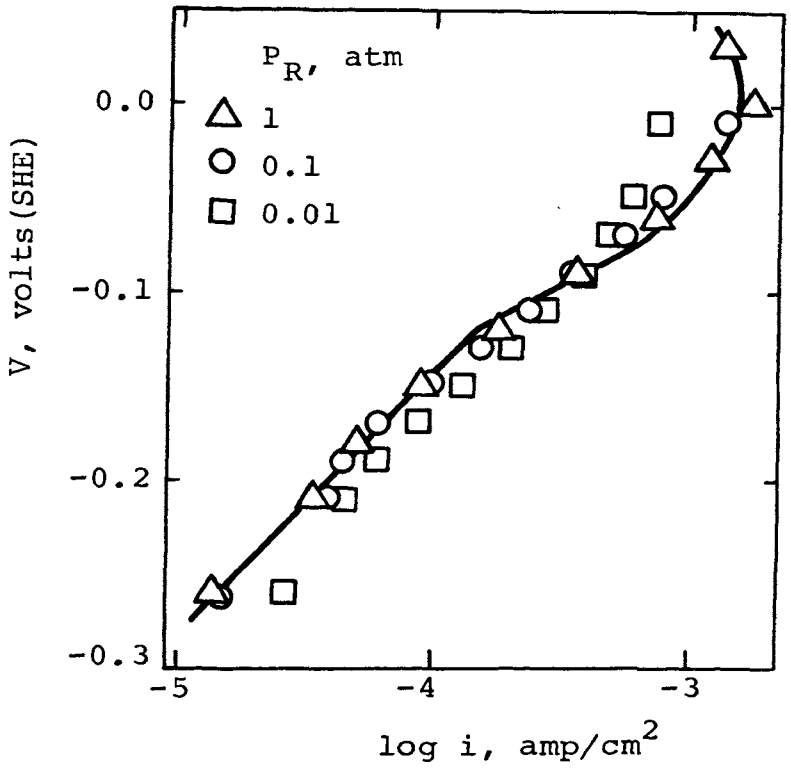

Figure 10. Polarization curves for the anodic oxidation of Grade-B butadiene on Pt at 70°C in 1 KOH.

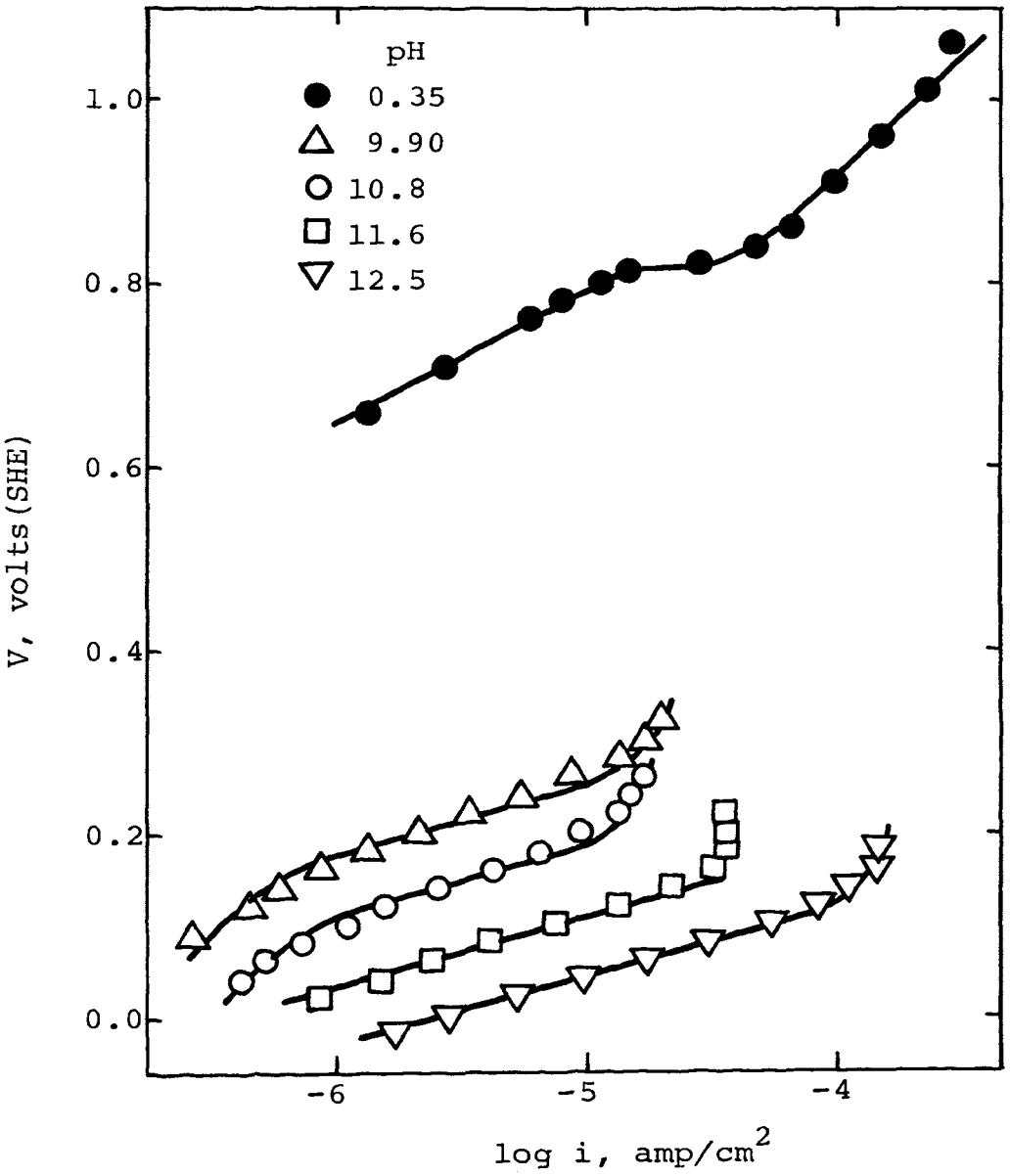

Figure 11. Polarization curves for the anodic oxidation of Grade-B butadiene on Au at 70°C (P_R = 1 atm).

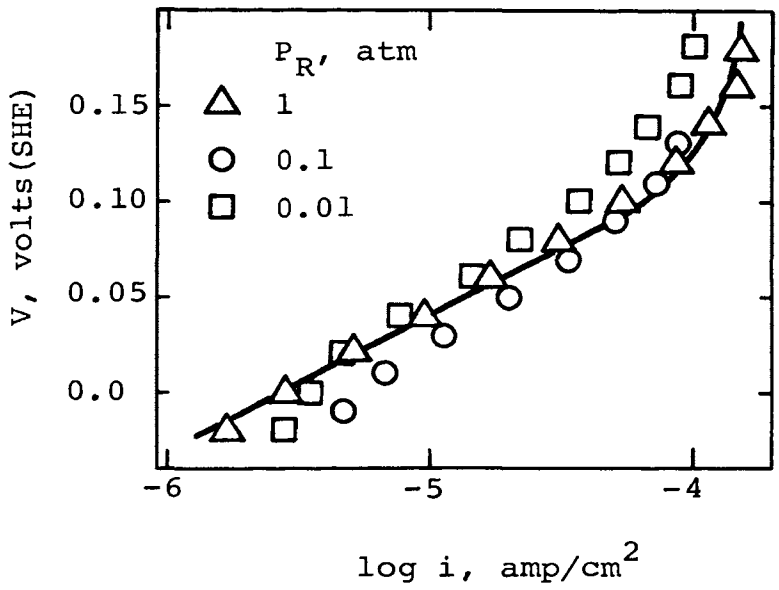

Figure 12. Polarization curves for the anodic oxidation of Grade-B butadiene on Au at 70°C in 1 N KOH.

0.35 and 12.5. The reduction in butadiene pressure considerably shortened the linear regions of the curves, both b.t.r. and a.t.r., as seen in Figures 9 and 10. The curves at reduced pressures fall below that of 1 atm, thus showing a negative pressure effect.

The effect of electrolyte pH on current $\partial \log i/\partial pH$ was calculated separately for both linear Tafel regions, i.e., b.t.r. ($\sim$140 mv slope) and a.t.r. ($\sim$70 mv slope). The potential chosen for the calculations was the same in both cases, 0.5 volt(SHE). Current values corresponding to a pH and a Tafel portion were obtained by extrapolating that portion of the curve to 0.5 V. The current values for the other Tafel portion were obtained similarly. These values of log i are plotted versus corresponding pH in Figure 13. For the case b.t.r., log i changed by one-half decade per unit pH in the pH range $\sim$2 to 13, while the change was practically zero in the pH range 0 to $\sim$2. A different relation was observed for case a.t.r. Here log i increased a decade per unit pH in the range $\sim$2 to 13, and as in the previous case, the change was negligibly small or zero in the pH range 0 to $\sim$2.

The relationship between potential and electrolyte pH is shown in Figure 14 for both b.t.r. and a.t.r. The plot was constructed in a manner similar to that described in the above paragraph in that the Tafel portions

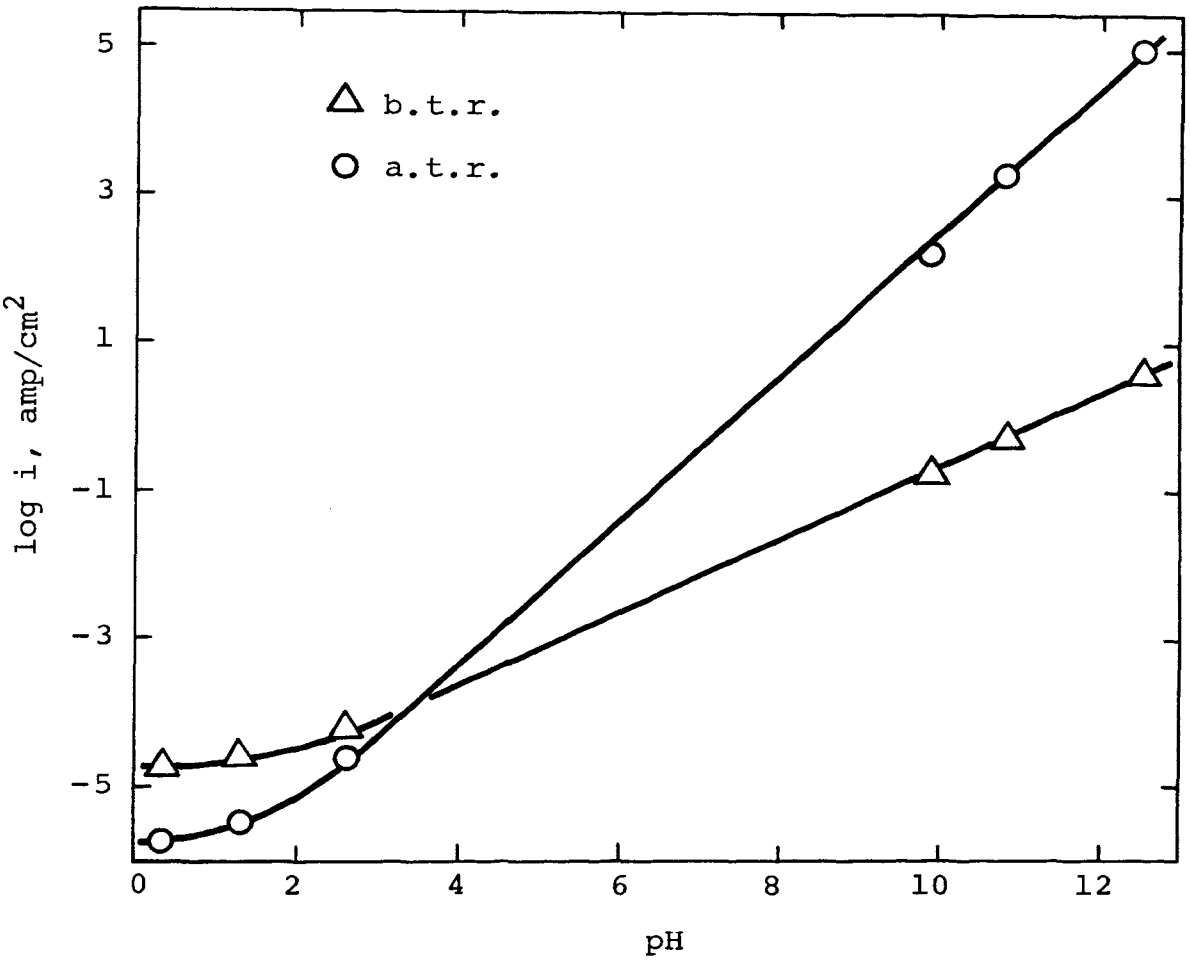

Figure 13. log i-pH relation at 0.5 volts(SHE) for the anodic oxidation of Grade-B butadiene on Pt at 70°C (P_R = 1 atm).

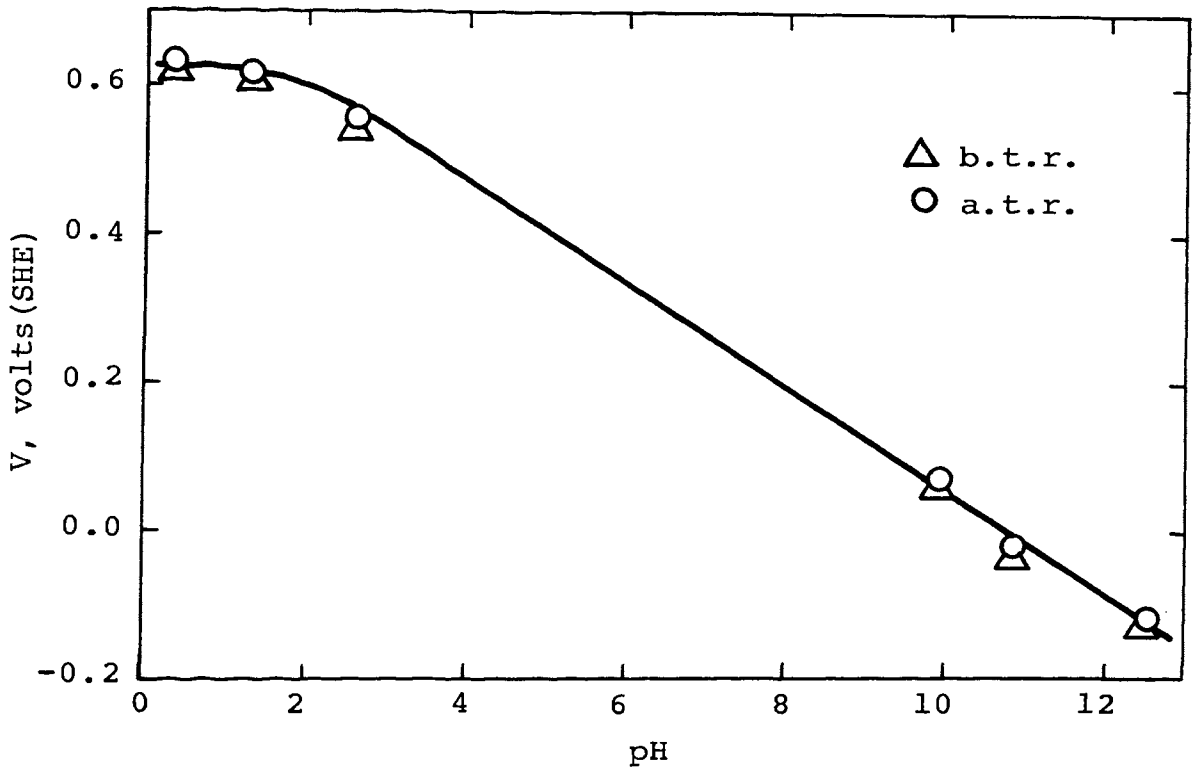

Figure 14. V-pH relation at 1.37×10^{-4} amp/cm^2 current density for the anodic oxidation of Grade-B butadiene on Pt at 70°C (P_R = 1 atm).

with their respective slopes were extrapolated to an arbitrarily fixed current density of 1.37×10^{-4} amp/cm^2 to obtain the potential values. The relation was same for the two cases. The potential decreased by ~ 70 mv per unit pH in the range ~ 2 to 13. The potential remained reasonably constant in pH range 0 to ~ 2.

(2) Gold. The reaction on the Au electrode at 1 atm C_4H_6 pressure was studied at pH's 0.35, 9.9, 10.8, 11.6, and 12.5. In acid solution, polymerization products were seen on the electrode surface after a certain period. At the end of an experiment, the Au foil appeared to be covered with a polymer film. No such film was noticed in the basic solutions, nor was there any discoloration of the anolyte. The Tafel slopes (Figure 11) in basic solutions are approximately 70 mv. Studies at 0.10 and 0.01 atm C_4H_6 pressure in pH 12.5 along with the corresponding study at 1 atm are shown in Figure 12. The linear portions of the curves at lower pressures are shorter than at 1 atm, but the slopes, although not as clearly defined as at 1 atm, can be seen to be approximately the same. The Tafel curve at $P_R = 0.1$ atm lies below while the curve at 0.01 atm lies above the plot for $P_R = 1$ atm. Thus, the pressure effect changes from positive to negative in going from $P_R = 0.01$ to 1 atm. Figures 15 and 16 show the effect of pH on log i and V, which were 1 and -70 mv, respectively.

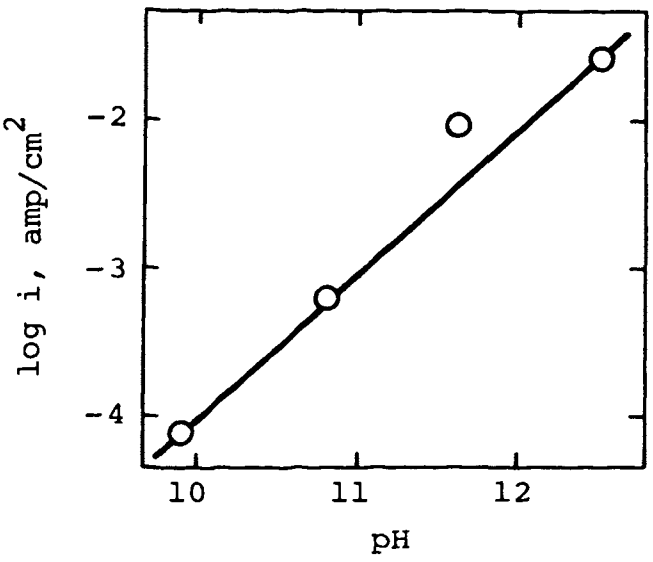

Figure 15. log i-pH relation at 0.1 volts(SHE) for the anodic oxidation of Grade-B butadiene on Au at 70°C (P_R = 1 atm).

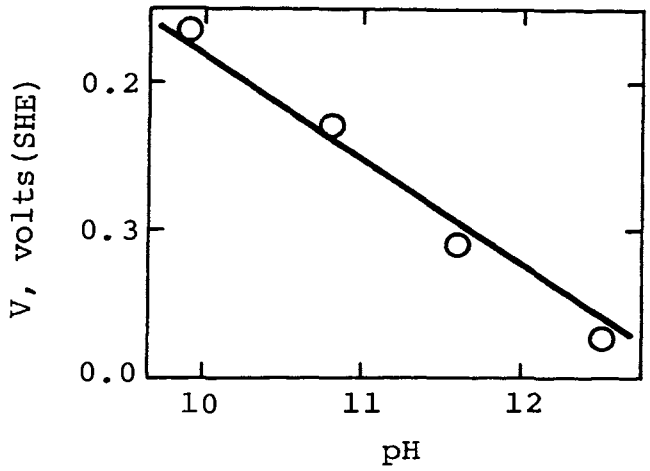

Figure 16. V-pH relation at 6.67 x 10^{-6} amp/cm^2 current density for the anodic oxidation of Grade-B butadiene on Au at 70°C (P_R = 1 atm).

D. Current-Partial Pressure Studies

1. Apparatus. The apparatus was the same as described previously.

2. Procedure. The procedure up to obtaining a rest potential was the same as for the current-potential studies. At 1 atm C_4H_6 pressure, a potential within the linear Tafel region was impressed on the anode and a steady state current obtained. The C_4H_6 pressure was then reduced and its corresponding steady state current obtained. The partial pressure was varied in the order 1.0, 0.3, 0.1, 0.03, and 0.01 atm.

3. Data and results. Pressure studies on the Pt electrode were made in 1 N H_2SO_4 and 1 N KOH, and on the Au electrode in 1 N KOH. The resulting data are reported in Appendix D, and log i vs. log P_R plots are shown in Figures 17 to 19.

On the Pt electrode, the current increased with decreasing C_4H_6 partial pressure, i.e., the system exhibited a negative pressure effect. The negative effect was more pronounced in acidic than in basic solutions. This confirms the observations in section C regarding the pressure effect. On Au, an inversion point was observed. The current increased with decreasing C_4H_6 partial pressure down to 0.1 atm, then decreased with further pressure decreases. Similar effects are seen by comparing the Tafel plots at different partial

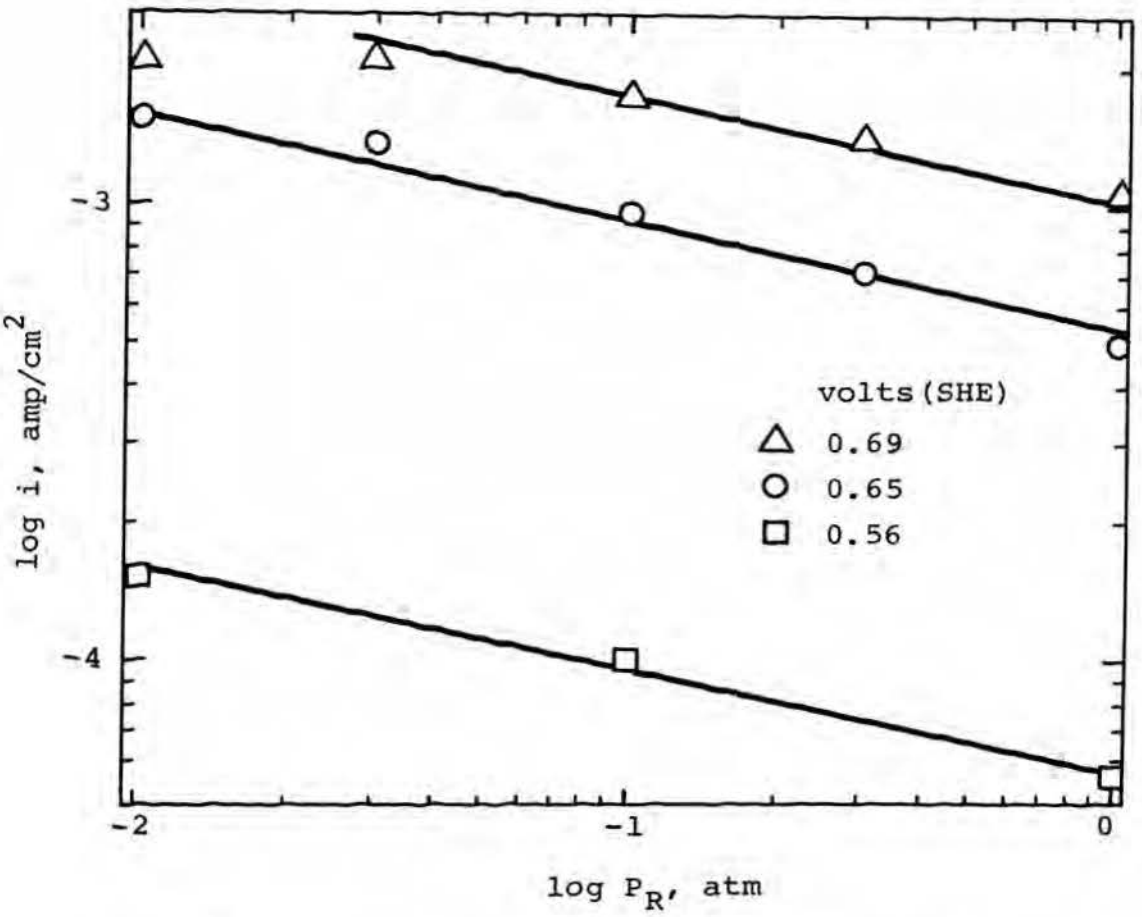

Figure 17. Current-partial pressure relation for the anodic oxidation of Grade-B butadiene on Pt at 70°C in 1 N H_2SO_4. (Curves represent theoretically calculated values)

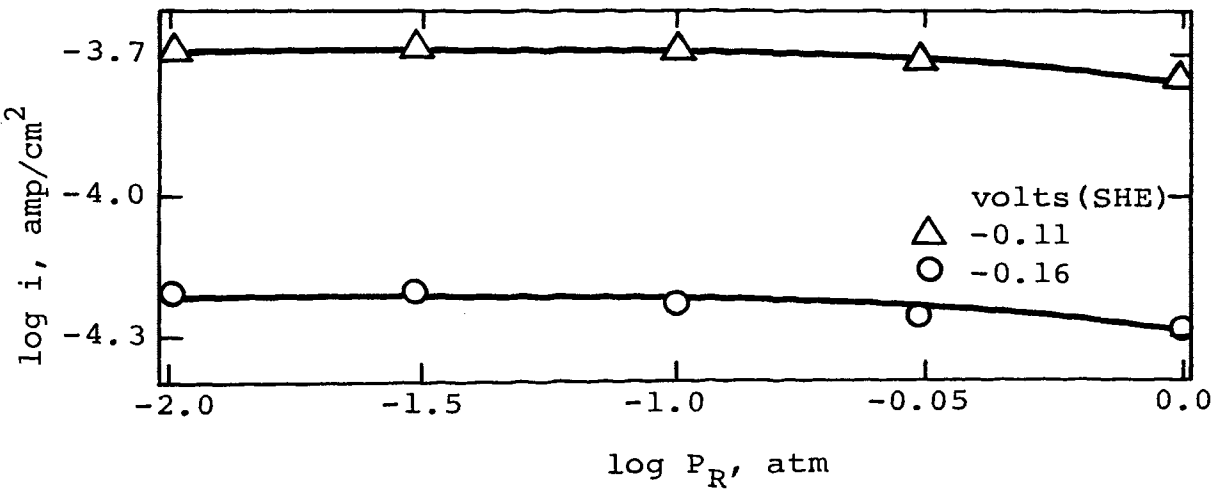

Figure 18. Current-partial pressure relation for the anodic oxidation of Grade-B butadiene on Pt at 70°C in 1 N KOH. (Curves represent theoretically calculated values)

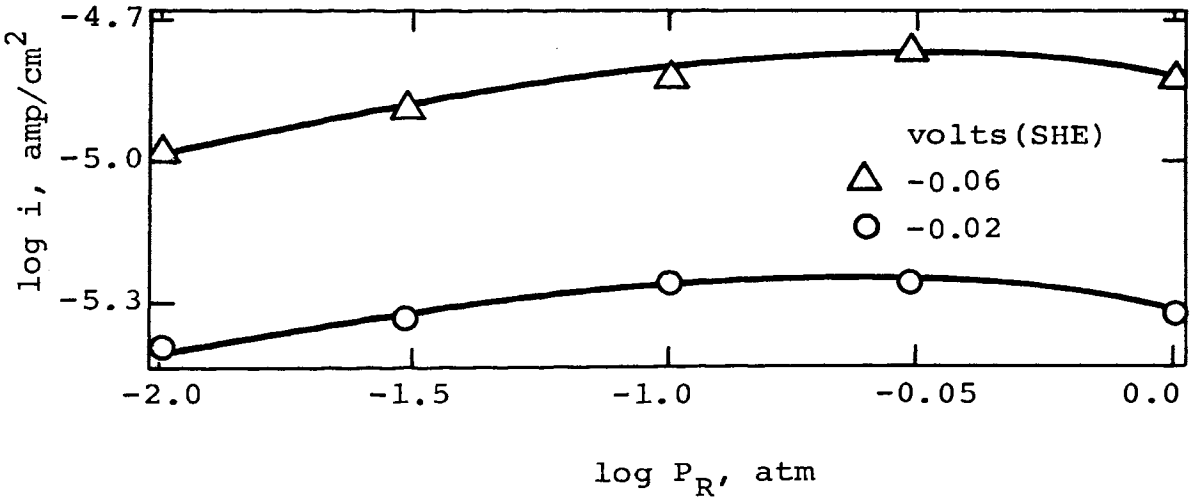

Figure 19. Current-partial pressure relation for the anodic oxidation of Grade-B butadiene on Au at 70°C in 1 N KOH. (Curves represent theoretically calculated values)

pressures in section C.

E. Current-Temperature Studies

1. Apparatus. The apparatus employed in these experiments was the same as described previously.

2. Procedure. The procedure followed to obtain the rest potential was the same as for the current-potential studies except the temperature was initially at 80°C. The anode potential was then set and held constant at a value within the linear Tafel region and the current allowed to reach a steady value. At this time, the temperature was lowered from 80°C by 5°C. When the thermometer in the anolyte indicated the desired temperature, the value of the current was noted and the temperature again decreased. In this manner, current readings were taken at 80, 75, 70, 65, and 60°C at a fixed potential. To find the effect of temperature at another potential, the anolyte was heated again to 80°C and the measurements repeated. In this manner, three sets of readings were obtained at potentials within the linear Tafel regions.

3. Data and results. All temperature studies were done at 1 atm C_4H_6 pressure. The reaction on Pt was studied in 1 N H_2SO_4 and 1N KOH, and on Au in 1 N KOH. The data have been tabulated in Appendix D. Arrhenius plots are shown in Figures 20 to 22. The apparent activation energies were calculated and are shown in

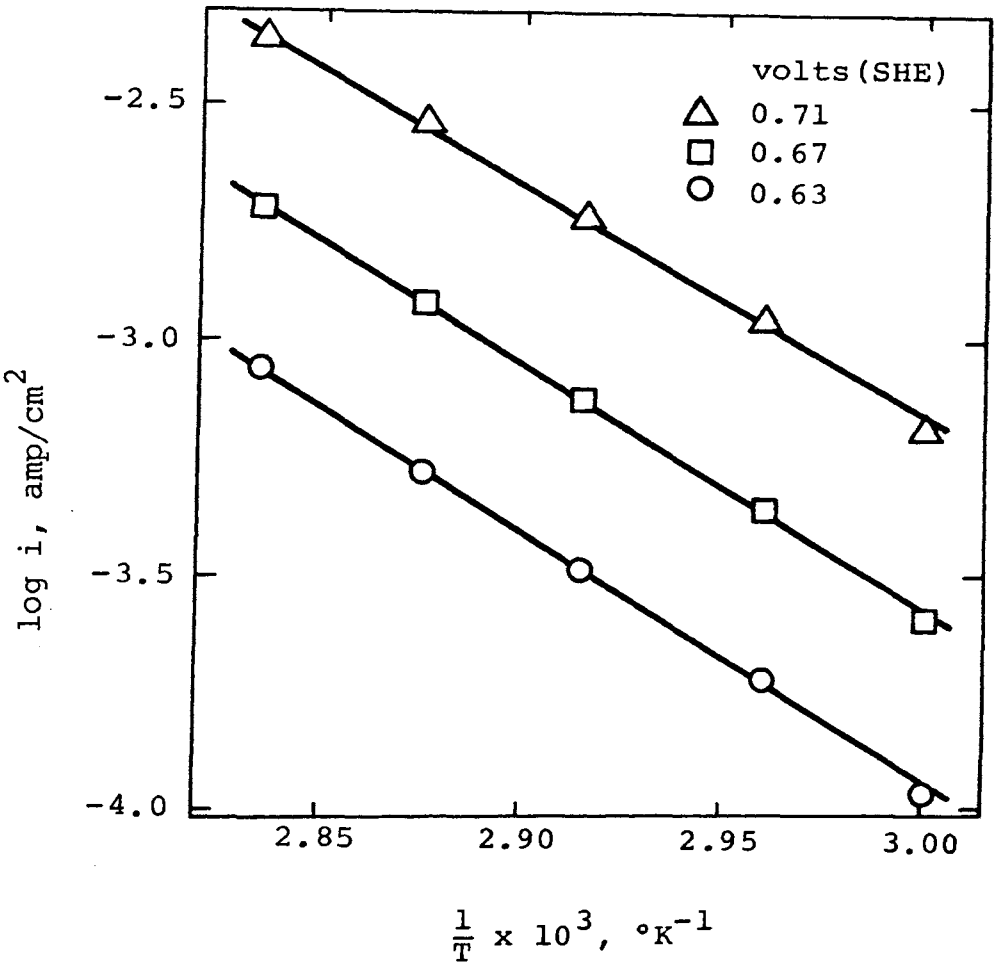

Figure 20. Current-temperature relation for the anodic oxidation of Grade-B butadiene on Pt in 1 N H_2SO_4 (P_R = 1 atm).

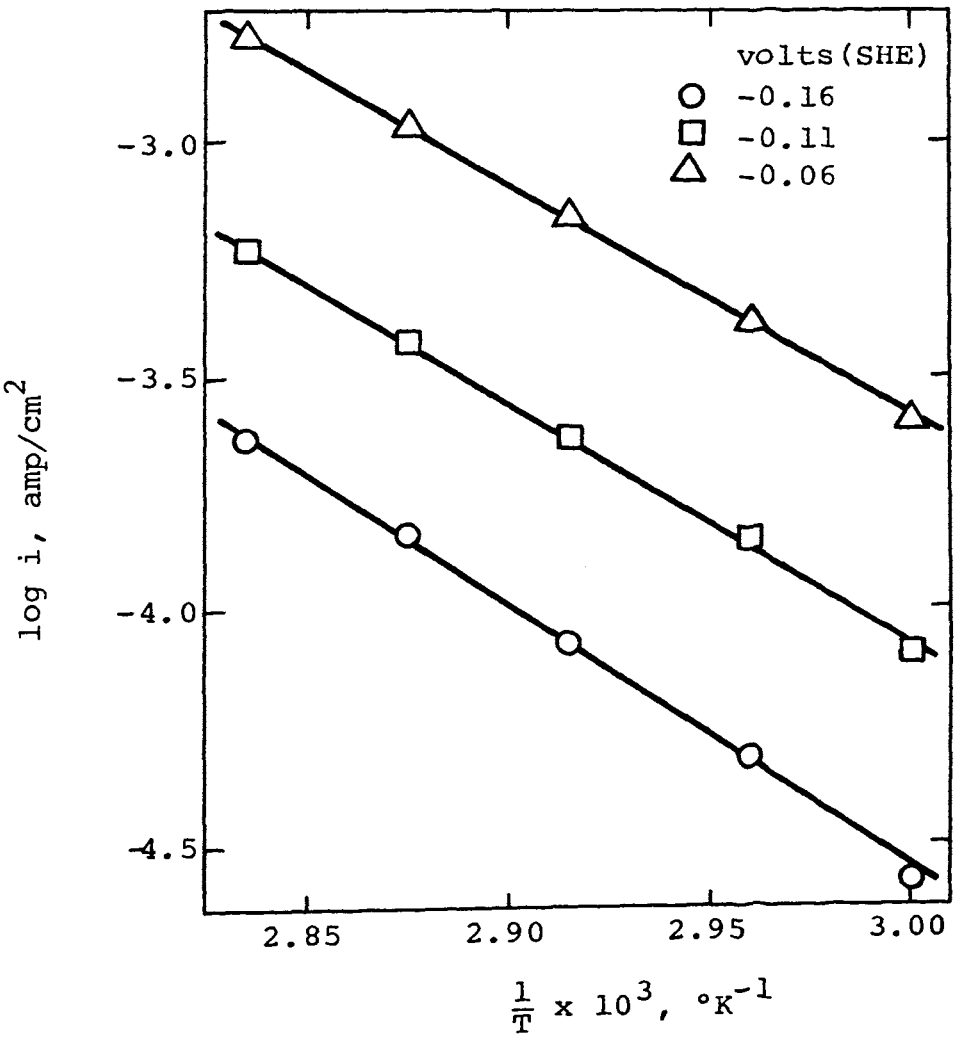

Figure 21. Current-temperature relation for the anodic oxidation of Grade-B butadiene on Pt in 1 N KOH (P_R = 1 atm).

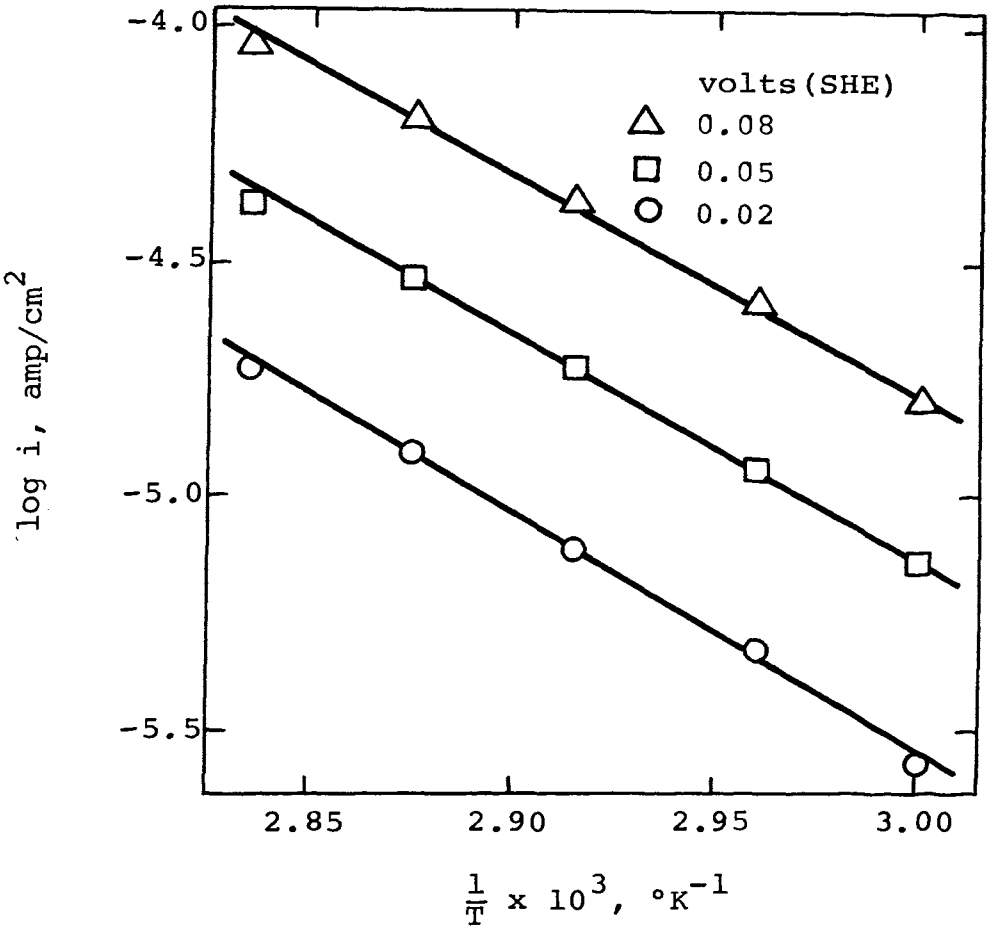

Figure 22. Current-temperature relation for the anodic oxidation of Grade-B butadiene on Au in 1 N KOH (P_R = 1 atm).

Table VI, along with the corresponding $\partial E'_a/\partial V$ values.

F. Coulombic Efficiency Studies

1. Apparatus. The principal apparatus was similar to that described previously and shown in Figure 3. The potentiostat was replaced by a constant voltage d.c. power supply and a high resistor in series with the cell. The galvanostatic circuit is shown in Figure 23. The air condenser on the anodic compartment was connected to a cold-trap maintained at 0°C for condensing the by-products in the exit gas. Subsequently, in the case of the acidic electrolyte, the non-condensables were introduced at the bottom of a column filled with saturated $Ba(OH)_2$ solution for absorbing CO_2. In the case of the basic electrolyte, no such column was necessary as the CO_2 was absorbed in the electrolyte itself.

2. Procedure. The rest potential was obtained in the same manner as for the potentiostatic experiments. The stopcock between the cell compartments was closed and the current adjusted to a desired value by varying the voltage applied with the power supply. The efficiencies were determined at potentials in the linear Tafel region. It was necessary to pass current for about a day or more in order to produce a quantity of CO_2 that could be estimated with reasonable accuracy. Frequent checks of the potential were made to insure that it remained within the linear Tafel region.

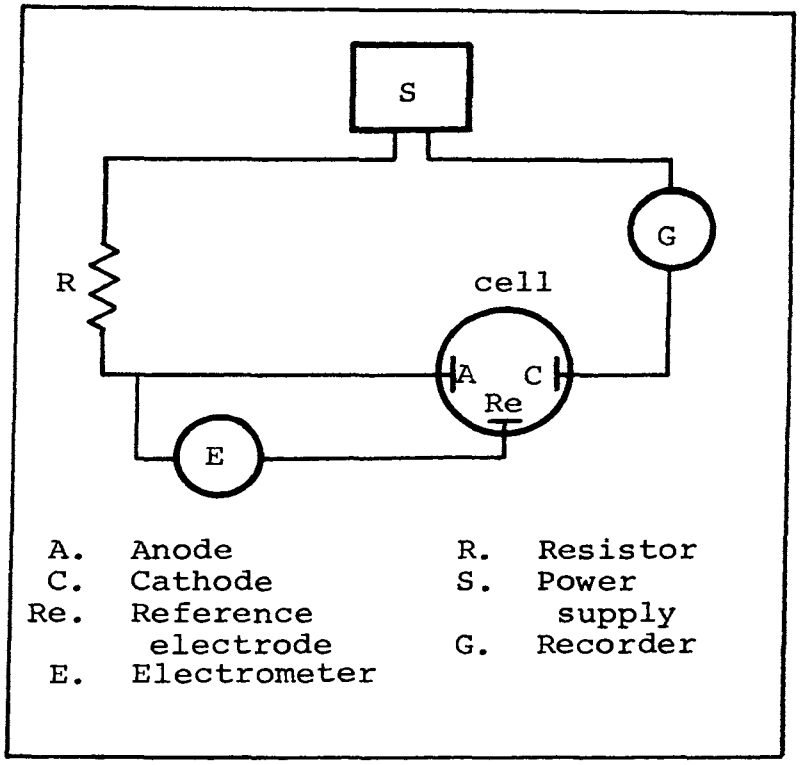

Figure 23. Electrical circuit used for galvanostatic studies in the anodic oxidation of butadiene.

TABLE VI

APPARENT ACTIVATION ENERGIES FOR THE ANODIC OXIDATION OF GRADE-B BUTADIENE ON Pt AND Au (P_R = 1 atm)

Electrode	Solution	Potential	Activation Energy	$\partial E_a'/\partial V$
		V(SHE)	Kcal/mole	Kcal/volt
Pt	1 N H_2SO_4	0.628*	24.2	
		0.668**	23.0	-22.5
		0.708**	22.1	
Pt	1 N KOH	-0.161*	24.3	
		-0.111**	22.0	-22.5
		-0.061**	20.9	
Au	1 N KOH	0.019	22.5	-23.3
		0.049	21.8	-23.3
		0.079	21.1	

* b.t.r.

** a.t.r.

The carbon dioxide produced by the anodic oxidation of C_4H_6 during a known period of time was used to calculate the coulombic efficiency. In the case of the acidic electrolyte (1 N H_2SO_4), samples of the $Ba(OH)_2$ solution from the absorption column were titrated before and after the run with HCl solution using a phenolphthalein indicator, thus the CO_2 absorbed during the experiment was determined. In the case of the basic electrolyte (1 N KOH), a known quantity of standardized solution was charged into the cell at the beginning and analyzed again after the run. The analysis for CO_2 was made by titrating the electrolyte with HCl using methylorange and phenolphthalein indicators. Details of the analytical procedure can be found in Vogel.[24]

The material collected in the cold trap and a sample of the anolyte were analyzed with a flame-ionization gas chromatograph.

3. Data and results. The efficiencies on Pt in 1 N H_2SO_4 at 5 ma current over 20 hours for two different runs were found to be 82 and 87 $\pm$ 5 percent. In 1 N KOH at 3 ma current over 25 hours, they were 91 and 94 $\pm$ 5 percent. The efficiencies on Au in 1 N KOH at 1 ma current over 30 hours were 69 and 73 $\pm$ 10 percent. Sample calculations are shown in Appendix D.

For Pt, the 1 N H_2SO_4 anolyte and condensate showed the presence of a by-product when analyzed on a gas

chromatograph. None was found for 1 N KOH. In the case of Au, an anolyte analysis showed no by-product.

IV. DISCUSSION

In this chapter, mechanisms for the electro-oxidation of butadiene on Pt and Au are postulated and the developed rate equations compared with the experimental data. As the proposed mechanisms differ with most reported in the literature for unsaturated hydrocarbons, they are also discussed in the light of that work.

A. Summary of Experimental Results

The reaction parameters obtained on Pt and Au in the previous chapter are summarized below and also presented in Table VII.

1. Platinum. Polarization curves for Grade-A butadiene at 70°C and 80°C both had Tafel slopes of ∿140 mv. The pH effects, $\partial \log i/\partial pH$ and $\partial V/\partial pH$, in neutral to basic solutions were approximately 0.5 and -70 mv, respectively.

For Grade-B butadiene, there were two linear Tafel sections in both acidic and basic solutions. The slope was ∿140 mv at low and ∿70 mv at high overpotentials. The pH effect, $\partial \log i/\partial pH$, was approximately zero in strongly acidic solutions both at low and high overpotentials, whereas it was 0.5 in basic and weakly acidic solutions at low overpotentials and unity at high

TABLE VII

KINETIC PARAMETERS FOR THE ANODIC OXIDATION OF GRADE-B BUTADIENE AT 70°C

Electrode	Electrolyte	$\partial V/\partial \log i$	$\partial V/\partial pH$	$\partial \log i/\partial pH$	$\partial i/\partial P_R$
Pt(b.t.r.)	strong acids	$2(2.3RT/F)$	~ 0	~ 0	<0
Pt(a.t.r.)	strong acids	$2.3RT/F$	~ 0	~ 0	<0
Pt(b.t.r.)	base and weak acids	$2(2.3RT/F)$	$-2.3RT/F$	0.5	<0
Pt(a.t.r.)	base and weak acids	$2.3Rt/F$	$-2.3RT/F$	1	<0
Au	base	$2.3RT/F$	$-2.3RT/F$	1	<0 (1 to 0.1 atm) >0 (0.1 to 0.01 atm)

overpotentials. Throughout this chapter henceforth, all the results and discussion pertain to Grade-B butadiene unless mentioned otherwise. The system showed a negative pressure effect, $\partial i/\partial P_R < 0$, at both low and high overpotentials. The effect was more pronounced in acidic than in basic solutions. The apparent energies of activation at low overpotentials were 24.2 and 24.3 Kcal/mole in 1 N H_2SO_4 and 1 N KOH, respectively. Since the temperature effect could be studied at only one potential in the 140 mv Tafel region, $\partial E'_a/\partial V$ could not be evaluated. The apparent activation energies at high overpotentials varied from 23.0 to 22.1 Kcal/mole in 1 N H_2SO_4 and 22.0 to 20.9 in 1 N KOH. The values of $\partial E'_a/\partial V$ were -22.5 Kcal/volt in both acid and base in the 70 mv Tafel region. The coulombic efficiencies for C_4H_6 oxidation to CO_2 in 1 N H_2SO_4 and 1 N KOH were 85 and 93 $\pm$ 5 percent, respectively.

2. Gold. The reaction could not be studied in acidic solutions due to polymer formation on the electrode. The Tafel slope in basic solutions was $\sim$70 mv. The pH effects, $\partial \log i/\partial pH$ and $\partial V/\partial pH$, were unity and -70 mv, respectively. An inversion point was observed in the partial pressure effect in 1 N KOH. The current increased with decreasing C_4H_6 pressure down to 0.1 atm, then decreased with further pressure decreases. The apparent activation energies in 1 N KOH ranged from

22.5 to 21.1 Kcal/mole with $\partial E'_a/\partial V$ equal to -23.3 Kcal/volt. The coulombic efficiency in 1 N KOH was 72 $\pm$ 10 percent.

B. Comparison of Present Work with that Reported in Literature

The polarization curves obtained with Grade-A butadiene on Pt (Figure 5) were similar to those reported by Bockris, et. al.[17] The linear Tafel region was about two decades in length with a slope of $\sim$140 mv. The pH effect estimated from the limited amount of data was approximately 0.5. For both these studies, the butadiene was obtained from the same source (Matheson Co.). The minimum purity of the Grade-A used in this study was 99.4 percent and that used by Bockris, et. al., (Piersma)[25] was 99.0 percent.

Polarization curves obtained with Grade-A butadiene on Pt were different from those with Grade-B (Figure 8). A transition region was found in the Tafel plots for the latter which had $\sim$140 and 70 mv slopes below and above the transition regions, respectively. The difference in the results appears to be due to the greater amounts of impurities in the other two grades (from Matheson). The source of Grade-B butadiene was different (Phillips Petroleum Co.) and the minimum purity was listed as 99.5 percent. The Grade-B butadiene was further purified (see experimental section) prior to

electrolysis. Gas chromatographic analyses of grades A and B are shown in Appendix B for comparison purposes. Since significantly greater amounts of impurities are evident in the Grade-A material, its kinetic parameters are not considered applicable to butadiene and will be omitted from further discussion.

C. Postulation of a Reaction Mechanism

Comparisons of the reaction mechanisms proposed previously for the oxidation of unsaturated hydrocarbons on Pt and Au show them to differ for the various hydrocarbons on the same metal as well as for the same hydrocarbon on the two metals. It will be shown shortly that of all the mechanisms that have been proposed, none completely explain the kinetic parameters observed for butadiene.

The existence of such problems might have been anticipated due to the previous way that the potentials (the driving force for the reactions) have been expressed. In most cases, the rate equations were developed using potentials expressed on the normal hydrogen scale. A more logical choice would seem to be the rational scale which refers potentials to the p.z.c. The logic of such a choice can be arrived at if one considers the appropriateness of basing the potential driving force on a null-value applicable to the electrode under consideration (e.g., the p.z.c.), rather than an arbitrarily

selected value such as that for the standard hydrogen electrode. This becomes especially apparent when one sees that the p.z.c. and reaction rates may both be affected by compositional changes in the electrolyte (e.g., pH), but in an unequal manner.

1. Potential of zero charge. It is necessary to know the p.z.c.-pH relationship for both Pt and Au as the pH effect is the parameter most probably affected by changes in the p.z.c. In case of Au, we shall use the results of Bode, et. al.,[8] for solutions containing $SO_4^=$ and assume that solutions containing $CO_3^=$ behave similarly. Thus, for Au:

$$V_{pzc} = V^o_{pzc} - \zeta pH \qquad (4.1)$$

where

$$\zeta \simeq 0 \text{ (acids)} \qquad (4.1a)$$

$$\simeq 2.3RT/F \text{ (bases)} \qquad (4.1b)$$

V_{pzc} and V^o_{pzc} are the potentials of zero charge (volts, SHE) at the desired and zero pH, respectively.

For Pt, no information is available on the p.z.c. shift in alkaline and weakly acidic solutions containing $CO_3^=$ and $SO_4^=$ ions. Here we will use the relationship obtained by Bockris, et. al.,[9] for ClO_4^- ions, which was identical to relation (4.1) with

$$\zeta = 2.3RT/F \quad (pH = \sim 3 \text{ to } 13) \qquad (4.1c)$$

As shown in Figure 1, ClO_4^- and $SO_4^=$ ions do give identical results for Au. In the present study, the electrodes were activated by anodic and cathodic pulsing prior to use. Therefore, for Pt in strong acid solutions containing $SO_4^=$ ions, we will use the results reported by the Russian workers,[7,10] i.e., relation 4.1 with

$$\zeta = 0 \text{ to } 0.018 \text{ (pH = 0 to } \sim 3) \qquad (4.1d)$$

2. Applicability of oxidation mechanisms from the literature to butadiene. The oxidation mechanisms previously proposed for C_2H_2 on Pt,[18] C_2H_2 and C_2H_4 on Au,[20,21] and for alkenes on Pt[17] are examined here for their applicability to C_4H_6 oxidation on Pt and Au.

a. Acetylene-Pt mechanism. The reaction sequence proposed by Johnson, et. al.,[18] for C_2H_2 on Pt is,

$$C_2H_2 = C_2H_2(ads) \qquad (4.2)$$

$$H_2O = OH(ads) + H^+ + e \qquad (4.3)$$

or,
$$OH^- = OH(ads) + e \qquad (4.4)$$

$$C_2H_2(ads) + OH(ads) \xrightarrow{rds} \xrightarrow{H_2O} \cdots \rightarrow CO_2, H^+, e \qquad (4.5)$$

Approximating θ_T by θ_R, the rate equation is

$$i = zFk(a_{H^+})^{-1}\theta_R(1-\theta_R)\exp(VF/RT) \qquad (4.6)$$

The kinetic parameters from this equation are: Tafel

slope = 2.3RT/F, pH effect (on log i) = unity, pH effect (on potential) = -2.3RT/F, and a negative pressure effect when $\theta_R > 0.5$. In this development, V is volts(SHE) and the shift in the p.z.c. on Pt was not considered.

In the present work with C_4H_6, a Tafel slope of 2.3RT/F was observed on Au and a.t.r. on Pt. pH effects of unity (on log i) and -2.3RT/F (on V) were observed for both Pt and Au in basic solutions, but were zero in acid on Pt (there is no comparable data in acid for Au). The pressure effect was negative on Pt, but changed from negative to positive with decreasing pressures for Au. This change for Au would be expected if θ_R decreased below 0.5. Thus, the mechanism by Johnson, et. al., satisfies the kinetic parameters obtained for C_4H_6 on Au in base and on Pt in base a.t.r. However, a different mechanism would be needed to explain the behavior on Pt in acidic solutions.

If one uses the rational potential ν rather than V, the rate equations become,

$$i = zFk(a_{H^+})^{-1}\theta_R(1-\theta_R)\exp(\nu F/RT) \qquad (4.7)$$

$$\text{or} \quad i = zFk(a_{H^+})^{-1}\theta_R(1-\theta_R)\exp\{(V-V^o_{pzc}+\zeta\ pH)F/RT\} \qquad (4.8)$$

Now, pH effects of unity and -2.3RT/F for log i and V, respectively, are obtained for strong acids where $\zeta = 0$ for both Pt and Au. In bases, where $\zeta = 2.3RT/F$, pH

effects of two and -2(2.3RT/F) would be obtained. As these were not observed experimentally, the C_2H_2 mechanism will not explain the effects for C_4H_6.

b. Alkene-Pt mechanism. It was reported,[17] as shown in Table I, that a number of unsaturated hydrocarbons oxidize on Pt in an identical manner. The reaction sequence proposed for them was,

$$R = R(ads) \tag{4.9}$$

$$H_2O \xrightarrow{rds} OH(ads) + H^+ + e \tag{4.10}$$

$$R(ads) + OH(ads) \rightarrow ROH(ads) \text{ or } R^{\cdot}(ads) + H_2O \tag{4.11}$$

$$ROH(ads) \text{ or } R^{\cdot}(ads) \rightarrow \text{Products} \tag{4.12}$$

This sequence is similar to that proposed for C_2H_2 except that the r.d.s. has changed from a chemical step to an electron discharge reaction and accounts for the Tafel slopes of 140 mv. A rate equation was developed on the basis of the rational potential,

$$i = zFk(1-\theta_T)\exp(\alpha\nu F/RT) \tag{4.13}$$

Again, θ_T was approximated by θ_R to give,

$$i = zFk(1-\theta_R)\exp(\alpha\nu F/RT) \tag{4.14}$$

When ν is replaced by V and using $\zeta = 2.3RT/F$ and $\alpha = 0.5$,

$$i = zFk(1-\theta_R)\exp(2.3pH/2)\exp\{(V-V^{o}_{pzc})F/2RT\} \tag{4.15}$$

Thus, the kinetic parameters are $\partial V/\partial \log i = 2(2.3RT/F)$, $\partial V/\partial pH = -2.3RT/F$, and $\partial \log i/\partial pH = 0.5$. A negative pressure effect arises from the factor $(1-\theta_R)$ which was further approximated as proportional to $P_R^{-1/n}$. These parameters were in agreement with their results (shown in Table I).

The use of the rational potential was necessary to explain the pH effect of 0.5. Otherwise, the rate equation would be

$$i = zFk(1-\theta_R)\exp(\alpha VF/RT) \qquad (4.16)$$

This gives a pH effect of zero contrary to the observations. In basic solutions, OH^- ions would be expected to discharge more readily than H_2O but they lead to anomalous pH effects with either ν or V. No explanation was offered as to why H_2O should discharge in preference to OH^-.

This mechanism would satisfactorily explain the results for butadiene on Pt b.t.r., i.e., where the Tafel slope is 140 mv. To obtain the correct pH effect, $\partial \log i/\partial pH = 0$ and $\partial V/\partial pH = 0$ in strong acid, and $\partial \log i/\partial pH = 0.5$ and $\partial V/\partial pH = -2.3RT/F$ in base, ζ values of zero for strong acid and $2.3RT/F$ for base must be used.

A negative pressure effect was observed by Bockris, et. al., as predicted by equation 4.14. The effect $(\partial \log i/\partial \log P_R)$ reported for butadiene on Pt in acid

was -0.13. The value obtained in the present work was about -0.25 in acid and -0.13 in base (see Figures 17 and 18). This difference in the observations may have been due to presence of higher impurities (primarily the additive catechol) in the C_4H_6 used by the previous investigators.

To explain the behavior on Pt a.t.r. and on Au (Tafel slopes = 70 mv), the r.d.s. of the alkenes mechanism would have to change to a chemical step following the electron discharge step. The mechanisms would then be similar to that proposed for acetylene which was shown inadequate in the previous section. It is therefore concluded that the alkene-Pt mechanism is also inadequate for the present work.

c. Acetylene, ethylene-Au mechanism.[20,21]

For C_2H_2, two reaction mechanisms (one b.t.r and another a.t.r.) were proposed:

b.t.r.

$$C_2H_2 = C_2H_2(ads) \quad (4.17)$$

$$H_2O \overset{rds}{\rightarrow} OH(ads) + H^+ + e \quad (4.18)$$

and/or,

$$OH^- \overset{rds}{\rightarrow} OH(ads) + e \quad (4.19)$$

$$C_2H_2(ads) + OH(ads) \rightarrow \text{products} \quad (4.20)$$

a.t.r.

$$C_2H_2 = C_2H_2(ads) \quad (4.17)$$

$$C_2H_2(ads) + H_2O \xrightarrow{rds} C_2H_2OH(ads) + H^+ + e \quad (4.21)$$

and/or,

$$C_2H_2(ads) + OH^- \rightarrow C_2H_2OH(ads) + e \quad (4.22)$$

The corresponding rate equations were,

$$i = zF(k_b a_W + k'_b a_{OH^-})(1-\theta_R)\exp(\alpha VF/RT) \quad (4.23)$$

$$i = zF(k_a a_W + k'_a a_{OH^-})\theta_R \exp(\alpha VF/RT) \quad (4.24)$$

In equation 4.23, θ_T was approximated by θ_R. The water or OH^- discharge is identical to that for alkenes, as discussed in the preceding section. The case a.t.r. is not applicable for butadiene on Pt as it leads to a positive pressure effect.

As in the case of C_2H_2, two reaction mechanisms were proposed for the C_2H_4 oxidation on Au. The mechanism proposed in basic solutions b.t.r. was identical to that for C_2H_2 a.t.r. The second mechanism (see page 35) was quite different and involved the formation of a carbonium ion, $C_2H_4^+$, previously postulated by Dahms, et. al.[23] The rate equation for this sequence is,

$$i = zFka_w\theta_R\exp(VF/RT) \quad (4.25)$$

A positive pressure effect is also predicted by this equation and again is unsuitable for C_4H_6 on either Pt or Au.

3. A mechanism for the anodic oxidation of butadiene. A sequence of reactions that leads to an explanation of the observed kinetic parameters in this work has been found. The development of the scheme along with the assumptions involved is presented here.

The adsorption of C_4H_6 on the electrode substrate prior to oxidation is assumed to be relatively fast as has been found for other hydrocarbons in the works cited previously. It is further assumed that adsorption occurs under Langmuir conditions. Since organic adsorption is a replacement reaction, H_2O and C_4H_6 compete for the same active sites, so it is also assumed that H_2O adsorbs and under Langmuir conditions. The main reaction product from C_4H_6 oxidation both on Pt and Au was CO_2 as was with other hydrocarbons on Pt. Since oxygen must be supplied and the only oxygen source available in the aqueous electrolytes is H_2O or a species derived therefrom,* water in some form (or a derivative) is considered to participate in the r.d.s.

The parameters presented in Table VII are based on potentials relative to the standard hydrogen electrode. These have been converted to the rational scale and these results are shown in Table VIII. The transformation procedure is shown in Appendix D. The modified parameters show that there is no direct effect of pH on the

*Anions such as $SO_4^=$ present in the electrolyte have never been found to directly participate in the reaction.

oxidation reaction on either Pt or Au, thus suggesting adsorbed water is participating in the r.d.s.

The negative pressure effect with C_4H_6 on Pt in the present work has been observed with other similar hydrocarbons on Pt in previous studies. A negative pressure effect on Au was observed only in certain cases. Two conclusions might be drawn from such behavior: (1) upon adsorption, the organic species break into two or more similar species which are involved in the r.d.s., or (2) a species not derived from the organic species is involved in the r.d.s. Since C_4H_6 shows a negative pressure effect on Pt of roughly the same degree as C_2H_2 and C_2H_4, the first supposition is discarded in favor of the second.

In the formulation of electrochemical rate equations from a mechanism, it is customary to take the value of the transfer coefficient α as constant and equal to 0.5 for both forward and backward reactions. The effect of potential or other variables upon its value is not explicitly known. With $\alpha = 0.5$ and Langmuir type adsorption, the Tafel slopes of $2.3RT/\alpha F$ and $2.3RT/F$ signify the rate determining steps to be the first electron transfer and a chemical reaction following the first electron transfer, respectively. This suggests a sequence for C_4H_6 oxidation on Pt and Au as,

TABLE VIII

MODIFIED PARAMETERS FOR THE ANODIC OXIDATION

OF GRADE-B BUTADIENE AT 70°C

Electrode	Electrolyte	$\partial\nu/\partial\log i$	$\partial\nu/\partial pH$	$\partial\log i/\partial pH$	$\partial i/\partial P_R$
Pt(b.t.r.)	strong acids	2(2.3RT/F)	0	0	<0
Pt(a.t.r.)	strong acids	2.3RT/F	0	0	<0
Pt(b.t.r.)	base and weak acids	2(2.3RT/F)	0	0	<0
Pt(a.t.r.)	base and weak acids	2.3RT/F	0	0	<0
Au	base	2.3RT/F	0	0	<0 (1 to 0.1 atm) >0 (0.1 to 0.01 atm)

$$H_2O = H_2O(ads) \quad (4.26)$$

$$R = R(ads) \quad (4.27)$$

$$R(ads) + H_2O(ads) \rightarrow RHOH^+(ads) + e \quad (4.28)$$

$$RHOH^+(ads) + H_2O \rightarrow \overset{H_2O}{\cdots} \rightarrow CO_2, H^+, e, \text{ etc.} \quad (4.29)$$

The rate determining step is reaction 4.28 when the Tafel slope is $2.3RT/\alpha F$ and is reaction 4.29 when it is $2.3RT/F$. The corresponding rate equations are developed by considering the reactions preceding the r.d.s. to be in quasi-equilibrium and those following the r.d.s. to be fast and having no effect on it (i.e., assuming the reaction products to be rapidly consumed and removed). The rational potential will be considered the potential driving force that affects the rate of reaction.

a. Case I (Tafel slope = $2.3RT/\alpha F$). Considering reaction 4.28 to be the r.d.s. and water to adsorb on a single site, reaction 4.26 gives,

$$k_1 a_W (1-\theta_T) = k_{-1}\theta_W \quad (4.30)$$

or

$$\theta_W = K_1(1-\theta_T) \quad (4.31)$$

where, θ_T is the total fractional coverage of the surface, and $K_1 (= a_W k_1/k_{-1})$ can be considered constant as a_W is practically constant in the dilute electrolytes used in these studies. From reaction 4.27,

$$k_2 P_R (1-\theta_T)^n = k_{-2}\theta_R \quad (4.32)$$

or $\theta_R = K_2 P_R (1-\theta_T)^n$ (4.33)

where, K_2 ($= k_2/k_{-2}$) is the equilibrium constant for the adsorption step 4.27.* The rate of reaction 4.28 can be written as:

$$i = zFk_3\theta_R\theta_W \exp(\alpha\nu F/RT) \quad (4.34)$$

Substituting for θ_W from equation 4.31 and combining the constant gives,

$$i = zFk'\theta_R(1-\theta_T)\exp(\alpha\nu F/RT) \quad (4.35)$$

where, $k' = K_1 k_3$.

b. Case II (Tafel slope = 2.3RT/F). For this case, reaction 4.28 is also considered to be at equilibrium and reaction 4.29 becomes the r.d.s. Equations 4.31 and 4.33 for θ_W and θ_R are unchanged while reaction 4.28 gives

$$k_3\theta_R\theta_W \exp(\alpha\nu F/RT) = k_{-3}\theta_{RW^+} \exp[-(1-\alpha)\nu F/RT] \quad (4.36)$$

or $\theta_{RW^+} = K_3\theta_R\theta_W(\nu F/RT)$ (4.37)

where, K_3 ($= k_3/k_{-3}$) is the equilibrium constant for the

*It should be noted that the adsorption of R by replacing adsorbed water leads to an isotherm, $\theta_R = KP_R(\theta_W)^n = K_2P_R(1-\theta_T)^n$ which is the same as eqn. 4.33.

reaction and θ_{RW}^+ is the fractional coverage by the species $RHOH^+$. The rate of reaction 4.29 can be written as,

$$i = zFk_4 a_W \theta_{RW}^+ \qquad (4.38)$$

Substituting for θ_{RW}^+, and combining constants gives,

$$i = zFk'' \theta_R (1-\theta_T) \exp(\nu F/RT) \qquad (4.39)$$

where, $k'' = K_1 K_3 k_4 a_W$.

D. Correlation of Experimental Results with the Theoretical Rate Equations

The rate equations developed in the previous section are tested in this section for their validity. An ability to correlate the observed results for C_4H_6 oxidation will lend support to the reaction mechanisms from which they were derived.

1. Polarization and pH relation.

a. Case I (Tafel slope = $2.3RT/\alpha F$). Taking the log of both sides of equation 4.35

$$\log i = \log zFk' + \log \theta_R (1-\theta_T) + \alpha\nu F/2.3RT \qquad (4.40)$$

Partial differentiation gives $\partial\nu/\partial \log i = 2.3RT/\alpha F$ (Tafel slope), $\partial\nu/\partial pH = 0$ (pH effect on potential), $\partial \log i/\partial pH = 0$ (pH effect on current). These values are the same as observed experimentally and are listed in Table VIII.

b. Case II (Tafel slope = 2.3RT/F). Proceeding as before with equation 4.39,

$$\log i = \log zFk'' + \log \theta_R(1-\theta_T) + \nu F/2.3RT \quad (4.41)$$

gives $\partial\nu/\partial\log i = 2.3RT/F$, $\partial\nu/\partial pH = 0$, and $\partial\log i/\partial pH = 0$. These parameters also agree well with those obtained experimentally and are shown in Table VIII.

2. Current-partial pressure relation. At constant potential and pH, equations 4.35 and 4.39 can be reduced to the following form:

$$i = k\theta_R(1-\theta_T) \quad (4.42)$$

The C_4H_6 adsorption isotherm is given by the equation 4.33,

$$\theta_R/(1-\theta_T)^n = K_2P_R \quad (4.33)$$

In the above two equations θ_T, when approximated by θ_R, gives,

$$i = k\theta_R(1-\theta_R) \quad (4.43)$$

and

$$\theta_R/(1-\theta_R)^n = K_2P_R \quad (4.44)$$

Thus, equations 4.43 and 4.44 give the predicted (mechanistic) effect of pressure on the reaction rate (current). As values of n and K_2 are not known, various values are assumed and their appropriateness checked by testing their ability to correlate the experimental data. Calculated and experimental current density are both plotted

against P_R in Figures 17 to 19 (points represent the experimental and curves the calculated values). In all the cases, good agreement within the experimental limits of accuracy were obtainable. The values of n and K_2 which gave the best fit were,

Pt in acid: $n = 4$ and $K_2 = 10^7$,

Pt in base: $n = 8$ and $K_2 = 10^5$,

Au in base: $n = 4$ and $K_2 = 50$.

The value of n for Pt in base is different from that in acid. Johnson, et. al.,[20,21] in studies of C_2H_2 and C_2H_4 oxidation on Au, found a similar difference (see pp. 35 to 37).

3. Current-temperature relation. The variation of the apparent activation energy with potential for Pt b.t.r. can be calculated from equation 4.35, and for Pt a.t.r. or Au from equation 4.39. The terms k' and k" are equivalent to chemical rate constants which, by use of the Arrhenius relationship, can be expressed as $A\exp(-E_a/RT)$. Substituting k' and taking the derivative of the log of both sides of equation 4.35 with respect to 1/T, one obtains

$$\partial \log i/\partial(1/T) = \frac{-E_a}{2.3R} + \frac{\alpha\nu F}{2.3R} = \frac{-E'_a}{2.3R} \qquad (4.45)$$

Using this expression, the variation of the apparent activation energy with potential is found to be

$$\frac{\partial E'_a}{\partial \nu} = -\alpha F = -11.5 \text{ Kcal/volt.} \qquad (4.46)$$

A similar treatment of equation 4.39 gives

$$\frac{\partial E'_a}{\partial \nu} = -F = -23.0 \text{ Kcal/volt} \qquad (4.47)$$

for Au and Pt a.t.r. These values agree well with those obtained experimentally.

E. Applicability of the Postulated Reaction Mechanism to Other Hydrocarbons

1. Acetylene on Pt. Letting the r.d.s. be reaction 4.29 in the mechanism sequence, the rate equation is

$$i = zFk''\theta_R(1-\theta_T)\exp(\nu F/RT) \qquad (4.35)$$

When ν is replaced by V with relation 4.1 and ζ is taken to be 2.3RT/F over the whole pH range (since a pH effect was also observed in acid solutions),

$$i = zFk''\theta_R(1-\theta_T)\exp[(V-V^o_{pzc} + \frac{2.3RT}{F}\text{ pH})F/RT] \qquad (4.48)$$

The kinetic parameters from this equation are, $\partial V/\partial \log i = 2.3RT/F$, $\partial V/\partial pH = -2.3RT/F$, $\partial \log i/\partial pH = 1$, $\partial E'_a/\partial V = -F$, and $\partial i/\partial P_R < 0$ when $\theta_R > (1-\theta_T)$. These parameters are the same as obtained from the mechanism, reactions (2.61) - (2.64), as proposed by Johnson, et. al.[18]

2. Alkenes on Pt. If reaction 4.28 in the sequence is the r.d.s.,

$$i = zFk'\theta_R(1-\theta_T)\exp(\alpha\nu F/RT) \tag{4.39}$$

Substituting for ν as above,

$$i = zFk'\theta_R(1-\theta_T)\exp[\alpha(V-V^o_{pzc} + \frac{2.3RT}{F}\ pH)F/RT] \tag{4.49}$$

The kinetic parameters from this equation are $\partial V/\partial \log i = 2.3RT/\alpha F$, $\partial V/\partial pH = -2.3RT/F$, $\partial \log i/\partial pH = 0.5$, $\partial E'_a/\partial V = -\alpha F$, and $\partial i/\partial P_R < 0$ when $\theta_R > (1-\theta_T)$. These parameters are in agreement with those obtained by Bockris, et. al.[17]

3. Ethylene on Au. Let the r.d.s. be reaction 4.28 in the oxidation sequence for the case where the Tafel slope was 2(2.3RT/F) i.e., b.t.r. in weak acid and base. The rate equation is,

$$i = zFk'\theta_R(1-\theta_T)\exp(\alpha\nu F/RT) \tag{4.35}$$

which reduces to

$$i = zFk'\theta_R(1-\theta_T)\exp[\alpha(V-V^o_{pzc} + \frac{2.3RT}{F}\ pH)F/RT] \tag{4.50}$$

when ν is replaced by V and $\zeta = 2.3RT/F$. Kinetic parameters derived from this equation are $\partial V/\partial \log i = 2.3RT/\alpha F$, $\partial E'_a/\partial V = -\alpha F$, $\partial \log i/\partial pH = 0.5$, and $\partial i/\partial P_R < 0$ when $\theta_R > (1-\theta_T)$.

The pH effect obtained here is different than that obtained from the rate equation proposed by Johnson, et. al.[21] The experimental value of $\partial \log i/\partial pH$ was

0.75[26] and this was interpreted as 1.0. It would be equally reasonable to interpret the value of 0.5, thus giving complete agreement between the observed and derived values.

If the r.d.s. were shifted to reaction 4.29 for the case where Tafel slope was 2.3RT/F, i.e., strong acids and a.t.r. in base, the corresponding rate equation would be,

$$i = zFk''\theta_R(1-\theta_T)\exp(\nu F/RT) \qquad (4.39)$$

In terms of V (ζ = 0 for acid and 2.3RT/F for base), the rate equation becomes:

For acid,

$$i = zFk''\theta_R(1-\theta_T)\exp[(V-V^o_{pzc})F/RT] \qquad (4.51)$$

and for base,

$$i = zFk''\theta_R(1-\theta_T)\exp[(V-V^o_{pzc} + \frac{2.3RT}{F}\,pH)F/RT] \qquad (4.52)$$

The respective parameters from these two equations are $\partial V/\partial \log i = 2.3RT/F$, $\partial E'_a/\partial V = -F$, $\partial i/\partial P_R > 0$ when $\theta_R < (1-\theta_T)$ and $\partial \log i/\partial pH = 0$ for acid, 1.0 for base. These again completely satisfy the requirements.

4. Acetylene on Au. Let the r.d.s be reaction 4.28 in the oxidation sequence, thereby giving the rate equation

$$i = zFk'\theta_R(1-\theta_T)\exp(\alpha\nu F/RT) \qquad (4.35)$$

Replacing ν with V and $\zeta = 0$ for acid and 2.3RT/F for base gives:

For acid,

$$i = zFk'\theta_R(1-\theta_T)\exp[\alpha(V-V^o_{pzc})F/RT] \qquad (4.53)$$

and for base,

$$i = zFk'\theta_R(1-\theta_T)\exp[\alpha(V-V^o_{pzc} + \frac{2.3RT}{F}\,pH)F/RT] \qquad (4.54)$$

The derivatives, $\partial V/\partial \log i = 2.3RT/F$, $\partial E'_a/\partial V = -F$, and $\partial i/\partial P_R < 0$ when θ_R is greater than $(1-\theta_T)$ but > 0 when θ_R is less than $(1-\theta_T)$, obtained from the above two equations are in agreement with the observed results. The derivative $\partial \log i/\partial pH = 0$ for acid is in agreement but $\partial \log i/\partial pH = 0.5$ in base is different than reported (see Table III). An examination of the experimental results obtained by Reed[27] shows that $\partial \log i/\partial pH = 0.75$ b.t.r. and ~ 0.85 a.t.r. As mentioned in the previous section, these values might also be interpreted as 0.5, as was done in the case of C_2H_4, thus resolving the differences. At least in one case, b.t.r., it would not be unreasonable to do so.

V. RECOMMENDATIONS

Anodic oxidation of unsaturated hydrocarbons is a complex sequential reaction with the possibility of parallel reactions occurring. Steady state techniques used in the present study of C_4H_6 oxidation yield only limited data with which to follow the progress of the reaction. Therefore, transient methods are recommended for obtaining the kinetic parameters, electrode surface coverage, and reaction-intermediate identification. Rotating ring and disc electrode assemblies should be employed to obtain the reaction order of the limiting reactant and also for intermediate identification. These methods, by providing complementary and additional kinetic parameters, would help in a more complete elucidation of the oxidation reaction. A reference to these techniques can be found in the Hand Book of Fuel Cell Technology.[28]

It is further suggested that hydrocarbon oxidation be carefully studied on activated and non-activated electrodes to ascertain accurately the pH effect on reaction in acids. The order of reaction with respect to H_2O should be ascertained by using different concentrations of electrolytes, e.g., phosphoric acid, to possibly confirm the present findings for C_4H_6.

VI. APPENDICES

APPENDIX A

NOTATION

a	=	Chemical potential
A	=	Frequency factor in Arrhenius equation
A_H	=	Surface excess of adsorbed hydrogen in the metal
a.t.r.	=	Above transition region
b.t.r.	=	Below transition region
c	=	Coordination number on the surface
C_{dl}	=	Capacity of double layer
C_R	=	Concentration of hydrocarbon, gmole/liter
C_ϕ	=	Pseducapacitance
e	=	Electron
	=	Charge on an electron
E	=	Electrode potential
	=	Energy of interaction between dipoles in eqns. 2.34 and 2.35
E'_a	=	Apparent energy of activation, Kcal/mole
E_1, E_2	=	Total energy of a H_2O molecule on the surface in the two possible orientations
E_1^c, E_2^c	=	Non field dependent energy of interaction of H_2O on the surface in the two possible orientations
E_m	=	Potential of maximum adsorption
F	=	Faraday constant

ΔG^{o}_{ad}	=	Standard free energy of electrosorption
$\Delta G_{s,W}$	=	Free energy of adsorption of water from solution
$\Delta G_{s,R}$	=	Free energy of adsorption of organic from solution
$\Delta G_{v,W}$	=	Free energy of adsorption of water from the vapor phase at 1 atm
$\Delta G_{v,R}$	=	Free energy of adsorption of organic from the vapor phase at 1 atm
$\Delta G_{p,W}$	=	$-RT \ln(p_W)$
$\Delta G_{p,R}$	=	$-RT \ln(p_R)$
$\Delta G_{d,R}$	=	$-RT \ln(C_R/C_{sat,R})$, free energy of dilution from $C_{sat,R}$ to C_R
i	=	Current density, amp/cm^2
I	=	Current, amp
k,k',k"	=	Rate constants
K	=	Equilibrium constant
K_c	=	Concentration equilibrium constant
K_p	=	Pressure equilibrium constant
n	=	Number of sites required for adsorption
NHE	=	Normal hydrogen electrode
N_t	=	N_1+N_2
N_1,N_2	=	Number of water molecules on the surface in the two possible orientations
P	=	Pressure, atm

P_R	=	Partial pressure of the species R, atm
p.z.c.	=	Potential of zero charge
q_m	=	Excess charge on the electrode
q_s	=	Charge on the solution side
R	=	Gas constant, 1.987 cal/gmole °K
	=	Hydrocarbon, acetylene, butadiene, etc.
SHE	=	Standard hydrogen electrode
T	=	Temperature, °K
V	=	Potential, volts(SHE)
V_m	=	Measured potential, volts
V_{pzc}	=	Potential of zero charge, volts(SHE)
V^o_{pzc}	=	Potential of zero charge at zero pH, volts (SHE)
X	=	Mole fraction
z	=	Number of excess electrons in the electrode
	=	Total number of electrons involved in the reaction
γ	=	Surface tension
θ	=	Fractional coverage of the surface
ν	=	Rational potential, volts
ϕ	=	Galvani or inner potential, volts
μ	=	Chemical potential
$\bar{\mu}$	=	Electrochemical potential
Γ	=	Surface excess, gmole/cm^2
ρ	=	Dipole moment

Subscripts

i	=	Species i
R	=	Hydrocarbon
sat	=	Saturated
sol	=	Solution
W	=	Water

APPENDIX B

MATERIALS

The following is a list of the materials and reagents used in this investigation. More detailed information of the reagents may be obtained from the chemical catalogue of the respective supplier.

1. Barium Hydroxide. Fisher Certified Reagent grade, Fisher Scientific Co., Fairlawn, N.J. (used for analysis)

2. 1,3-Butadiene (Grade-A). Instrument grade, minimum purity 99.4%, Matheson Scientific Co., Joliet, Ill.

3. 1,3-Butadiene (Grade-B). Special Purity grade, minimum purity 99.5%, Phillips Petroleum Co., Bartlesville, Oklahoma. (GC analysis is shown on the next page)

4. Gold. 0.005 inch thick sheet, Engelhard Industries Inc., Newark, N.J.

5. Hydrochloric Acid. Reagent A.C.S. grade, Fisher Scientific Co., Fairlawn, N.J. (used for CO_2 analysis)

6. Mercurous Chloride. Fisher Certified Reagent grade, Fisher Scientific Co., Fairlawn, N.J. (used in reference electrode)

7. Mercurous Sulfate. Reagent grade, Matheson Coleman & Bell, Norwood, Ohio. (used in reference electrode)

Gas Chromatograph of Grade-A and Grade-B Butadiene

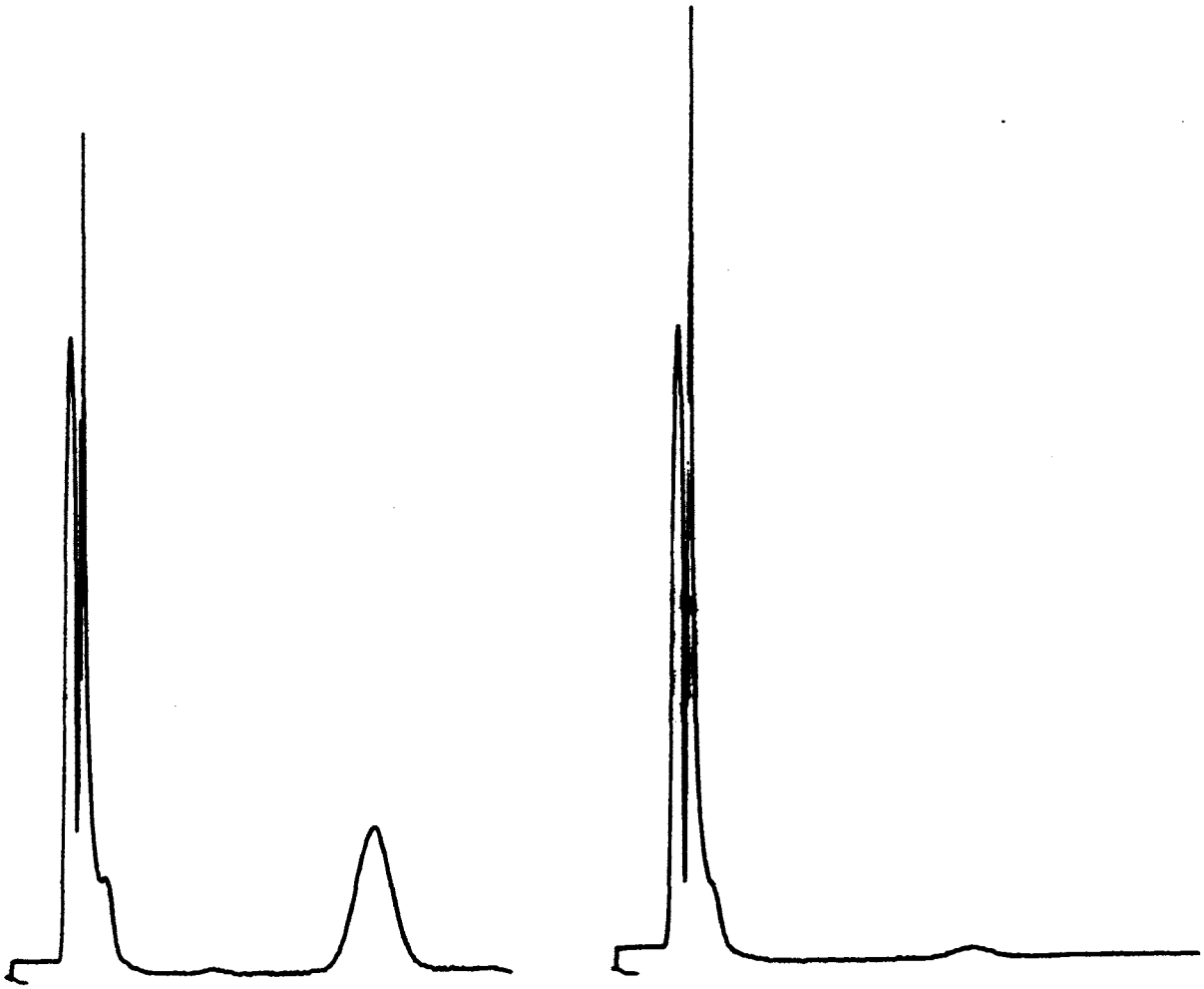

Grade-A

Grade-B

8. Nitrogen. Prepurified grade, Matheson Scientific Co., Joliet, Ill.

9. Platinum. 52-mesh gauze, Engelhard Industries Inc., Newark, N.J.

10. Potassium Carbonate. Certified A.C.S. grade, Fisher Scientific Co., Fairlawn, N.J.

11. Potassium Chloride. Fisher Certified Reagent grade, Fisher Scientific Co., Fairlawn, N.J. (used in reference electrode)

12. Potassium Hydroxide. Certified A.C.S. grade, Fisher Scientific Co., Fairlawn, N.J.

13. Potassium Sulfate. Certified A.C.S. grade, Fisher Scientific Co., Fairlawn, N.J.

14. Sulfuric Acid. Reagent A.C.S. grade, Fisher Scientific Co., Fairlawn, N.J.

APPENDIX C

APPARATUS

The following is a list of the principal components used in this investigation.

1. Ammeter. Ultra high sensitivity volt-ohm-microammeter, Simpson 269, Simpson Electric Co., Chicago, Ill.

2. Electrometer. Multi-range type, Model 610B, Keithley Instruments Inc., Cleveland, Ohio.

3. Gas Chromatograph. Model 810 Research Chromatograph, F & M Scientific Corporation, Avondale, Pa.

4. Gas Proportioner. Matheson Model 665, Dual-flow control, Matheson Scientific Co., East Rutherford, N.J.

5. Potentiostat. Wenking 6356, Gerhard Bank Elektronic, Gottinger, West Germany.

6. Power Resistor. Decade Box, Model 240-C, Clarostat Mfg. Co., Inc., Dover, N.H.

7. Power Supply. Sorenson, QRB (0.75 amp, 40 v) D.C. power supply, Raytheon Co., South Norwalk, Conn.

8. Recorder. Esterline Angus Graphic Ammeter, 0-1 amp, Esterline Angus, Indianapolis, Ind.

9. Temperature Controller. Matheson Lab-Stat, S. No. BS 2041, Matheson Scientific Co., East Rutherford, N.J.

10. Variac. Adjust-A-Volt, Type 500B, Standard Elct. Product Co., Dayton, Ohio.

APPENDIX D

SAMPLE CALCULATIONS

1. Sample calculations to obtain modified parameters for butadiene oxidation.

$$\nu = V - V_{pzc}$$

$$V_{pzc} = V^{o}_{pzc} - \zeta\ pH$$

$$\nu = V - V^{o}_{pzc} + \zeta\ pH$$

Therefore,

$$\partial\nu/\partial pH = \zeta$$

$$\partial\nu/\partial pH = \partial V/\partial pH + \zeta$$

$$\partial\nu/\partial \log i = \partial V/\partial \log i$$

$$\partial \log i/\partial pH = (\partial \log i/\partial pH)_{V} - (\partial \log i/\partial\nu)_{pH}(\partial\nu/\partial pH)_{V}$$

$$= (\partial \log i/\partial pH)_{V} - \zeta/(\partial\nu/\partial \log i)_{pH}$$

Taking for example the parameters for Au, Table VII, we have,

$$\partial V/\partial pH = -2.3RT/F$$

$$\partial V/\partial \log i = 2.3RT/F$$

$$\partial \log i/\partial pH = 1$$

substituting these values and $\zeta(=2.3RT/F)$ for Au into the derivatives with rational potentials gives,

$$\partial\nu/\partial pH = -2.3RT/F + \zeta$$

$$= 0$$

$$\partial\nu/\partial \log i = 2.3RT/F$$

$$\partial \log i/\partial pH = 1 - \zeta/(2.3RT/F)$$

$$= 0$$

2. Sample calculations to obtain coulombic efficiency of C_4H_6 oxidation to CO_2.

The coulombic efficiency is the actual amount of CO_2 formed during the experiment divided by the theoretical amount formed if the oxidation were complete.

The oxidation equation for butadiene is

$$C_4H_6 + 8\ H_2O = 4\ CO_2 + 22\ H^+ + 22\ e$$

Therefore, by Faraday's law, the amount of CO_2 formed by passage of I amperes in t seconds will be

$$W_t = \frac{(4)(44)I\ t}{22\ F}$$

e.g., 5 ma for 20 hours should yield

$$W_t = \frac{(4)(44)(5 \times 10^{-3})\ (20 \times 3600)}{(22)\quad (96500)} = 0.0299 \text{ gms.}$$

If the actual amount formed in this period is $W_e = 0.0245$ gms, the coulombic efficiency is

$$\text{eff.} = \frac{W_e}{W_t} = \frac{0.0245}{0.0299} = 0.82 \text{ or } 82\%$$

APPENDIX E

DATA

The following tables include the data obtained in the current-potential, current-partial pressure, and current-temperature studies. The measured potential V_m was converted to V(SHE) by the method described by Johnson, et. al.[18] The current density i was calculated by dividing the measured current I by the area of the electrode surface.

TABLE IX

CURRENT-POTENTIAL VALUES FOR THE ANODIC OXIDATION OF GRADE-A BUTADIENE ON Pt AT 80°C (P_R = 1 atm) IN 1 N H_2SO_4 (pH = 0.35)

V_m	V	I x 10^3	i x 10^3
volts(NSE)*	volts(SHE)	amp	amp/cm^2
0.15	0.448	1.0	0.14
0.10	0.498	1.5	0.21
0.05	0.548	2.8	0.38
0.00	0.598	6.0	0.82
-0.05	0.648	14	2.0
-0.10	0.698	36	4.9
-0.15	0.748	72	9.9

*Normal sulfate electrode

TABLE X

CURRENT-POTENTIAL VALUES FOR THE ANODIC OXIDATION OF GRADE-A BUTADIENE ON Pt AT 70°C (P_R = 1 atm) IN 1 N H_2SO_4 (pH = 0.35)

V_m	V	I x 10^3	i x 10^3
volts(NSE)	volts(SHE)	amp	amp/cm^2
0.15	0.458	0.56	0.077
0.10	0.508	0.80	0.11
0.05	0.558	1.4	0.19
0.00	0.608	3.0	0.41
-0.05	0.658	6.4	0.88
-0.10	0.708	15	2.1
-0.15	0.758	30	4.0

TABLE XI

CURRENT-POTENTIAL VALUES FOR THE ANODIC OXIDATION OF GRADE-A BUTADIENE ON Pt AT 70°C (P_R = 1 atm) IN 1 N K_2SO_4 (pH = 4.4)

V_m	V	I x 10^3	i x 10^3
volts(NSE)	volts(SHE)	amp	amp/cm^2
0.30	0.308	0.72	0.099
0.20	0.408	1.8	0.25
0.15	0.458	4.4	0.60
0.10	0.508	8.4	1.2
0.05	0.558	17	2.3
0.00	0.608	31	4.2
-0.05	0.658	50	6.9
-0.10	0.708	68	9.3

TABLE XII

CURRENT-POTENTIAL VALUES FOR THE ANODIC OXIDATION OF GRADE-A BUTADIENE ON Pt AT 70°C (P_R = 1 atm) IN 1 N K_2CO_3 (pH = 10.8)

V_m	V	I x 10^3	i x 10^3
volts(NCE)*	volts(SHE)	amp	amp/cm^2
0.40	-0.161	0.22	0.030
0.35	-0.111	0.34	0.047
0.30	-0.061	0.60	0.082
0.25	-0.011	1.5	0.21
0.20	0.039	4.5	0.62
0.15	0.089	12	1.6
0.10	0.139	21	2.9

*Normal calomel electrode

TABLE XIII

CURRENT-POTENTIAL VALUES FOR THE ANODIC OXIDATION OF GRADE-A BUTADIENE ON Pt AT 70°C (P_R = 1 atm) IN 1 N KOH (pH = 12.5)

V_m	V	I x 10^3	i x 10^3
volts (NCE)	volts (SHE)	amp	amp/cm^2
0.50	-0.261	0.32	0.044
0.45	-0.211	0.45	0.062
0.42	-0.181	0.62	0.085
0.39	-0.151	0.98	0.13
0.36	-0.121	1.7	0.23
0.33	-0.091	3.0	0.41
0.30	-0.061	5.2	0.72
0.27	-0.031	8.8	1.2
0.24	-0.001	14	1.9

TABLE XIV

CURRENT-POTENTIAL VALUES FOR THE ANODIC OXIDATION OF GRADE-B BUTADIENE ON Pt AT 70°C (P_R = 1 atm) IN 1 N H_2SO_4 (pH = 0.35)

V_m	V	I x 10^3	i x 10^3
volts(NSE)	volts(SHE)	amp	amp/cm^2
0.10	0.508	0.28	0.038
0.05	0.558	0.40	0.055
0.02	0.588	0.60	0.082
0.00	0.608	0.81	0.11
-0.02	0.628	1.2	0.16
-0.04	0.648	2.0	0.27
-0.06	0.668	3.6	0.49
-0.08	0.688	6.4	0.88
-0.10	0.708	11	1.5
-0.12	0.728	16	2.2
-0.14	0.748	24	3.3
-0.20	0.808	52	7.1
-0.25	0.858	80	11
-0.30	0.908	110	15

TABLE XV

CURRENT-POTENTIAL VALUES FOR THE ANODIC OXIDATION OF GRADE-B BUTADIENE ON Pt AT 70°C (P_R = 1 atm) IN H_2SO_4 + K_2SO_4 (pH = 1.3)

V_m	V	I x 10^3	i x 10^3
volts(NSE)	volts(SHE)	amp	amp/cm^2
0.10	0.508	0.35	0.048
0.06	0.548	0.46	0.063
0.04	0.568	0.60	0.080
0.02	0.588	0.80	0.11
0.00	0.608	1.1	0.15
-0.02	0.628	1.6	0.23
-0.04	0.648	2.9	0.40
-0.06	0.668	5.5	0.75
-0.08	0.688	9.8	1.3
-0.10	0.708	15	2.1
-0.12	0.728	22	3.0
-0.15	0.758	34	4.7
-0.20	0.808	56	7.7
-0.25	0.858	76	10

TABLE XVI

CURRENT-POTENTIAL VALUES FOR THE ANODIC OXIDATION OF GRADE-B BUTADIENE ON Pt AT 70°C (P_R = 1 atm) IN H_2SO_4 + K_2SO_4 (pH = 2.6)

V_m	V	I x 10^3	i x 10^3
volts(NSE)	volts(SHE)	amp	amp/cm^2
0.20	0.408	0.17	0.023
0.17	0.438	0.22	0.030
0.14	0.468	0.30	0.041
0.11	0.498	0.43	0.059
0.08	0.528	0.72	0.099
0.05	0.558	1.3	0.18
0.02	0.588	3.6	0.49
-0.01	0.618	8.8	1.2
-0.03	0.638	14	1.9
-0.05	0.658	20	2.7
-0.08	0.688	32	4.4
-0.10	0.708	41	5.6
-0.15	0.758	64	8.8

TABLE XVII

CURRENT-POTENTIAL VALUES FOR THE ANODIC OXIDATION OF GRADE-B BUTADIENE ON Pt AT 70°C (P_R = 1 atm) IN K_2SO_4 + K_2CO_3 (pH = 9.9)

V_m	V	I x 10^3	i x 10^3
volts(NCE)	volts(SHE)	amp	amp/cm^2
0.35	-0.111	0.055	0.0075
0.30	-0.061	0.12	0.017
0.25	-0.011	0.28	0.038
0.22	0.019	0.44	0.060
0.19	0.049	0.76	0.10
0.16	0.079	1.5	0.21
0.13	0.109	3.0	0.41
0.10	0.139	5.7	0.78
0.07	0.169	9.6	1.3
0.04	0.199	15	2.0
0.01	0.229	19	2.6
-0.01	0.249	20	2.7

TABLE XVIII

CURRENT-POTENTIAL VALUES FOR THE ANODIC OXIDATION OF GRADE-B BUTADIENE ON Pt AT 70°C (P_R = 1 atm) IN 1 N K_2CO_3 (pH = 10.8)

V_m	V	I x 10^3	i x 10^3
volts(NCE)	volts(SHE)	amp	amp/cm^2
0.45	-0.211	0.050	0.0069
0.40	-0.161	0.095	0.013
0.35	-0.111	0.18	0.025
0.30	-0.061	0.35	0.048
0.28	-0.041	0.52	0.071
0.26	-0.021	0.78	0.11
0.24	-0.001	1.2	0.16
0.22	0.019	2.0	0.28
0.20	0.039	3.4	0.47
0.18	0.059	5.5	0.75
0.16	0.079	8.3	1.1
0.14	0.099	12	1.6
0.11	0.129	18	2.4
0.08	0.159	23	3.2

TABLE XIX

CURRENT-POTENTIAL VALUES FOR THE ANODIC OXIDATION OF GRADE-B BUTADIENE ON Pt AT 70°C (P_R = 1 atm) IN 1 N KOH (pH = 12.5)

V_m	V	I x 10^3	i x 10^3
volts(NCE)	volts(SHE)	amp	amp/cm^2
0.55	-0.311	0.08	0.011
0.50	-0.261	0.10	0.014
0.45	-0.211	0.24	0.033
0.42	-0.181	0.36	0.049
0.39	-0.151	0.66	0.090
0.36	-0.121	1.3	0.18
0.33	-0.091	2.6	0.36
0.30	-0.061	5.2	0.71
0.27	-0.031	8.4	1.2
0.24	-0.001	12	1.7
0.21	0.029	10	1.4

TABLE XX

CURRENT-POTENTIAL VALUES FOR THE ANODIC OXIDATION OF GRADE-B BUTADIENE ON Pt AT 70°C (P_R = 0.1 atm) IN 1 N H_2SO_4 (pH = 0.35)

V_m	V	I x 10^3	i x 10^3
volts(NSE)	volts(SHE)	amp	amp/cm^2
0.10	0.508	0.44	0.060
0.05	0.558	0.76	0.10
0.03	0.578	0.96	0.13
0.01	0.598	1.3	0.18
-0.01	0.618	2.0	0.27
-0.03	0.638	3.0	0.41
-0.05	0.658	4.8	0.66
-0.07	0.678	7.9	1.1
-0.09	0.698	12	1.7
-0.11	0.718	18	2.5
-0.15	0.758	32	4.4
-0.20	0.808	49	6.7
-0.25	0.858	62	8.5

TABLE XXI

CURRENT-POTENTIAL VALUES FOR THE ANODIC OXIDATION OF GRADE-B BUTADIENE ON Pt AT 70°C (P_R = 0.01 atm) IN 1 N H_2SO_4 (pH = 0.35)

V_m	V	I x 10^3	i x 10^3
volts(NSE)	volts(SHE)	amp	amp/cm^2
0.10	0.508	0.59	0.081
0.05	0.558	1.1	0.15
0.03	0.578	1.6	0.22
0.01	0.598	2.5	0.34
-0.01	0.618	4.0	0.55
-0.03	0.638	5.8	0.80
-0.05	0.658	8.1	1.1
-0.07	0.678	10	1.4
-0.09	0.698	12	1.6
-0.11	0.718	13	1.8
-0.15	0.758	14	1.9
-0.20	0.808	16	2.2
-0.25	0.858	16	2.2

TABLE XXII

CURRENT-POTENTIAL VALUES FOR THE ANODIC OXIDATION OF GRADE-B BUTADIENE ON Pt AT 70°C (P_R = 0.1 atm) IN 1 N KOH (pH = 12.5)

V_m	V	I x 10^3	i x 10^3
volts(NCE)	volts(SHE)	amp	amp/cm^2
0.55	-0.311	0.02	0.0027
0.50	-0.261	0.10	0.014
0.45	-0.211	0.28	0.038
0.43	-0.191	0.32	0.044
0.41	-0.171	0.44	0.060
0.39	-0.151	0.68	0.093
0.37	-0.131	1.1	0.15
0.35	-0.111	1.7	0.23
0.33	-0.091	2.6	0.36
0.31	-0.071	3.8	0.52
0.29	-0.051	5.6	0.77
0.25	-0.011	10	1.4

TABLE XXIII

CURRENT-POTENTIAL VALUES FOR THE ANODIC OXIDATION OF GRADE-B BUTADIENE ON Pt AT 70°C (P_R = 0.01 atm) IN 1 N KOH (pH = 12.5)

V_m	V	I x 10^3	i x 10^3
volts(NCE)	volts(SHE)	amp	amp/cm^2
0.55	-0.311	0.12	0.016
0.50	-0.261	0.20	0.027
0.45	-0.211	0.32	0.044
0.43	-0.191	0.44	0.060
0.41	-0.171	0.64	0.088
0.39	-0.151	0.96	0.13
0.37	-0.131	1.4	0.20
0.35	-0.111	2.0	0.27
0.33	-0.091	2.6	0.36
0.31	-0.071	3.4	0.47
0.29	-0.051	4.3	0.59
0.25	-0.011	5.2	0.71

TABLE XXIV

CURRENT-POTENTIAL VALUES FOR THE ANODIC OXIDATION OF GRADE-B BUTADIENE ON Au AT 70°C (P_R = 1 atm) IN 1 N H_2SO_4 (pH = 0.35)

V_m	V	I x 10^6	i x 10^6
volts(NSE)	volts(SHE)	amp	amp/cm^2
0.00	0.608	20	1.3
-0.05	0.658	20	1.3
-0.10	0.708	40	2.7
-0.15	0.758	90	6.0
-0.17	0.778	120	8.0
-0.19	0.798	160	11
-0.20	0.808	210	14
-0.21	0.818	440	29
-0.23	0.838	700	47
-0.25	0.858	1000	67
-0.30	0.908	1500	99
-0.35	0.958	2100	140
-0.40	1.008	3100	210
-0.45	1.058	4400	290

TABLE XXV

CURRENT-POTENTIAL VALUES FOR THE ANODIC OXIDATION OF GRADE-B BUTADIENE ON Au AT 70°C (P_R = 1 atm) IN K_2SO_4 + K_2CO_3 (pH = 9.9)

V_m	V	I x 10^6	i x 10^6
volts(NCE)	volts(SHE)	amp	amp/cm^2
0.15	0.089	4.1	0.27
0.12	0.119	6.6	0.44
0.10	0.139	8.9	0.59
0.08	0.159	13	0.86
0.06	0.179	19	1.3
0.04	0.199	31	2.1
0.02	0.219	50	3.3
0.00	0.239	79	5.3
-0.02	0.259	130	8.5
-0.04	0.279	190	13
-0.06	0.299	240	16
-0.08	0.319	300	20

TABLE XXVI

CURRENT-POTENTIAL VALUES FOR THE ANODIC OXIDATION OF GRADE-B BUTADIENE ON Au AT 70°C (P_R = 1 atm) IN 1 N K_2CO_3 (pH = 10.8)

V_m	V	I x 10^6	i x 10^6
volts (NCE)	volts (SHE)	amp	amp/cm^2
0.20	0.039	6.1	0.41
0.18	0.059	7.6	0.51
0.16	0.079	11	0.71
0.14	0.099	16	1.1
0.12	0.119	22	1.5
0.10	0.139	36	2.4
0.08	0.159	61	4.1
0.06	0.179	93	6.2
0.04	0.199	140	9.2
0.02	0.219	200	13
0.00	0.239	210	14
-0.02	0.259	240	16

TABLE XXVII

CURRENT-POTENTIAL VALUES FOR THE ANODIC OXIDATION OF GRADE-B BUTADIENE ON Au AT 70°C (P_R = 1 atm) IN K_2SO_4 + KOH (pH = 11.6)

V_m	V	I x 10^6	i x 10^6
volts(NCE)	volts(SHE)	amp	amp/cm^2
0.25	-0.011	4.4	0.29
0.22	0.019	13	0.84
0.20	0.039	21	1.4
0.18	0.059	34	2.3
0.16	0.079	60	4.0
0.14	0.099	110	7.3
0.12	0.119	200	13
0.10	0.139	310	21
0.08	0.159	460	31
0.06	0.179	500	33
0.04	0.199	500	33
0.02	0.219	500	33

TABLE XXVIII

CURRENT-POTENTIAL VALUES FOR THE ANODIC OXIDATION OF GRADE-B BUTADIENE ON Au AT 70°C (P_R = 1 atm) IN 1 N KOH (pH = 12.5)

V_m	V	I x 10^6	i x 10^6
volts(NCE)	volts(SHE)	amp	amp/cm^2
0.26	-0.021	26	1.7
0.24	-0.001	42	2.8
0.22	0.019	76	5.1
0.20	0.039	140	9.5
0.18	0.059	260	17
0.16	0.079	450	30
0.14	0.099	780	52
0.12	0.119	1200	83
0.10	0.139	1700	110
0.08	0.159	2100	140
0.06	0.179	2100	140

TABLE XXIX

CURRENT-POTENTIAL VALUES FOR THE ANODIC OXIDATION OF GRADE-B BUTADIENE ON Au AT 70°C (P_R = 0.1 atm) IN 1 N KOH (pH = 12.5)

V_m	V	I x 10^6	i x 10^6
volts(NCE)	volts(SHE)	amp	amp/cm^2
0.25	-0.011	69	4.6
0.23	0.009	100	6.7
0.21	0.029	170	11
0.19	0.049	300	20
0.17	0.069	480	32
0.15	0.089	750	50
0.13	0.109	1100	71
0.11	0.129	1300	88
0.09	0.149	970	65
0.07	0.169	720	48

TABLE XXX

CURRENT-POTENTIAL VALUES FOR THE ANODIC OXIDATION OF GRADE-B BUTADIENE ON Au AT 70°C (P_R = 0.01 atm) IN 1 N KOH (pH = 12.5)

V_m	V	I x 10^6	i x 10^6
volts(NCE)	volts(SHE)	amp	amp/cm^2
0.26	-0.021	40	2.7
0.24	-0.001	49	3.3
0.22	0.019	73	4.9
0.20	0.039	110	7.6
0.18	0.059	210	14
0.16	0.079	320	21
0.14	0.099	530	35
0.12	0.119	770	51
0.10	0.139	1000	69
0.08	0.159	1300	88
0.06	0.179	1500	100

TABLE XXXI

CURRENT-PRESSURE VALUES FOR THE ANODIC OXIDATION OF GRADE-B BUTADIENE ON Pt AT 70°C IN 1 N H_2SO_4 (pH = 0.35)

V_m	V	P_R	I x 10^3	i x 10^3
volts(NSE)	volts(SHE)	atm	amp	amp/cm^2
0.05	0.558	1.0	0.40	0.055
		0.1	0.76	0.10
		0.01	1.1	0.15
-0.04	0.648	1.0	3.6	0.49
		0.3	5.2	0.71
		0.1	7.0	0.96
		0.03	10	1.4
		0.01	11	1.5
-0.08	0.688	1.0	7.8	1.1
		0.3	10	1.4
		0.1	12	1.7
		0.03	15	2.1
		0.01	15	2.1

TABLE XXXII

CURRENT-PRESSURE VALUES FOR THE ANODIC OXIDATION OF GRADE-B BUTADIENE ON Pt AT 70°C IN 1 N KOH (pH = 12.5)

V_m	V	P_R	$I \times 10^3$	$i \times 10^3$
volts(NCE)	volts(SHE)	atm	amp	amp/cm^2
0.40	-0.161	1.0	0.38	0.052
		0.3	0.40	0.055
		0.1	0.42	0.058
		0.03	0.48	0.065
		0.01	0.48	0.065
0.35	-0.111	1.0	1.3	0.18
		0.3	1.4	0.19
		0.1	1.5	0.21
		0.03	1.5	0.21
		0.01	1.5	0.21

TABLE XXXIII

CURRENT-PRESSURE VALUES FOR THE ANODIC OXIDATION OF GRADE-B BUTADIENE ON Au AT 70°C IN 1 N KOH (pH = 12.5)

V_m	V	P_R	I x 10^6	i x 10^6
volts(NCE)	volts(SHE)	atm	amp	amp/cm^2
0.22	0.019	1.0	71	4.7
		0.3	83	5.5
		0.1	82	5.5
		0.03	69	4.6
		0.01	60	4.0
0.18	0.059	1.0	22	1.5
		0.3	25	1.7
		0.1	23	1.5
		0.03	19	1.3
		0.01	16	1.1

TABLE XXXIV

CURRENT-TEMPERATURE VALUES FOR THE ANODIC OXIDATION OF GRADE-B BUTADIENE ON Pt IN 1 N H_2SO_4 (P_R = 1 atm)

V_m	V	T	I x 10^3	i x 10^3
volts(NSE)	volts(SHE)	°C	amp	amp/cm^2
-0.02	0.628	80	6.4	0.88
		75	3.8	0.52
		70	2.4	0.32
		65	1.4	0.19
		60	0.78	0.11
-0.06	0.668	80	14	1.9
		75	8.8	1.2
		70	5.4	0.74
		65	3.2	0.44
		60	1.9	0.26
-0.10	0.708	80	32	4.4
		75	21	2.9
		70	13	1.8
		65	8.0	1.1
		60	4.7	0.64

TABLE XXXV

CURRENT-TEMPERATURE VALUES FOR THE ANODIC OXIDATION OF GRADE-B BUTADIENE ON Pt IN 1 N KOH (P_R = 1 atm)

V_m	V	T	I x 10^3	i x 10^3
volts(NCE)	volts(SHE)	°C	amp	amp/cm^2
0.40	-0.161	80	1.7	0.24
		75	1.0	0.14
		70	0.60	0.08
		65	0.35	0.48
		60	0.19	0.26
0.35	-0.111	80	4.2	0.58
		75	2.7	0.37
		70	1.7	0.23
		65	1.0	0.14
		60	0.58	0.08
0.30	-0.061	80	12	1.7
		75	7.8	1.1
		70	5.0	0.69
		65	3.0	0.41
		60	1.8	0.25

TABLE XXXVI

CURRENT-TEMPERATURE VALUES FOR THE ANODIC OXIDATION OF GRADE-B BUTADIENE ON Au IN 1 N KOH (P_R = 1 atm)

V_m	V	T	I x 10^6	i x 10^6
volts (NCE)	volts (SHE)	°C	amp	amp/cm^2
0.22	0.019	80	280	19
		75	180	12
		70	120	7.7
		65	70	4.7
		60	40	2.7
0.19	0.049	80	640	43
		75	440	29
		70	280	19
		65	170	11
		60	110	7.3
0.16	0.079	80	1400	91
		75	960	64
		70	640	43
		65	390	26
		60	240	16

VII. BIBLIOGRAPHY

1. H. Davy, Ann. Phys., 8, 301 (1801).
2. G.E. Evans, "Future Commercial Application for Fuel Cells in the Chemical Industry," Paper presented at St. Louis, the AIChE National Meeting (1968).
3. B.J. Piersma and E. Gileadi, "Modern Aspects of Electrochemistry," No. 4, ed. J.O'M. Bockris, Plenum Press, New York (1966).
4. B.E. Conway, "Electrode Processes," The Roland Press Company, New York (1965).
5. S.D. Argade, Ph.D. Thesis, University of Pennsylvania (1968).
6. J.O'M. Bockris and S.D. Argade, J. Chem. Phys., 49,' 5133 (1968)
7. O.A. Petrii, A.N. Frumkin and Yu G. Kotlov, Elektrokhimiya URSS, 5, 476 (1969).
8. D.D. Bode, Jr., T.N. Andersen and H. Eyring, J. Phys. Chem., 71, 792 (1967).
9. E. Gileadi, S.D. Argade and J.O'M. Bockris, J. Phys. Chem., 71, 2044 (1966).
10. R.Kh. Burshtein, A.G. Pshenichnikov and L.A. Shevchenko, Elektrokhimiya URSS, 5, 332 (1969).
11. A.N. Frumkin, J. Electroanal. Chem., 9, 173 (1965); J. Electrochem. Soc., 113, 1024 (1966).

12. J.O'M. Bockris and D.A.J. Swinkels, J. Electrochem. Soc., 111, 736 (1964).

13. J.O'M. Bockris, M. Green and D.A.J. Swinkels, J. Electrochem Soc., 111, 743 (1964).

14. E. Gileadi, B.T. Rubin and J.O'M. Bockris, J. Phys. Chem., 69, 3335 (1965).

15. W. Heiland, E. Gileadi and J.O'M. Bockris, J. Phys. Chem., 70, 1207 (1966).

16. E. Gileadi, J. Electroanal. Chem., 11, 137 (1966).

17. J.O'M. Bockris, H. Wroblowa, E. Gileadi and B.J. Piersma, Trans. Faraday Soc., 61, 2531 (1965).

18. J.W. Johnson, H. Wroblowa and J.O'M. Bockris, J. Electrochem Soc., 111, 863 (1964).

19. J.O'M. Bockris, E. Gileadi and G.E. Stoner, J. Phys. Chem., 73, 427 (1969).

20. J.W. Johnson, J.L.Reed and W.J. James, J. Electrochem. Soc., 114, 573 (1967).

21. J.W. Johnson, S.C. Lai and W.J. James, Electrochim Acta, to be published.

22. M. Green, J. Weber and V. Drazic, J. Electrochem. Soc., 111, 721 (1964).

23. H. Dahms and J.O'M Bockris, J. Electrochem. Soc., 111, 6 (1964).

24. A.I. Vogel, "Quantitative Inorganic Analysis," 3rd ed., John Wiley and Sons, Inc., New York (1961).

25. B.J. Piersma, Ph.D. Thesis, University of Pennsylvania (1965).

26. S.C. Lai, Ph.D. Thesis, University of Missouri-Rolla (1968).

27. J.L. Reed, Ph.D. Thesis, University of Missouri-Rolla (1966).

28. S. Srinivasan and E. Gileadi, "Handbook of Fuel Cell Technology," ed. C. Berger, Prentice-Hall, Inc., New Jersey (1968).

VIII. VITA

Arun Kumar Agrawal was born on January 1, 1940, in Allahabad, India. He attended high school in Allahabad, graduating in 1953. He received a B.Sc. Ch.E. degree from Banaras Hindu University in 1962.

He came to the U.S.A. in September 1963 and pursued graduate studies at the University of Missouri-Rolla. He graduated in July 1965 with an M.S. in Chemical Engineering. During this period he held graduate assistantships in the Chemistry and Chemical Engineering Departments.

The author worked in Cleveland, Ohio for one and one-half years after the M.S., and rejoined the University of Missouri-Rolla in January 1967 for the Ph.D. degree. He received an assistantship from the Graduate Center for Materials Research while doing his dissertation research.